농학박사 학위논문

벼 도열병균의 발달과 병원성에 대한 수모화의 기능 구명

SUMOylation for fungal development and pathogenicity in the rice blast fungus, *Magnaporthe oryzae*

2022년 2월

서울대학교 대학원

농생명공학부 식물미생물학전공

임 유 진

SUMOylation for fungal development and pathogenicity in the rice blast fungus, *Magnaporthe oryzae*

A dissertation submitted in partial
fulfillment of the requirement for
the degree of

DOCTOR OF PHILOSOPHY

to the Faculty of
Department of Agricultural Biotechnology
at

SEOUL NATIONAL UNIVERSITY

by

You-Jin Lim

FEBRUARY 2022

농학박사 학위논문

벼 도열병균의 발달과 병원성에 대한 수모화의 기능 구명

지도교수 이 용 환

이 논문을 농학박사 학위논문으로 제출함
2021년 12월

서울대학교 대학원
농생명공학부 식물미생물학전공

임 유 진

임유진의 박사 학위논문을 인준함

2021년 12월

위 원 장 김 국 형 (인)

부 위 원 장 이 용 환 (인)

위 원 전 준 현 (인)

위 원 김 순 옥 (인)

위 원 손 호 경 (인)

A THESIS FOR THE DEGREE OF DOCTOR OF PHILOSOPHY

SUMOylation for fungal development and pathogenicity in the rice blast fungus, *Magnaporthe oryzae*

UNDER THE DIRECTION OF DR. YONG-HWAN LEE

SUBMITTED TO THE FACULTY OF THE GRADUATE SCHOOL OF SEOUL NATIONAL UNIVERSITY

BY

YOU-JIN LIM

PROGRAM IN PLANT MICROBIOLOGY
DEPARTMENT OF AGRICULTURAL BIOTECHNOLOGY

DECEMBER 2021

APPROVED AS A QUALIFIED THESIS OF YOU-JIN LIM
FOR THE DEGREE OF DOCTOR OF PHILOSOPHY
BY THE COMMITTEE MEMBERS

CHAIRMAN	Kook-Hyung Kim
VICE CHAIRMAN	Yong-Hwan Lee
MEMBER	Junhyun Jeon
MEMBER	Soonok Kim
MEMBER	Hokyung Son

ABSTRACT

SUMOylation for fungal development and pathogenicity in the rice blast fungus, *Magnaporthe oryzae*

You-Jin Lim
Program in Plant Microbiology
Department of Agricultural Biotechnology
The Graduate School
Seoul National University

The translation process is the final step in 'central dogma', the sequential conversion process into RNA and protein. However, organisms additionally achieve a diversity of biological functions through post-translational modifications (PTMs). The PTM processes including phosphorylation, methylation, acetylation, glycosylation, ubiquitination, and SUMOylation are involved in forming various proteome by binding a specific functional group or polypeptide to substrate proteins. SUMOylation, one of the well-conserved PTMs, regulates diverse biological processes including cell cycle, DNA repair, and transcriptional regulation with the participation of five key components, SUMO, E1-activating enzyme, E2-conjugating enzyme, E3 ligase, and protease. Most PTMs have been reported to be necessary for the development and pathogenicity, but the roles of SUMOylation are

not well understood in plant fungal pathogens. *Magnaporthe oryzae*, the rice blast fungus, is the most important fungal pathogen, causing socioeconomic damage by invading rice and wheat throughout the growing season and has been studied as a model organism for host-microbe interaction. In this study, to elucidate the roles of the SUMOylation in *M. oryzae*, SUMOylation components were identified for the first time in plant pathogenic fungi. Among the SUMOylation components, SUMO (MoSMT3), two E1-activating enzymes (MoAOS1 and MoUBA2), and E2-conjugating enzyme (MoUBC9) were crucial for mycelial growth, formation of conidia and infection structure, and pathogenicity. These components were essential for SUMOylation in *M. oryzae* and were associated with tolerance of nutrient starvation, interference of DNA repair, and oxidative stresses. In addition, four components located in the nucleus upon exposure to oxidative stress, which is one of the environmental stresses confronted when invading host plants. Taken together, this study provides the possibility of involvement between stress resistance and SUMOylation of nuclear proteins in *M. oryzae*, and a new perspective on the roles of SUMOylation in the pathogenicity of plant fungal pathogens. Ubiquitination, a well-known PTMs, adds ubiquitin to substrate protein by sequential participation of E1-activating enzymes, E2-conjugating enzymes, and E3 ligases, which share the same domains with SUMOylation, but are different from the SUMOylation components. Ubiquitination plays an important role in protein quality control by participating in the ubiquitin-proteasome system, unlike SUMOylation, and the E3 ligase is crucial for selecting the substrate for degradation. Although the roles of

ubiquitination on the pathogenicity of *M. oryzae* have been studied, but little is known about the understanding of the E3 ligases forming Skp1/Cullin/F-box (SCF) complex and the endoplasmic reticulum-associated degradation (ERAD) complex. In this study, we performed functional analysis of MoFBX15 (F-box only protein) and MoCUE1 (ubiquitin system component cue protein) that participate in each complex. MoFBX15 and MoCUE1 are required for the development and pathogenicity in *M. oryzae*. MoCUE1 is important for endoplasmic reticulum stress resistance and the secretion and translocation of cytoplasmic effectors, virulence factor in plant pathogens. In addition, in Δ*Mofbx15* and Δ*Mocue1*, SUMOylation as well as ubiquitination, decreased and the expression of SUMOylation protease coding genes that separate SUMO from the substrate was increased. This study helps to decipher the roles of ubiquitination in pathogenicity, and provides new insight on the crosstalk between ubiquitination and SUMOylation in rice blast fungus and other plant pathogenic fungi. This study provides a more comprehensive understanding of the roles of post-translational modification in the pathogenicity of fungal pathogens and illuminates the relationship between SUMOylation and ubiquitination, which are independent post-translational modifications that crosstalk with each other. Taken together, this work shed light on the post-translational modification in plant pathogenic fungi.

Keywords: *Magnaporthe oryzae*, pathogenicity, post-translational modification, rice blast disease, SUMOylation, ubiquitination

Student number: 2015-21792

CONTENTS

CHAPTER III. F-box only and CUE proteins are crucial ubiquitination-associated components for conidiation and pathogenicity in the rice blast fungus, *Magnaporthe oryzae*

LIST OF TABLES

CHAPTER I

CHAPTER II

CHAPTER III

LIST OF FIGURES

CHAPTER I

CHAPTER II

CHAPTER III

CHAPTER I

Solo or in concert:

SUMOylation roles in pathogenic fungi

This chapter is in preparation for publication.

ABSTRACT

SUMOylation is crucial for DNA replication and repair, transcription stability, and stress response. Although SUMOylation is conserved post-translational modification (PTM) in eukaryotes, the number, functions, and types of SUMOylation-associated components differ between kingdoms. Ubiquitination, a well-known PTM, shares several hallmarks with SUMOylation. However, extensive studies on the interaction between two PTMs are limited to yeast in fungi. Recently, the importance of SUMOylation for pathogenicity and possibility of crosstalks between two PTMs has emerged in pathogenic fungi. In this review, I summarize the recent findings of the difference of SUMOylation components in different kingdoms and describe the important roles of SUMOylation in fungal pathogens. In addition, I propose novel research area for SUMOylation, which regulates DNA and chromosome stabilization processes alone or together with the other PTMs in fungal pathogens. This review shed light on the crosstalk research platform of PTMs in fungi.

INTRODUCTION

Post-translational modifications (PTMs) induce the formation of various proteins by the addition of polypeptides or functional groups to proteins (Leach and Brown. 2012). PTMs regulate multiple processes in eukaryotes such as apoptosis, transcriptional regulation, DNA repair, cell cycle, and protein interaction (Enserink. 2015; He et al., 2017; Oh et al., 2012; Zhao. 2007). Ubiquitination is the most vigorously studied PTM and is involved in protein degradation via the ubiquitin-proteasome system (UPS) (Dielen et al., 2010). Some proteins with similarities to ubiquitin have been discovered and are termed ubiquitin-like modifiers (UBLs) (Kerscher et al., 2006).

Small ubiquitin-like modifier (SUMO) in UBLs has also been actively studied in recent years. As predicted from its full name, SUMOylation has common hallmarks with ubiquitination. The ubiquitin and SUMO form isopeptide bond to lysine (K) residues in their substrates via the sequential participation of E1-activating enzyme (E1), E2-conjugating enzyme (E2) and E3 ligase (E3) (Gill 2004). The ubiquitin and SUMO are initially synthesized with an inactivated precursor. After exposing the di-glycine residues on the C-terminus of ubiquitin and SUMO precursor by protease containing hydrolase function, the ubiquitin and SUMO are ATP-dependently activated by binding to the cysteine (C) residue of E1. The ubiquitin and SUMO are serially transferred to the C residues of E2 and substrates with or without mediation by E3. Subsequently, ubiquitin and SUMO are separated from modified substrates by protease containing isopeptidase function and the modifiers are reused as

components of reversible pathway (Figure 1) (Enserink. 2015; Gill 2004; Morrell and Sadanandom. 2019). Unlike ubiquitination, E1 is a heterodimer in SUMOylation and E3 is not essential to modification and target selection but is only involved in enhancing modification efficiency when non-covalently bound to substrates (Gill. 2004; Morrell and Sadanandom. 2019). The consensus SUMO-binding motif is ΨKxE/D (Ψ and x represent hydrophobic residue and any residue, respectively) but other binding motifs such as inverted motif and consensus motif with additional hydrophobic or acidic residues are found in recent studies (Garvin and Morris. 2017; Liu et al., 2018; Yang et al., 2006). However, a consensus ubiquitin-binding motif does not exist (Akimov et al., 2018). Non-consensus motifs, ubiquitin interaction motifs (UIMs) and SUMO interaction motifs (SIMs), are existed and involved in non-covalent bonds with each modifier and substrate. The UIMs is xAcAcAcxΨxxAΨxxSxxAcx, where Ac and Ψ represent acidic and hydrophobic residues and SIMs have consisted of $\Psi\Psi x\Psi Ac_n$, ΨΨDLT, and $Ac_n\Psi\Psi x\Psi$ (Ac_n represents 2-5 acidic residues) (Garvin and Morris. 2017; Jardin et al., 2015; Lambrughi et al., 2021). Ubiquitination has been studied about E4 elongase and functions of mono-, multi-, and poly-ubiquitination which K residue (K6, K11, K27, K29, K33, K48, and K63) of ubiquitin is participated to form poly chain. The SUMO E4 elongases PIAL1, PIAL2, and ZNF451 have been reported in *Arabidopsis thaliana* and *Homo sapiens* and these elongases enhance chain formation (Eisenhardt et al., 2015; Hoppe. 2005; Li and Ye. 2008; Matic et al., 2008; Tomanov et al., 2014), but the specific roles of mono- and poly-SUMOylation has not yet been clearly elucidated (Figure 1).

Ubiquitin and SUMO were first discovered in 1975 and 1995, respectively, and have since been studied in model organisms such as human, mouse, *A. thaliana*, and yeast (Celen and Sahin. 2020; Goldstein et al., 1975; Meluh and Koshalnd. 1995). However, compared to ubiquitination, SUMOylation is less fully understood in many species, including fungal pathogens, and because of these differences between ubiquitin and SUMO, the two PTMs have been studied as independent pathways (Gill, 2004). In recent studies, several researchers have investigated whether ubiquitination and SUMOylation interact with each other (Lamoliatte et al., 2017; Parker and Ulrich, 2012). In this review, I summarize recent understating of the role of SUMOylation in mammal and plant fungal pathogens and provide future perspectives on crosstalk between ubiquitination and SUMOylation in fungi.

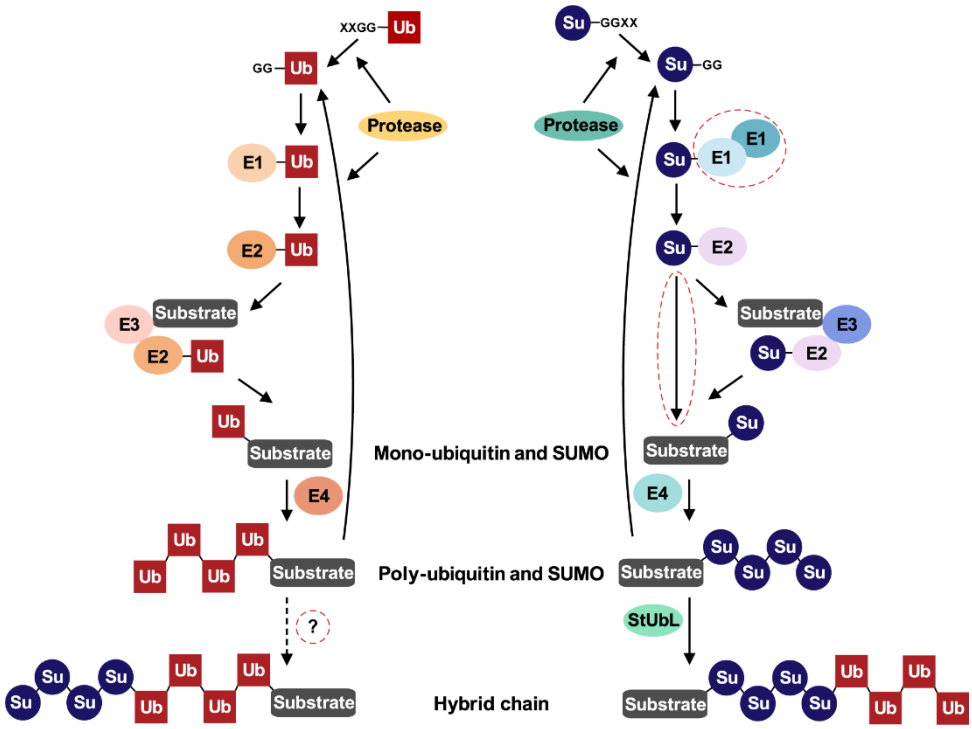

Figure 1. Reversible ubiquitination and SUMOylation pathways and linkage types of ubiquitin and SUMO on the substrates. Schematic illustration of the sequential ubiquitination and SUMOylation pathways. The enzymes E1, E2, and E3 are essential for the modification of substrates by ubiquitin, while E4 enzyme is only involved in poly-chain formation on the substrates. Protease has dual hydrolase and isopeptidase functions. Most SUMOylation processes are similar with the ubiquitination pathway, but, unlike ubiquitination, E1 has activity as a heterodimer and E3 is not crucial for SUMOylation. Moreover, the SUMO-ubiquitin hybrid chain is well understood, but ubiquitin-SUMO hybrid chain formation has not been clearly elucidated. Ub, ubiquitin; Su, SUMO; E1, E1-activating enzymes; E2, E2-conjugating enzyme; E3, E3 ligase; E4, E4 elongase; StUbL, SUMO targeted ubiquitin ligase.

I. Differences between SUMOylation components in mammal, plant, and fungi

The SUMOylation roles and components in mammal and plant have been well studied, including their involvement in abiotic stress responses and immune responses during infection by pathogenic fungi (Augustine et al., 2016; Benlloch and Lois. 2018; Colignon et al., 2017; Enserink. 2015; Morrell and Sadanandom. 2019; Verma et al., 2018; Yang et al., 2017). Among fungi, the function of these components and SUMOylated targets have been most vigorously studied in *Saccharomyces cerevisiae* (Esteras et al., 2017), but the understanding of the SUMOylation pathway in pathogenic fungi is still lacking. Compared to mammal and plant, fungi have a relatively small number of SUMOylation-associated components (Table 1).

Table 1. SUMOylation-associated components in *H. sapiens*, *A. thaliana*, *S.cerevisiae*, and *M. oryzae*.

Class of components	*H. sapiens*	*A. thaliana*	*S.cerevisiae*	*M. oryzae*
SUMO	SUMO1[1] SUMO2[1] SUMO3[1] SUMO4[2] SUMO5[3]	SUM1[4] SUM2[4] SUM3[4] SUM4[4] SUM5[4] SUM6[4] SUM7[4] SUM8[4]	SMT3[5]	MoSMT3[6]
E1	SAE1[7] SAE2[7]	SAE1a[8] SAE1b[8] SAE2[8]	AOS1[9] UBA2[9]	MoAOS1[6] MoUBA2[6]
E2	UBC9/UBE2I[10]	SCE1[11]	UBC9[12]	MoUBC9[6]
E3	PIAS1[13] PIASxα[13] PIASxβ[13] PIAS3[13] PIASy[13] KAP1[14] CBX4/PC2[15] MMS21[16] RANBp2[17] HDAC4[18]	SIZ1[19] MMS21/HPY2[20]	SIZ1[21] SIZ2/NFI1[22] MMS21[23] CST9/ZIP3[24]	MoSIZ1[25] MoSIZ2[6] MoMMS21[6]
E4	ZNF451[26]	PIAL1[27] PIAL2[27]		
Protease	SENP1[28]	ULP1a/ELS1[31]	ULP1/PLI1[39]	MoULP1[25]

	SENP2[28]	ULP1b/ELS2[31]	ULP2[40]	MoULP2[25]
	SENP3[28]	ULP1c/OTS2[32]	WSS1[41]	MoWSS1[25]
	SENP5[28]	ULP1d/OTS1[33]		
	SENP6[28]	ESD4[34]		
	SENP7[28]	ASP1/SPF1[35]		
	DESI1[29]	SPF2[35]		
	DESI2[29]	DESI1[36]		
	USPL1[30]	DESI2A[36]		
		DESI2B[36]		
		DESI3A[36]		
		DESI3B[36]		
		DESI3C[36]		
		DESI4A[36]		
		DESI4B[36]		
		FUG1[37]		
		UBP6[38]		
		UBP7[38]		

[1]Saitoh and Hinchey. 2005; [2]Wang and She. 2008; [3]Liang et al., 2016; [4]Kurepa et al., 2003; [5]Seufert et al., 1995; [6]Lim et al., 2018; [7]Gong et al., 1999; [8]Castaño-Miquel et al., 2013; [9]Johnson et al., 1997; [10]Bernier-Villamor et al., 2002; [11]Saracco et al., 2007; [12]Johnson and Blobel. 1997; [13]Schmidt and Müller. 2002; [14]Liang et al., 2011; [15]Kagey et al., 2003; [16]Potts and Yu. 2005; [17] Tatham et al., 2005; [18]Zhao et al., 2005; [19]Catala et al., 2007; [20]Ishida et al., 2012; [21]Takahashi et al., 2001; [22]Johnson and Gupta. 2001; [23]Hoch et al., 2008; [24]Cheng et al., 2006; [25]Liu et al., 2018; [26]Eisenhardt et al., 2015; [27]Tomanov et al., 2014; [28]Mendes et al., 2016; [29]Shin et al., 2012; [30]Schulz et al., 2012; [31]Hermkes et al., 2011; [32]Colby et al., 2006; [33]Cheng et al., 2006; [34]Murtas et al., 2003; [35]Liu et al., 2017; [36]Orosa et al., 2018; [37]Lois. 2010; [38]Morrell and Sadanandom. 2019; [39]Li and Hochstrasser. 1999; [40]Li and Hochstrasser. 2000; [41]Balakirev et al., 2015

E1-activating enzyme, SUMO, and E4 elongase

Except for some plant species, the E1 of most species gain activity after forming a heterodimer with two proteins (SAE1/AOS1-SAE2/UBA2) (Enserink. 2015; Gong et al., 1999; Lim et al., 2018). Among plants, *A. thaliana* and some *Brassicaceae* have two types of E1 heterodimer composed of three E1 subunits (SAE1a-SAE2 or SAE1b-SAE2) due to the duplication of SAE1 (Castaño-Miquel et al., 2013). SAE1a and SAE1b do not have fully redundant functions. Compared to SAE1b, the SAE1a has higher SUMO conjugation efficiency and higher thioester binding levels to SAE2-SUMO (Castaño-Miquel et al., 2013).

In *H. sapiens*, five SUMO isoforms are present. SUMO1 is related to mono-SUMOylation and the termination of poly-chain formation, while SUMO2, SUMO3, SUMO4, and SUMO5 are involved in poly-SUMOylation (Liang et al., 2016; Saitoh and Hinchey. 2000; Wang and she. 2008). In *A. thaliana*, SUM1 and SUM2 participate in poly-SUMOylation, but SUM3 has no motif for forming SUMO chains and the functions of other SUMO proteins are still undefined (Budhiraja et al., 2009; Colby et al., 2006; Kurepa et al., 2003). However, fungi have only one SUMO protein (Lim et al., 2018), it strongly supports that the type of SUMO involved in mono- and poly-SUMOylation appears to have increased with evolution.

In a recent study of human and plant, a new type of SUMOylation-associated component, E4 elongase, was discovered. E4 elongase is related to formation of poly-SUMO chains on substrates (Eisenhardt et al., 2015; Tomanov et al., 2014). In human, ZNF451 has dual functions with E3 ligase and E4 elongase activities, and

zinc-finger domain and SUMO-interacting motifs (SIMs) are essential for the activity of this enzyme (Eisenhardt et al., 2015). In *A. thaliana*, the SP-RING domain [containing a zinc finger MIZ-type (Zf-MIZ) domain; IPR004181] and SIM1 of PIAL1 and PIAL2 are important for E4 elongase activity. An E3 ligase of *A. thaliana*, SIZ1, also contains a Zf-MIZ domain. The function of SIZ1 overlaps with that of PIAL1 and PIAL2, but PIAL1 and PIAL2 are involved in chain extension not SUMO conjugation while SIZ1 is only involved in SUMO conjugation (Tomanov et al., 2014). In fungi, there is no E4 elongase, but E2-conjugating enzyme, UBC9, also acts as a factor for SUMO chain formation via non-covalent interaction (Klug et al., 2013). However, it is still unclear how poly-SUMO chains are assembled in fungi. In *H. sapiens*, SENP6 and SENP7 are involved in SUMO2/3 chain-specific editing (Nayak and Müller, 2014). In order to determine the function of poly-SUMOylation, proteomic research is ongoing in human such as by identifying targets of the chain-specific isopeptidase SENP6. The targets of SENP6, which are poly-SUMOylation substrates, are involved in DNA repair, cell cycle progression, and chromosome segregation (Keiten-Schmitz et al., 2019; Liebelt et al., 2019; Wagner et al., 2019). In addition, SENP7 is related to chromatin remodeling and dynamics (Garvin et al., 2013). Unlike ubiquitination, the functions according to the type of chain formed on K residues have not been studied in detail, but it is assumed that poly-SUMOylation is involved in the DNA-associated process (Liebelt et al., 2019).

II. Roles of SUMOylation in fungal pathogens

Mammal pathogenic fungi

Candida albcians, *Candida glabrata*, *Aspergillus nidulans* are the most medically important pathogenic fungi in mammals. *Candida* spp. and *A. nidulans* are representative yeast and filamentous form of opportunistic fungal pathogens that cause mucosal candidemia and pulmonary aspergillosis to immune deficiency patients, respectively (Grosset et al., 2016; Paulussen et al., 2017). In *C. albicans*, SUMOylation components including SMT3, AOS1, UBA2, UBC9, MMS21, and ULP2 are important for morphological change, cell differentiation, and sensitivity to DNA damage, cell wall, and thermal stresses, but not essential for viability (Islam *et al*., 2019; Leach *et al*., 2011). In addition, WOS1, an E3 ligase, regulates CO_2-induced switching from a white to purple cell formation (Yan *et al*., 2015). A total of 31 SUMOylated proteins have been identified in *C. albicans* and 373 genes are deferentially expressed in MMS21, an E3 ligase, deletion mutant (Islam *et al*., 2019; Leach *et al*., 2011). SUMOylated substrates of *C. albicans* are involved in stress response, cell cycle progression, cytoskeleton and polarized growth, microtubule, secretion, endocytosis, and nuclear pore complex (Leach *et al*., 2011; Islam *et al*., 2019). In *C. glabrata*, two E3 ligases (SIZ1 and SIZ2) and two proteases (ULP1 and ULP2) are predominantly nuclear localization but are also localized in cytosolic spots. SIZ2 and ULP2 are required for growth, DNA damage and oxidative stress tolerance, repression of pseudohyphal structure formation, and SUMOylation. In particular, Ulp2 is crucial for fungal virulence (Gujjula *et al*., 2016).

In *A. nidulans*, *SumO*, *AosA*, *UbaB*, *UbcN*, *SizA*, *UlpA*, and *UlpB* are important for growth, asexual and sexual reproduction, and responses to DNA damage, nutrient starvation, and temperature stresses but they are not essential for viability (Harting

et al., 2013; Wong *et al*., 2008). A total of 149 SUMOylated proteins have been identified in *A. nidulans*, most of the SUMOylated proteins are related to transcription regulation, RNA processing, DNA replication, DNA repair, and cell cycle progression (Horio et al., 2019). In addition, some SUMOylation and ubiquitination components have also been detected to be SUMO-modified (Harting et al., 2013; Horio et al., 2019).

Plant pathogenic fungi

The functions of SUMOylation components and profiling of SUMOylated proteins have been studied relatively recently in plant pathogenic fungi. *Magnaporthe oryzae* is the most of the critical phytopathogen that cause severe rice and wheat blast disease (Dean et al., 2012; Malaker et al., 2016). In *M. oryzae*, deletion mutants of SUMO (MoSMT3), two E1 enzymes (MoAOS1 and MoUBA2), one E2 enzyme (MoUBC9), one E3 enzyme (MoSIZ1) exhibited pleiotropic phenotypes, including defect of conidiation, septum formation, tolerance to stress, pathogenicity, and SUMOylation (Lim et al., 2018; Liu et al., 2018) (Table 2). In addition, SUMOylation of four septins is very essential for fungal virulence and arrangement of septins in appressoria and SUMOylation is associated with localization of effector proteins in *M. oryzae* (Liu et al., 2018). A total of 940 proteins related to translation, ribosome biogenesis, nutrient assimilation and utilization, and stress responses are predicted to be SUMOylated. In addition, a large number of SUMOylated proteins are involved in pathogenesis such as HSP70 family, ROS-scavenging enzymes, fatty acid and glycogen metabolism-, cell cycle-, and cell wall-related proteins (Liu et al., 2018). In *Aspergillus flavus*, SUMO is important for

growth, cell separation, stress sensitivities, asexual and sexual reproduction, aflatoxin production and pathogenicity, but it is not essential for viability (Nie *et al.*, 2016)

III. Roles of ubiquitination in *Magnaporthe oryzae*

Ubiquitination roles have been actively studied on plant pathogens including *M. oryzae* (Cai et al., 2020; Guo et al., 2015; Li et al., 2020; Lim and Lee. 2020; Oh et al., 2012; Prakash et al., 2016; Que et al., 2020; Shi et al., 2016; Shi et al., 2019; Wang et al., 2018; Yang et al., 2020). MGG_01282, ubiquitin component, is required for fungal development, N-starvation stress response, and pathogenicity (Oh et al., 2012). MoRAD6, E2-conjugating enzyme, is interacted with E3-ligase including MoBRE1, MoUBR1, and MoRAD18 and each interaction is involved in histone monoubiquitination, post-replication repair, and degradation of N-end rule substrate (Shi et al., 2016). SCF complex is the most well-known ubiquitin E3 ligase complex and is composed of SKP1, CUL1, and F-box proteins (FBXs). MoSKP1 is essential for viability and silencing strain has a defect in fungal development, conidiation, septum formation, response to cell wall integrity stress, and pathogenicity (Prakash et al., 2016). MoGRR1, FBXs with LRR motif, is important for fungal development, conidiation, stress response, sexual development, and pathogenicity (Guo et al., 2015; Shi et al., 2019). MoFBX15, F-box only protein, MoCDC4, and MoFWD1, FBXs with WD40 repeats are required for fungal development, conidiation, pathogenicity, and stress tolerance and F-box domain of these proteins are important for pleiotropic

defect (Lim and Lee. 2020; Shi et al., 2019). In addition, MoFWD1 is involved in the degradation of FRQ protein, circadian regulator, and induced activation of white color transcription factor (Shi et al., 2019). HECT E3 ligase, MoUPL3, is essential for forming penetration structure and pathogenicity (Li et al., 2020). Ubiquitin proteases have dual functions as deubiquitinating enzyme and isopeptidase, MoUBP1, MoUBP3, MoUBP4, MoUBP6, MoUBP8, MoUBP12, MoUBP13, MoUBP14, MoUBP15, and MoUBP16, deubiquitinating enzymes, are required for fungal development, pathogenicity, and deubiquitination (Cai et al., 2020; Que et al., 2020; Wang et al., 2018; Yang et al., 2020). MoCUE1, ER-associated degradation (ERAD) mechanism component, is required for fungal growth, conidiation, ER stress resistance, ubiquitination and SUMOylation level, cytoplasmic effector localization and translocation, and pathogenicity (Lim and Lee. 2020) (Table 2).

Table 2. Previous studies and functional roles of ubiquitination and SUMOylation-associated genes in *M. oryzae*

	Class	Locus number	Protein name	Phenotypes	Roles in biological function
Ubiquitination	Ub	MGG_01282[1]		Grow ↓ , Con ↓ , Germ ↓ , App ↓ , Patho ↓ [a]	Abnormal septum formation
	E2	MGG_01756[2]	MoRAD6	Grow ↓ , Con ↓ , Germ ↓ , App ↓ , Patho ↓	
	E3	MGG_04978[3]	MoSKP1	Grow ↓ , Con ↓ , Germ ↓ , App ↓ , Patho ↓	Abnormal septum formation
		MGG_13065[4,5]	MoGRR1	Grow ↓ , Con ↓ , App ↓ , Patho ↓	Sensitive to stress
		MGG_00139[2]	MoBRE1	Grow ↓ , Con ↓ , Germ ↓ , App ↓ , Patho ↓	
		MGG_13171[2]	MoUBR1	Grow ↓ , Con ↓ , Germ ↓ , App ↓ , Patho ↓	
		MGG_04175[2]	MoRAD18	Con ↑	
		MGG_08345[5]	MoCDC4	Grow ↓ , Con ↓ , Germ ↓ , App ↓ , Patho ↓	Abnormal septum formation
		MGG_09696[5]	MoFWD1	Grow ↓ , Con ↓ , Germ ↓ , App ↓ , Patho ↓	
		MGG_00768[5,6]	MoFBX15	Grow ↓ , Con ↓ , Germ ↓ , App ↓ , Patho ↓	Abnormal septum formation, Sensitive to stress
		MGG_03841[7]	MoUPL3	App ↓ , Patho ↓	Effector secretion
		MGG_01077[5]		-	
		MGG_06117[5]		-	
		MGG_07421[5]		-	
		MGG_07448[5]		-	
		MGG_08019[5]		-	
		MGG_09760[5]		-	
		MGG_11604[5]		-	
		MGG_13493[5]		-	
		MGG_13660[5]		-	
		MGG_15933[5]		-	

		MGG_16709[5]		-	
		MGG_06372[5]		-	
		MGG_00261[5]		-	
		MGG_10415[5]		-	
		MGG_09240[5]		-	
		MGG_13129[5]		-	
		MGG_06215[5]		-	
	Protease	MGG_04031[8]	MoUBP1	Grow ↓ , Con ↓ , App ↓ , Patho ↓	Abnormal septum formation, Sensitive to stress
		MGG_00877[8]	MoUBP2		Sensitive to stress
		MGG_05996[8]	MoUBP3	Grow ↓ , Con ↓ , App ↓ , Patho ↓	Abnormal septum formation, Sensitive to stress
		MGG_04957[8,9]	MoUBP4	Grow ↓ , Con ↓ , App ↓ , Patho ↓	Abnormal septum formation, Sensitive to stress
		MGG_02970[8]	MoUBP6	Con ↓ , Germ ↓ , App ↓ , Patho ↓	Sensitive to stress
		MGG_03527[8,10]	MoUBP8	Grow ↓ , Con ↓ , Germ ↓ , App ↓ , Patho ↓	Abnormal septum formation, Sensitive to stress
		MGG_05666[8]	MoUBP12	Con ↓ , App ↓ , Patho ↓	Sensitive to stress
		MGG_09907[8]	MoUBP13	Con ↓ , Patho ↓	
		MGG_08270[8,11]	MoUBP14	Grow ↓ , Con ↓ , Germ ↓ , App ↓ , Patho ↓	Abnormal septum formation, Sensitive to stress, Protein degradation
		MGG_05002[8]	MoUBP15	Patho ↓	
		MGG_04494[8]	MoUBP16	Con ↓ , App ↓	
	Other	MGG_12163[6]	MoCUE1	Grow ↓ , Con ↓ , Patho ↓	Sensitive to stress, Effector secretion
SUMOylation	SUMO	MGG_05737[12,13]	MoSMT3	Grow ↓ , Con ↓ , Germ ↓ , App ↓ , Patho ↓	Abnormal septum formation, Sensitive to stress, Effector secretion

E1	MGG_01669[12,13]	MoAOS1	Grow ↓ , Con ↓ , Germ ↓ , App ↓ , Patho ↓	Abnormal septum formation, Sensitive to stress
	MGG_06733[12,13]	MoUBA2	Grow ↓ , Con ↓ , Germ ↓ , App ↓ , Patho ↓	Abnormal septum formation, Sensitive to stress
E2	MGG_09970[12,13]	MoUBC9	Grow ↓ , Con ↓ , Germ ↓ , App ↓ , Patho ↓	Abnormal septum formation, Sensitive to stress
E3	MGG_08837[13]	MoSIZ1	Grow ↓ , Con ↓ , Germ ↓ , App ↓ , Patho ↓	Abnormal septum formation, Sensitive to stress

[a] Grow, Growth; Con, Conidiation; Germ, Conidial germination; App, Appressorium formation; Patho, Pathogenicity

[1]Oh et al., 2012; [2]Shi et al., 2016; [3]Prakash et al., 2016; [4]Guo et al., 2015; [5]Shi et al., 2019; [6]Lim and Lee. 2020; [7]Li et al., 2020; [8]Wang et al., 2018; [9]Que et al., 2020; [10]Yang et al., 2020; [11]Cai et al., 2020; [12]Lim et al., 2018; [13]Liu et al., 2018

IV. Crosstalk between SUMOylation and ubiquitination in fungi

Various PTMs, including phosphorylation, acetylation, methylation, ubiquitination, and SUMOylation, interact with each other (Duan and Walther. 2015). Chromatin condensation is related to quinary interactions between phosphorylation, acetylation, methylation, ubiquitination, and SUMOylation in histone proteins (Cheung et al., 2000; Krogan et al., 2003; Zhang and Reinberg. 2001). However, herein, I mainly focus on crosstalk between SUMOylation and ubiquitination. In human and plant, several studies have suggested that SUMOylation and ubiquitination are related (Cuijpers et al., 2017; Lamoliatte et al., 2017; McManus et al., 2017; Praefcke et al., 2012; Ulrich. 2008). The overexpression or loss of functions of SUMOylation- and ubiquitination-associated components are overlapped, except for protein degradation, which is a specific role of ubiquitination (Celen and Sahin. 2020; Garvin and Morris. 2017; Park et al., 2011; Zhang et al., 2015; Zhou and Zheng. 2017). In pathogenic fungi, unlike human and plant, the interaction between the SUMO and ubiquitin pathway is poorly understood, and the web that interconnects phenotypes of SUMOylation- and ubiquitination-associated components remain unclear (Figure 2). However, the possibility of crosstalk between the two pathways was studied in rice blast fungus. In *M. oryzae*, MoFBX15 and MoCUE1, ubiquitination-associated components, are related to induction of SUMOylation under heat stress condition and transcript expression of deSUMOylation proteases (Lim and Lee. 2020). In addition, ubiquitination-associated components such as MoUBA1 (E1) and MoUBR1 (E3) are SUMOylated

in *M. oryzae* (Liu et al., 2018). Several pieces of evidence for direct or indirect crosstalk between SUMO and ubiquitin in yeast are described in detail below.

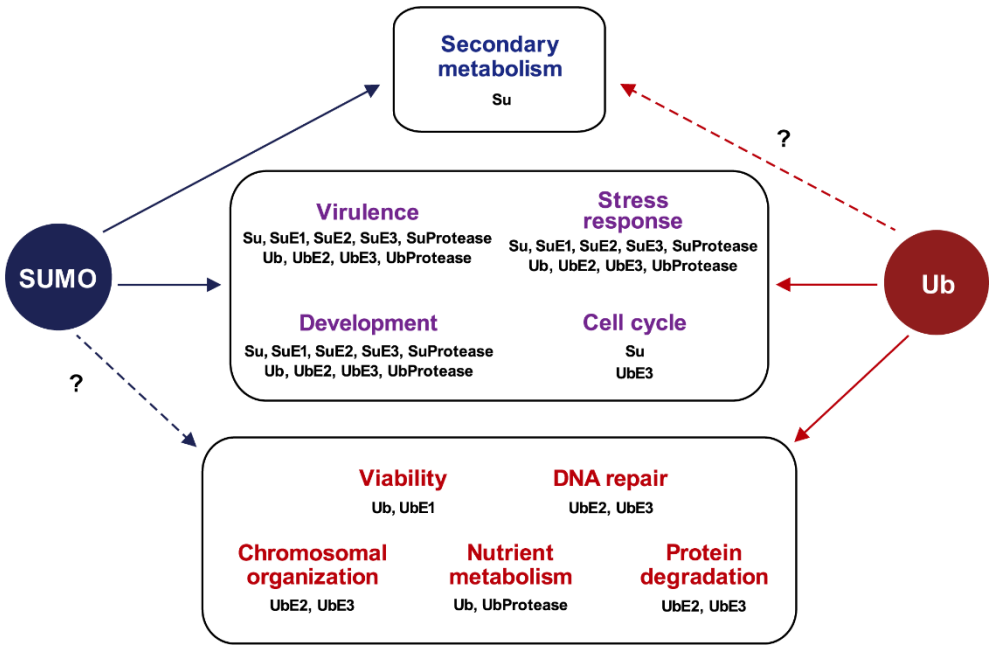

Figure 2. Phenotypes of SUMOylation- and ubiquitination-associated components in plant and mammal pathogenic fungi. The phenotypes are based on functional studies of the overexpression or loss of function of SUMOylation- and ubiquitination-associated components. The web of phenotypic crosstalk between SUMOylation and ubiquitination is still incompleted in fungal pathogens. Su, SUMO; SuE1, SUMO E1-activating enzyme; SuE2, SUMO E2-conjugating enzyme; SuE3, SUMO E3 ligase; SuProtease, SUMO Protease; Ub, ubiquitin; UbE1, Ubiquitin E1-activating enzyme; UbE2, Ubiquitin E2-conjugating enzyme; UbE3, Ubiquitin E3 ligase; UbProtease, Ubiquitin Protease

SUMO-targeted ubiquitin ligase (StUbL) and SUMO-ubiquitin hybrid chain specific receptors

Poly-SUMO chain gives rise to the SUMO-targeted ubiquitin ligase (StUbL) pathway (Mullen et al., 2008; Sriramachandran and Dohmen. 2014). SIMs of StUbL recognize poly-SUMO of SUMOylated substrates and add ubiquitin on the poly-SUMO chain or substrates (Wilson and Heaton, 2008). StUbL is important for cellular processes, including DNA repair, mitosis, and DNA replication, to retain genome stability (Nie et al., 2017). Yeast has four StUbLs, including SLX5-SLX8 heterodimer, ULS1/RIS1, and RAD18 (Sriramachandran and Dohmen. 2014). SLX5 recognizes SUMOylated CSE4, kinetochore protein, and proteolysis is induced to prevent mislocalization of CSE4, thereby maintaining genome stability (Ohkuni et al., 2016). ULS1 has dual functions, including SWI/SNF family ATPase and StUbL activities. ULS1 inhibits the accumulation of poly-SUMOylated RAP1 to prevent telomere-telomere fusion (Garza and Pillus. 2013). ULS1 interacts physically with SUMOylated YEN1, a nuclease that cleaves holiday junctions during homologous recombination. ULS1 plays an important role in DNA repair by genetically interacting with another holiday junction cleaving nuclease, MUS81 (Bauer et al., 2019). RAD18 is related to the ubiquitination of SUMOylated proliferating cell nuclear antigen (PCNA), a cofactor of DNA polymerase. In response to DNA damage, RAD18 controls DNA synthesis and repair process and is complexed with ubiquitin E2 to participate in the mono-ubiquitination of PCNA (Geng et al., 2010; Han et al., 2014; Hibbert et al., 2011). However, the RAD18 preference for SUMOylated substrates is not conserved in all species. Human RAD18, an ortholog of yeast RAD18, does not contain SIMs and does not act as StUbL (Parker and Ulrich.

2012).

WSS1, a SUMO-ubiquitin hybrid chain specific protease of yeast, has important roles not only as a SUMO isopeptidase but also in the deubiquitination of SUMO-ubiquitin hybrid chains (Balakirev et al., 2015; Mullen et al., 2010). In yeast, UFD1, a cofactor of CDC48 ATPase with NPI4, has an ubiquitin-interacting motif (UIM) and SIM. These two interaction motifs help to recognize the SUMO-ubiquitin hybrid chain and to organize the repair factors (Nie and Boddy. 2016; Sato et al., 2019).

SUMO and ubiquitin modification on the same substrates

PTMs, including SUMOylation, ubiquitination, acetylation, and methylation occur at K residues of proteins associated with the regulation of various biological processes (Li et al., 2018). PCNA, a DNA sliding clamp, is modified by SUMOylation and ubiquitination. SUMO is added at K127 and K164, but K164 of PCNA is a major SUMOylation and ubiquitination site (Papouli et al., 2005). Although modifiers are added to the same K residue of PCNA, the roles of PCNA are differ depending on the type of modifier (Gali *et al*., 2012; Northam and Trujillo. 2016; Zhang *et al*., 2011). SUMOylated PCNA is involved in the inhibition of homologous recombination during unperturbed S-phase and the recruitment and stabilization of anti-recombinogenic helicase SRS2. Ubiquitinated PCNA is involved in function of helicases, including RAD5 and MPH1 as well as fork regression (Gali *et al*., 2012; Northam and Trujillo. 2016; Zhang *et al*., 2011). Histone protein H2B is modified on different K residues by different two PTMs

(Trujillo *et al*., 2011). SUMOylation occurs on K6-7 and K16-17, but K6-7 residues are more important for the SUMOylation level in yeast. SUMOylated H2B is required for transcription suppression of the regulatory pathway genes *Gal1*, *Suc2*, and *Trp3* (Nathan et al., 2006). Ubiquitination at K123 of H2B functions in the restoration of chromatin, reassembly and stabilization of nucleosome, and replication fork progression (Chandrasekharan et al., 2009; Hung et al., 2017). Ubiquitination at K123 of H2B inhibits SUMOylation at K6-7 of H2B (Nathan et al., 2006). Proteasome participation in protein quality control is an important major function of ubiquitination (Tanaka. 2009). The proteasome is consisted of more than 45 subunits, some of which simultaneously have SUMOylation and ubiquitination sites (Cui et al., 2014). Ubiquitination at K71, K84, K99, and K268 of RPN10, a proteasome consisting subunit, inhibits interaction with other poly-ubiquitinated substrates by interrupting UIM in RPN10 and regulates the recruitment of modified substrates to the proteasome (Isasa et al., 2010). RPN10 is also SUMOylated, but its function is not yet understood (Cui et al., 2014).

PERSPECTIVE

This review summarized the latest research on how SUMOylation-associated components of fungi differ from those of mammals and plants as well as the roles of SUMOylation in fungal pathogens. Furthermore, I summarized studies of the interaction between SUMO and ubiquitin, a cousin of SUMO, that is not an independent pathway component with SUMO in fungi. SUMOylation is conserved and essential for transcriptional regulation, cell cycle, DNA maintenance, and chromatin assembly in eukaryotes (Alonso et al., 2015; Su et al., 2020). Particularly, SUMOylation is indispensable for virulence and environmental stress response in mammal and plant fungal pathogens (Lim et al., 2018; Sahu et al., 2020).

Two areas, poly-SUMOylation and crosstalk between SUMO and ubiquitin, are have not yet been explored in pathogenic fungi. In human and *A. thaliana*, E4 elongases that assemble the poly-SUMO chain have been discovered (Eisenhardt et al., 2015; Tomanov et al., 2014). In human, poly-SUMOylation is speculated to be involved in chromosome segregation, DNA repair, and cell cycle based on target proteins profiling and depletion experiment of poly-SUMO chain-specific isopeptidases (Liebelt et al., 2019). However, poly-SUMOylation is still requires further understanding in fungi. In case of ubiquitin, poly-ubiquitination has redundant roles with mono-ubiquitination, but mono-ubiquitination is more important for chromatin regulation, protein trafficking while poly-ubiquitination is more responsible for protein degradation and autophagy (Kocaturk and Gozuacik. 2018; Ze'ev. 2016). In line with these findings, the study of poly-SUMOylation will

contribute to our comprehensive understanding of the functional roles of SUMO-dependent regulatory pathway. Many PTMs, including phosphorylation, acetylation, methylation, ubiquitination, and SUMOylation, exhibit crosstalk with each other (Duan and Walther. 2015). Among fungi, the interactions between SUMO and ubiquitin have been extensively studied in yeast and the most representative interaction-associated component is StUbL. Some receptor proteins recognize SUMO-ubiquitin hybrid chain that is formed by StUbL (Mullen et al., 2008; Sriramachandran and Dohmen. 2014). In addition, as SUMO and ubiquitin both modify K residues of substrates, it is assumed that SUMO and ubiquitin are more likely to interact with each other than other PTMs (Li et al., 2018). Most SUMO and ubiquitin interaction-associated components and modified substrates are essential to cellular processes because they are involved in DNA repair and replication, chromosome stabilization and assembly, and host immunity (Nie et al., 2017; Zhang and Zeng. 2020). However, fewer studies have been conducted in pathogenic fungi; thus our knowledge of SUMO-ubiquitin interactions is less advanced than in mammals and plants. Mammalian and plant fungal pathogens are important because they regulate immunity and viability of the host during infection and colonization (Lim et al., 2018; Sahu et al., 2020). Therefore, it is essential to study how PTMs interactions in fungal pathogens affects not only the pathogens but also the host during host-microbe interaction.

LITERATURE CITED

Akimov, V., Barrio-Hernandez, I., Hansen, S. V., Hallenborg, P., Pedersen, A. K., Bekker-Jensen, D. B., Puglia, M., Christensen, S. D. K., Vanselow, J. T., Nielsen, M. M., Kratchmarova, I., Kelstrup, C. D., Olsen, J. V. and Blagoev, B. 2018. UbiSite approach for comprehensive mapping of lysine and N-terminal ubiquitination sites. Nat. Struct. Mol. Biol. 25:631-640.

Alonso, A., Greenlee, M., Matts, J., Kline, J., Davis, K. J. and Miller, R. K. 2015. Emerging roles of sumoylation in the regulation of actin, microtubules, intermediate filaments, and septins. Cytoskeleton. 72:305-339.

Augustine, R. C., York, S. L., Rytz, T. C. and Vierstra, R. D. 2016. Defining the SUMO system in maize: SUMOylation is up-regulated during endosperm development and rapidly induced by stress. Plant Physiol. 171:2191-2210.

Balakirev, M. Y., Mullally, J. E., Favier, A., Assard, N., Sulpice, E., Lindsey, D. F., Rulina, A. V., Gidrol, X. and Wilkinson, K. D. 2015. Wss1 metalloprotease partners with Cdc48/Doa1 in processing genotoxic SUMO conjugates. Elife, 4:e06763

Bauer, S. L., Chen, J. and Astrom, S. U. 2019. Helicase/SUMO-targeted ubiquitin ligase Uls1 interacts with the holliday junction resolvase Yen1. PLoS One. 14:e0214102.

Benlloch, R. and Lois, L. M. 2018. Sumoylation in plants: mechanistic insights and its role in drought stress. J. Exp. Bot. 69:4539-4554.

Bernier-Villamor, V., Sampson, D. A., Matunis, M. J. and Lima, C. D. 2002.

Structural basis for E2-mediated SUMO conjugation revealed by a complex between ubiquitin-conjugating enzyme Ubc9 and RanGAP1. Cell. 108:345-356.

Budhiraja, R., Hermkes, R., Müller, S., Schmidt, J., Colby, T., Panigrahi, K., Coupland, G. and Bachmair, A. 2009. Substrates related to chromatin and to RNA-dependent processes are modified by Arabidopsis SUMO isoforms that differ in a conserved residue with influence on desumoylation. Plant Physiol. 149:1529-1540.

Cai, X., Wang, Z., Hou, Y., Liu, C., Hendy, A., Xing, J. and Chen, X. L. 2020. Systematic characterization of the ubiquitin-specific proteases in *Magnaporthe oryzae*. Phytopathology. 2:1-12.

Castaño-Miquel, L., Seguí, J., Manrique, S., Teixeira, I., Carretero-Paulet, L., Atencio, F. and Lois, L. M. 2013. Diversification of SUMO-activating enzyme in Arabidopsis: implications in SUMO conjugation. Mol. Plant. 6:1646-1660.

Catala, R., Ouyang, J., Abreu, I. A., Hu, Y., Seo, H., Zhang, X., and Chua, N. H. 2007. The Arabidopsis E3 SUMO ligase SIZ1 regulates plant growth and drought responses. The Plant Cell. 19:2952-2966.

Celen, A. B. and Sahin, U. 2020. Sumoylation on its 25th anniversary: mechanisms, pathology, and emerging concepts. FEBS J. 287:3110-3140.

Chandrasekharan, M. B., Huang, F. and Sun, Z. W. 2009. Ubiquitination of histone H2B regulates chromatin dynamics by enhancing nucleosome stability. Proc. Natl. Acad. Sci. U.S.A. 106:16686-16691.

Cheng, C. H., Lo, Y. H., Liang, S. S., Ti, S. C., Lin, F. M., Yeh, C. H., Huang, H.-Y.

and Wang, T. F. 2006. SUMO modifications control assembly of synaptonemal complex and polycomplex in meiosis of *Saccharomyces cerevisiae*. Genes Dev. 20:2067-2081.

Cheung, P., Tanner, K. G., Cheung, W. L., Sassone-Corsi, P., Denu, J. M. and Allis, C. D. 2000. Synergistic coupling of histone H3 phosphorylation and acetylation in response to epidermal growth factor stimulation. Mol. Cell. 5:905-915.

Colby, T., Matthäi, A., Boeckelmann, A. and Stuible, H. P. 2006. SUMO-conjugating and SUMO-deconjugating enzymes from Arabidopsis. Plant Physiol. 142:318-332.

Colignon, B., Dieu, M., Demazy, C., Delaive, E., Muhovski, Y., Raes, M. and Mauro, S. 2017 Proteomic Study of SUMOylation During *Solanum tuberosum*-*Phytophthora infestans* Interactions. Mol. Plant Microbe Interact. 30:855-865.

Cuijpers, S. A., Willemstein, E. and Vertegaal, A. C. 2017. Converging small ubiquitin-like modifier (SUMO) and ubiquitin signaling: improved methodology identifies co-modified target proteins. Mol. Cell. Proteom. 16:2281-2295.

Cui, Z., Scruggs, S. B., Gilda, J. E., Ping, P. and Gomes, A. V. 2014. Regulation of cardiac proteasomes by ubiquitination, SUMOylation, and beyond. J. Mol. Cell. Cardiol, 71: 32-42.

Dean, R., Van Kan, J. A. L, Pretorius, Z. A., Hammond-Kosack, K. E., Di Pietro, A., Spanu, P. D., Rudd, J. J., Dickman, M., Kahmann, R., Ellis, J. and Foster, G. D. 2012. The Top 10 fungal pathogens in molecular plant pathology. Mol.

Plant Pathol. 13:414-430.

Dielen, A. S., Badaoui, S., Candresse, T. and German-Retana, S. 2010. The ubiquitin/26S proteasome system in plant–pathogen interactions: a never-ending hide-and-seek game. Mol. Plant Pathol. 11:293-308.

Duan, G. and Walther, D. 2015. The roles of post-translational modifications in the context of protein interaction networks. PLoS Comput. Biol. 11:e1004049.

Eisenhardt, N., Chaugule, V. K., Koidl, S., Droescher, M., Dogan, E., Rettich, J., Sutinen, P., Imanishi, S.Y., Hofmann, K., Palvimo, J, J. and Pichler, A. 2015. A new vertebrate SUMO enzyme family reveals insights into SUMO-chain assembly. Nat. Struct. Mol. Biol. 22:959-967.

Enserink, J. M. 2015. Sumo and the cellular stress response. Cell Div. 10:1-13.

Esteras, M., Liu, I. C., Snijders, A. P., Jarmuz, A. and Aragon, L. 2017. Identification of SUMO conjugation sites in the budding yeast proteome. Microb. Cell. 4:331-341.

Gali, H., Juhasz, S., Morocz, M., Hajdu, I., Fatyol, K., Szukacsov, V., Burkovics, P. and Haracska, L. 2012. Role of SUMO modification of human PCNA at stalled replication fork. Nucleic Acids Res. 40:6049-6059.

Garza, R., and Pillus, L. 2013. STUbLs in chromatin and genome stability. Biopolymers. 99:146-154.

Garvin, A. J., Densham, R. M., Blair-Reid, S. A., Pratt, K. M., Stone, H. R., Weekes, D., Lawrence, K. J. and Morris, J. R. 2013. The deSUMOylase SENP7 promotes chromatin relaxation for homologous recombination DNA repair. EMBO Rep. 14:975-983.

Garvin, A. J. and Morris, J. R. 2017. SUMO, a small, but powerful, regulator of

double-strand break repair. Philos. Trans. R. Soc. Lond., B, Biol. Sci. 372:20160281.

Geng, L., Huntoon, C. J. and Karnitz, L. M. 2010. RAD18-mediated ubiquitination of PCNA activates the fanconi anemia DNA repair network. J. Cell Biol. 191:249-257.

Gill, G. 2004. SUMO and ubiquitin in the nucleus: different functions, similar mechanisms? Genes Dev. 18:2046-2059.

Goldstein, G., Scheid, M., Hammerling, U., Schlesinger, D. H., Niall, H. D. and Boyse, E. A. 1975. Isolation of a polypeptide that has lymphocyte-differentiating properties and is probably represented universally in living cells. Proc. Natl. Acad. Sci. U.S.A. 72:11-15.

Gong, L., Li, B., Millas, S. and Yeh, E. T. 1999. Molecular cloning and characterization of human AOS1 and UBA2, components of the sentrin-activating enzyme complex. FEBS Lett. 448:185-189.

Grosset, M., Desnos-Ollivier, M., Godet, C., Kauffmann-Lacroix, C. and Cazenave-Roblot, F. 2016. Recurrent episodes of Candidemia due to *Candida glabrata*, *Candida tropicalis* and *Candida albicans* with acquired echinocandin resistance. Med. Mycol. Case Rep. 14:20-23.

Gujjula, R., Veeraiah, S., Kumar, K., Thakur, S. S., Mishra, K. and Kaur, R. 2016. Identification of components of the SUMOylation Machinery in *Candida glabrata*: role of deSUMOylation peptidase CgUlp2 in virulence. J. Biol. Chem. 291:19573-19589.

Guo, M., Gao, F., Zhu, X., Nie, X., Pan, Y. and Gao, Z. 2015. MoGrr1, a novel F-box protein, is involved in conidiogenesis and cell wall integrity and is

critical for the full virulence of *Magnaporthe oryzae*. Appl. Microbiol. Biotechnol. 99:8075-8088.

Han, J., Liu, T., Huen, M. S., Hu, L., Chen, Z. and Huang, J. 2014. SIVA1 directs the E3 ubiquitin ligase RAD18 for PCNA monoubiquitination. J. Cell. Biol. 205:811-827.

Harting, R., Bayram, O., Laubinger, K., Valerius, O. and Braus, G. H. 2013. Interplay of the fungal sumoylation network for control of multicellular development. Mol. Microbiol. 90:1125-1145.

He, Z., Huang, T., Ao, K., Yan, X. and Huang, Y. 2017. Sumoylation, phosphorylation, and acetylation fine-tune the turnover of plant immunity components mediated by ubiquitination. Front. Plant Sci. 8:1682.

Hermkes, R., Fu, Y. F., Nürrenberg, K., Budhiraja, R., Schmelzer, E., Elrouby, N., Dohmen, R. J., Bachmair, A. and Coupland, G. 2011. Distinct roles for Arabidopsis SUMO protease ESD4 and its closest homolog ELS1. Planta. 233:63-73.

Hibbert, R. G., Huang, A., Boelens, R. and Sixma, T. K. 2011. E3 ligase Rad18 promotes monoubiquitination rather than ubiquitin chain formation by E2 enzyme Rad6. Proc. Natl. Acad. Sci. U.S.A. 108:5590-5595.

Hoppe, T. 2005. Multiubiquitylation by E4 enzymes: 'one size' doesn't fit all. Trends Biochem. Sci. 30:183-187.

Horio, T., Szewczyk, E., Oakley, C. E., Osmani, A. H., Osmani, S. A. and Oakley, B. R. 2019. SUMOlock reveals a more complete *Aspergillus nidulans* SUMOylome. Fungal Genet. Biol. 127:50-59.

Hung, S. H., Wong, R. P., Ulrich, H. D. and Kao, C. F. 2017. Monoubiquitylation of

histone H2B contributes to the bypass of DNA damage during and after DNA replication. Proc. Natl. Acad. Sci. U.S.A. 114:E2205-E2214.

Isasa, M., Katz, E. J., Kim, W., Yugo, V., Gonzalez, S., Kirkpatrick, D. S., Thomson, T. M., Finley, D, Gygi, S. P. and Crosas, B. 2010. Monoubiquitination of RPN10 regulates substrate recruitment to the proteasome. Mol. Cell. 38:733-745.

Ishida, T., Yoshimura, M., Miura, K. and Sugimoto, K. 2012. MMS21/HPY2 and SIZ1, two Arabidopsis SUMO E3 ligases, have distinct functions in development. PloS ONE. 7: e46897.

Islam, A., Tebbji, F., Mallick, J., Regan, H., Dumeaux, V., Omran, R. P. and Whiteway, M. 2019. Mms21: a putative SUMO E3 ligase in Candida albicans that negatively regulates invasiveness and filamentation, and is required for the genotoxic and cellular stress response. Genetics. 211:579-595.

Johnson, E. S. and Blobel, G. 1997. Ubc9p is the conjugating enzyme for the ubiquitin-like protein Smt3p. J. Biol. Chem. 272:26799-26802.

Johnson, E. S. and Gupta, A. A. 2001. An E3-like factor that promotes SUMO conjugation to the yeast septins. Cell. 106:735-744.

Johnson, E. S., Schwienhorst, I., Dohmen, R. J. and Blobel, G. 1997. The ubiquitin-like protein Smt3p is activated for conjugation to other proteins by an Aos1p/Uba2p heterodimer. EMBO J. 16:5509-5519.

Kagey, M. H., Melhuish, T. A. and Wotton, D. 2003. The polycomb protein Pc2 is a SUMO E3. Cell. 113:127-137.

Keiten-Schmitz, J., Schunck, K. and Muller, S. 2019. SUMO chains rule on

chromatin occupancy. Front. Cell Dev. Biol, 7:343.

Kerscher, O., Felberbaum, R. and Hochstrasser, M. 2006. Modification of proteins by ubiquitin and ubiquitin-like proteins. Annu. Rev. Cell Dev. Biol, 22:159-180.

Klug, H., Xaver, M., Chaugule, V. K., Koidl, S., Mittler, G., Klein, F. and Pichler, A. 2013. Ubc9 sumoylation controls SUMO chain formation and meiotic synapsis in *Saccharomyces cerevisiae*. Mol. Cell. 50:625-636.

Kocaturk, N. M. and Gozuacik, D. 2018. Crosstalk between mammalian autophagy and the ubiquitin-proteasome system. Front. Cell Dev. Biol. 6:128.

Krogan, N. J., Dover, J., Wood, A., Schneider, J., Heidt, J., Boateng, M. A., Dean, K., Ryan, O. W., Golshani, A., Johnston, M., Greenblatt, J. F. and Shilatifard, A. 2003. The Paf1 complex is required for histone H3 methylation by COMPASS and Dot1p: linking transcriptional elongation to histone methylation. Mol. Cell. 11:721-729.

Kurepa, J., Walker, J. M., Smalle, J., Gosink, M. M., Davis, S. J., Durham, T. L., Sung, D.-Y. and Vierstra, R. D. 2003. The small ubiquitin-like modifier (SUMO) protein modification system in Arabidopsis accumulation of sumo1 and-2 conjugates is increased by stress. J. Biol. Chem. 278:6862-6872.

Lambrughi, M., Maiani, E., Aykac Fas, B., Shaw, G. S., Kragelund, B. B., Lindorff-Larsen, K., Teilum, K., Invernizzi, G. and Papaleo, E. 2021. Ubiquitin Interacting Motifs: duality between structured and disordered motifs. Front. Mol. Biosci. 8:494.

Lamoliatte, F., McManus, F. P., Maarifi, G., Chelbi-Alix, M. K. and Thibault, P. 2017. Uncovering the SUMOylation and ubiquitylation crosstalk in human cells

using sequential peptide immunopurification. Nat. Commun. 8:14109.

Leach, M. D. and Brown, A. J. 2012. Posttranslational modifications of proteins in the pathobiology of medically relevant fungi. Eukaryot. Cell. 11:98-108.

Leach, M. D., Stead, D. A., Argo, E. and Brown, A. J. 2011. Identification of sumoylation targets, combined with inactivation of SMT3, reveals the impact of sumoylation upon growth, morphology, and stress resistance in the pathogen *Candida albicans*. Mol. Biol. Cell. 22:687-702.

Li, G., Qi, X., Sun, G., Rocha, R. O., Segal, L. M., Downey, K. S., Wright, J. D. and Wilson, R. A. 2020. Terminating rice innate immunity induction requires a network of antagonistic and redox-responsive E3 ubiquitin ligases targeting a fungal sirtuin. New Phytol. 226: 523-540.

Li, G. X. H., Vogel, C. and Choi, H. 2018. PTMscape: an open source tool to predict generic post-translational modifications and map modification crosstalk in protein domains and biological processes. Mol. Omics. 14:197-209.

Li, S. J. and Hochstrasser, M. 1999. A new protease required for cell-cycle progression in yeast. Nature. 398:246-251.

Li, S. J. and Hochstrasser, M. 2000. The yeast ULP2 (SMT4) gene encodes a novel protease specific for the ubiquitin-like Smt3 protein. Mol. Cell. Biol. 20:2367-2377.

Li, W. and Ye, Y. 2008. Polyubiquitin chains: functions, structures, and mechanisms. Cell. Mol. Life Sci. 65:2397-2406.

Liang, Q., Deng, H., Li, X., Wu, X., Tang, Q., Chang, T. H., Peng, H., Rauscher III, F. J., Ozato, K. and Zhu, F. 2011. Tripartite motif-containing protein 28 is a small ubiquitin-related modifier E3 ligase and negative regulator of IFN

regulatory factor 7. J. Immunol. 187:4754-4763.

Liang, Y. C., Lee, C. C., Yao, Y. L., Lai, C. C., Schmitz, M. L. and Yang, W. M. 2016. SUMO5, a novel poly-SUMO isoform, regulates PML nuclear bodies. Sci. Rep. 6:1-15.

Liebelt, F., Jansen, N. S., Kumar, S., Gracheva, E., Claessens, L. A., Verlaan-de Vries, M., Willemstein, E. and Vertegaal, A. C. O. 2019. The poly-SUMO2/3 protease SENP6 enables assembly of the constitutive centromere-associated network by group deSUMOylation. Nat. Commun. 10:1-18

Lois, L. M. 2010. Diversity of the SUMOylation machinery in plants. Biochem. Soc. Trans. 38: 60-64.

Lim, Y.-J., Kim, K.-T. and Lee, Y.-H. 2018. SUMOylation is required for fungal development and pathogenicity in the rice blast fungus *Magnaporthe oryzae*. Mol. Plant Pathol. 19: 2134-2148.

Lim, Y. -J. and Lee, Y. -H. 2020. F-box only and CUE proteins are crucial ubiquitination-associated components for conidiation and pathogenicity in the rice blast fungus, *Magnaporthe oryzae*. Fungal Genet. Biol. 144:103473.

Liu, C., Li, Z., Xing, J., Yang, J., Wang, Z., Zhang, H., Chen, D., Peng, Y. –L. and Chen, X. -L. 2018. Global analysis of sumoylation function reveals novel insights into development and appressorium-mediated infection of the rice blast fungus. New Phytol. 219:1031-1047.

Liu, L., Jiang, Y., Zhang, X., Wang, X., Wang, Y., Han, Y., Coupland, G., Jin, J. B., Searle, I., Fu, Y. –F. and Chen, F. 2017. Two SUMO proteases SUMO PROTEASE RELATED TO FERTILITY1 and 2 are required for fertility in Arabidopsis. Plant Physiol. 175:1703-1719.

Malaker, P. K., Barma, N. C., Tiwary, T. P., Collis, W. J., Duveiller, E. P., Singh, K., Joshi, A. K., Singh, R. P., Braun, H.-J., Peterson, G. L., Pedley, K. F., Farman, M. L. and Valent, B. 2016. First report of wheat blast caused by *Magnaporthe oryzae* pathotype *triticum* in Bangladesh. Plant Dis. 100:2330.

Matic, I., van Hagen, M., Schimmel, J., Macek, B., Ogg, S. C., Tatham, M. H., Hay, R. T., Lamond, A. I., Mann, M. and Vertegaal, A. C. O. 2008. In vivo identification of human small ubiquitin-like modifier polymerization sites by high accuracy mass spectrometry and an in vitro to in vivo strategy. Mol. Cell. Proteom. 7:132-144.

McManus, F. P., Lamoliatte, F. and Thibault, P. 2017. Identification of cross talk between SUMOylation and ubiquitylation using a sequential peptide immunopurification approach. Nat. Protoc. 12:2342-2358.

Meluh, P. B. and Koshland, D. 1995. Evidence that the MIF2 gene of *Saccharomyces cerevisiae* encodes a centromere protein with homology to the mammalian centromere protein CENP-C. Mol. Biol. Cell. 6:793-807.

Mendes, A. V., Grou, C. P., Azevedo, J. E. and Pinto, M. P. 2016. Evaluation of the activity and substrate specificity of the human SENP family of SUMO proteases. Biochim. Biophys. Acta Mol. Cell Res. 1863:139-147.

Morrell, R. and Sadanandom, A. 2019. Dealing with stress: a review of plant SUMO proteases. Front. Plant Sci. 10:1122.

Mullen, J. R. and Brill, S. J. 2008. Activation of the Slx5–Slx8 ubiquitin ligase by poly-small ubiquitin-like modifier conjugates. J. Biol. Chem. 283:19912-19921.

Mullen, J. R., Chen, C. F. and Brill, S. J. 2010. Wss1 is a SUMO-dependent

isopeptidase that interacts genetically with the Slx5-Slx8 SUMO-targeted ubiquitin ligase. Mol. Cell. Biol. 30:3737-3748.

Murtas, G., Reeves, P. H., Fu, Y. F., Bancroft, I., Dean, C. and Coupland, G. 2003. A nuclear protease required for flowering-time regulation in Arabidopsis reduces the abundance of SMALL UBIQUITIN-RELATED MODIFIER conjugates. The Plant Cell. 15:2308-2319.

Nathan, D., Ingvarsdottir, K., Sterner, D. E., Bylebyl, G. R., Dokmanovic, M., Dorsey, J. A., Whelan, K. A., Krsmanovic, M., Lane, W. S., Meluh, P. B., Johnson, E. S. and Berger, S. L. 2006. Histone sumoylation is a negative regulator in *Saccharomyces cerevisiae* and shows dynamic interplay with positive-acting histone modifications. Genes Dev. 20:966-976.

Nayak, A. and Müller, S. 2014. SUMO-specific proteases/isopeptidases: SENPs and beyond. Genome Biol. 15:1-7.

Nie, M. and Boddy, M. N. 2016. Cooperativity of the SUMO and ubiquitin pathways in genome stability. Biomolecules, 6:14.

Nie, M., Moser, B. A., Nakamura, T. M. and Boddy, M. N. 2017. SUMO-targeted ubiquitin ligase activity can either suppress or promote genome instability, depending on the nature of the DNA lesion. PLoS Genet. 13:e1006776.

Nie, X., Yu, S., Qiu, M., Wang, X., Wang, Y., Bai, Y., Zhang, F. and Wang, S. 2016. *Aspergillus flavus* SUMO contributes to fungal virulence and toxin attributes. J. Agric. Food Chem. 64:6772-6782.

Northam, M. R. and Trujillo, K. M. 2016. Histone H2B mono-ubiquitylation maintains genomic integrity at stalled replication forks. Nucleic Acids Res. 44:9245-9255.

Oh, Y., Franck, W. L., Han, S. O., Shows, A., Gokce, E., Muddiman, D. C. and Dean, R. A. 2012. Polyubiquitin is required for growth, development and pathogenicity in the rice blast fungus *Magnaporthe oryzae*. PLoS One. 7:e42868.

Ohkuni, K., Takahashi, Y., Fulp, A., Lawrimore, J., Au, W. C., Pasupala, N., Levy-Myers, R., Warren, J., Strunnikov, A., Baker, R. E., Kerscher, O., Bloom, K. and Basrai, M. A. 2016. SUMO-targeted ubiquitin ligase (STUbL) Slx5 regulates proteolysis of centromeric histone H3 variant Cse4 and prevents its mislocalization to euchromatin. Mol. Biol. Cell. 27:1500-1510.

Orosa, B., Yates, G., Verma, V., Srivastava, A. K., Srivastava, M., Campanaro, A., Vega, D. D., Fernandes, A., Zhang, C., Lee, J., Bennett, M. J. and Sadanandom, A. 2018. SUMO conjugation to the pattern recognition receptor FLS2 triggers intracellular signalling in plant innate immunity. Nat. Commun. 9:1-12.

Papouli, E., Chen, S., Davies, A. A., Huttner, D., Krejci, L., Sung, P. and Ulrich, H. D. 2005. Crosstalk between SUMO and ubiquitin on PCNA is mediated by recruitment of the helicase Srs2p. Mol. Cell. 19:123-133.

Park, H. J., Kim, W. Y., Park, H. C., Lee, S. Y., Bohnert, H. J. and Yun, D. J. 2011. SUMO and SUMOylation in plants. Mol. Cells. 32:305.

Parker, J. L. and Ulrich, H. D. 2012. A SUMO-interacting motif activates budding yeast ubiquitin ligase Rad18 towards SUMO-modified PCNA. Nucleic Acids Res. 40:11380-11388.

Paulussen, C., Hallsworth, J. E., Alvarez-Perez, S., Nierman, W. C., Hamill, P. G., Blain, D., Rediers, H. and Lievens, B. 2017. Ecology of aspergillosis:

insights into the pathogenic potency of *Aspergillus fumigatus* and some other *Aspergillus* species. Microb. Biotechnol. 10:296-322.

Praefcke, G. J., Hofmann, K. and Dohmen, R. J. 2012. SUMO playing tag with ubiquitin. Trends Biochem. Sci. 37:23-31.

Prakash, C., Manjrekar, J. and Chattoo, B. B. 2016. Skp1, a component of E3 ubiquitin ligase, is necessary for growth, sporulation, development and pathogenicity in rice blast fungus (*Magnaporthe oryzae*). Mol. Plant Pathol. 17:903-919.

Que, Y., Xu, Z., Wang, C., Lv, W., Yue, X., Xu, L., Tang, S., Dai, H. and Wang, Z. 2020. The putative deubiquitinating enzyme MoUbp4 is required for infection-related morphogenesis and pathogenicity in the rice blast fungus *Magnaporthe oryzae*. Curr. Genet. 66, 561-576.

Sahu, M. S., Patra, S., Kumar, K. and Kaur, R. 2020. SUMOylation in Human Pathogenic Fungi: Role in Physiology and Virulence. J. Fungi. 6:32.

Saitoh, H. and Hinchey, J. 2000. Functional heterogeneity of small ubiquitin-related protein modifiers SUMO-1 versus SUMO-2/3. J. Biol. Chem. 275:6252-6258.

Saracco, S. A., Miller, M. J., Kurepa, J. and Vierstra, R. D. 2007. Genetic analysis of SUMOylation in Arabidopsis: conjugation of SUMO1 and SUMO2 to nuclear proteins is essential. Plant Physiol. 145:119-134.

Sato, Y., Tsuchiya, H., Yamagata, A., Okatsu, K., Tanaka, K., Saeki, Y. and Fukai, S. 2019. Structural insights into ubiquitin recognition and Ufd1 interaction of Npl4. Nat. Commun. 10:1-13.

Schmidt, D. and Müller, S. 2002. Members of the PIAS family act as SUMO ligases

for c-Jun and p53 and repress p53 activity. Proc. Natl. Acad. Sci. U.S.A. 99:2872-2877.

Schulz, S., Chachami, G., Kozaczkiewicz, L., Winter, U., Stankovic-Valentin, N., Haas, P., Hofmann, K., Urlaub, H., Ovaa, H., Wittbrodt, J., Meulmeester, E. and Melchior, F. 2012. Ubiquitin-specific protease-like 1 (USPL1) is a SUMO isopeptidase with essential, non-catalytic functions. EMBO Rep. 13:930-938.

Seufert, W., Futcher, B. and Jentsch, S. 1995. Role of a ubiquitin-conjugating enzyme in degradation of S-and M-phase cyclins. Nature. 373:78-81.

Shi, H. B., Chen, G. Q., Chen, Y. P., Dong, B., Lu, J. P., Liu, X. H. and Lin, F. C. 2016. MoRad6-mediated ubiquitination pathways are essential for development and pathogenicity in *Magnaporthe oryzae*. Environ. Miicrobiol. 18:4170-4187.

Shi, H. B., Chen, N., Zhu, X. M., Liang, S., Li, L., Wang, J. Y., Lu, J. P., Lin, F. C. and Liu, X. H. 2019. F-box proteins MoFwd1, MoCdc4 and MoFbx15 regulate development and pathogenicity in the rice blast fungus *Magnaporthe oryzae*. Environ. Microbiol. 21:3027-3045.

Shin, E. J., Shin, H. M., Nam, E., Kim, W. S., Kim, J. -H., Oh, B. -H. and Yun, Y. 2012. DeSUMOylating isopeptidase: a second class of SUMO protease. EMBO Rep. 13:339-346.

Sriramachandran, A. M. and Dohmen, R. J. 2014. SUMO-targeted ubiquitin ligases. Biochim. Biophys. Acta Mol. Cell Res. 1843:75-85.

Su, S., Zhang, Y. and Liu, P. 2020. Roles of Ubiquitination and SUMOylation in DNA Damage Response. Curr. Issues Mol. Biol. 35:59-84.

Takahashi, Y., Kahyo, T., Toh-e, A., Yasuda, H. and Kikuchi, Y. 2001. Yeast Ull1/Siz1 is a novel SUMO1/Smt3 ligase for septin components and functions as an adaptor between conjugating enzyme and substrates. J. Biol. Chem. 276:48973-48977.

Tanaka, K. 2009. The proteasome: overview of structure and functions. Proc. Jpn. Acad., Ser. B. 85:12-36.

Tatham, M. H., Kim, S., Jaffray, E., Song, J., Chen, Y. and Hay, R. T. 2005. Unique binding interactions among Ubc9, SUMO and RanBP2 reveal a mechanism for SUMO paralog selection. Nature Struct. Mol. Biol. 12:67-74.

Tomanov, K., Zeschmann, A., Hermkes, R., Eifler, K., Ziba, I., Grieco, M., Novatchkova, M., Hofmann, K., Hesse, H. and Bachmair, A. 2014. Arabidopsis PIAL1 and 2 promote SUMO chain formation as E4-type SUMO ligases and are involved in stress responses and sulfur metabolism. Plant Cell. 26:4547-4560.

Trujillo, K. M., Tyler, R. K., Ye, C., Berger, S. L. and Osley, M. A. 2011. A genetic and molecular toolbox for analyzing histone ubiquitylation and sumoylation in yeast. Methods, 54:296-303.

Ulrich, H. D. 2008. The fast-growing business of SUMO chains. Mol. Cell. 32:301-305.

Verma, V., Croley, F. and Sadanandom, A. 2018. Fifty shades of SUMO: its role in immunity and at the fulcrum of the growth-defence balance. Mol. Plant Pathol. 19:1537-1544.

Wagner, K., Kunz, K., Piller, T., Tascher, G., Holper, S., Stehmeier, P., Keiten-Schmitz, J., Schick, M., Keller, U. and Müller, S. 2019. The SUMO

isopeptidase SENP6 functions as a rheostat of chromatin residency in genome maintenance and chromosome dynamics. Cell Rep. 29:480-494.

Wang, C. Y. and She, J. X. 2008. SUMO4 and its role in type 1 diabetes pathogenesis. Diabetes/Metab. Res. Rev. 24:93-102.

Wang, Z., Zhang, H., Liu, C., Xing, J. and Chen, X. L. 2018. A deubiquitinating enzyme Ubp14 is required for development, stress response, nutrient utilization, and pathogenesis of *Magnaporthe oryzae*. Front. Microbiol. 9: 769.

Wilson, V. G. and Heaton, P. R. 2008. Ubiquitin proteolytic system: focus on SUMO. Expert Rev. Proteom. 5:121-135.

Wong, K. H., Todd, R. B., Oakley, B. R., Oakley, C. E., Hynes, M. J. and Davis, M. A. 2008. Sumoylation in *Aspergillus nidulans*: sumO inactivation, overexpression and live-cell imaging. Fungal Genet. Biol. 45:728-737.

Yan, M., Nie, X., Wang, H., Gao, N., Liu, H. and Chen, J. 2015. SUMOylation of Wor1 by a novel SUMO E3 ligase controls cell fate in *Candida albicans*. Mol. Microbiol. 98:69-89.

Yang, J., Chen, D., Matar, K. A. O., Zheng, T., Zhao, Q., Xie, Y., Gao, X., Li, M., Wang, B. and Lu, G. D. 2020. The deubiquitinating enzyme MoUbp8 is required for infection-related development, pathogenicity, and carbon catabolite repression in *Magnaporthe oryzae*. Appl. Microbiol. Biotechnol. 104:5081-5094.

Yang, Y., He, Y., Wang, X., Liang, Z., He, G., Zhang, P., Zhu, H., Xu, N. and Liang, S. 2017. Protein SUMOylation modification and its associations with disease. Open Biol. 7: 170167.

Ze'ev, A. R. 2016. Monoubiquitination in proteasomal degradation. Proc. Natl. Acad. Sci. U.S.A. 113:8894-8896.

Zhao, J. 2007. Sumoylation regulates diverse biological processes. Cell Mol. Life Sci. 64:3017-3033.

Zhao, X., Sternsdorf, T., Bolger, T. A., Evans, R. M. and Yao, T. P. 2005. Regulation of MEF2 by histone deacetylase 4-and SIRT1 deacetylase-mediated lysine modifications. Mol. Cell. Biol. 25:8456-8464.

Zhang, W., Qin, Z., Zhang, X. and Xiao, W. 2011. Roles of sequential ubiquitination of PCNA in DNA-damage tolerance. FEBS Lett. 585:2786-2794.

Zhang, Y. and Reinberg, D. 2001. Transcription regulation by histone methylation: interplay between different covalent modifications of the core histone tails. Genes Dev. 15:2343-2360.

Zhang, Z., Li, J., Liu, H., Chong, K. and Xu, Y. 2015. Roles of ubiquitination-mediated protein degradation in plant responses to abiotic stresses. Environ. Exp. Bot. 114:92-103.

Zhang, Y. and Zeng, L. 2020. Crosstalk between ubiquitination and other posttranslational protein modifications in plant immunity. Plant Communications, 1:100041.

Zhou, B. and Zeng, L. 2017. Conventional and unconventional ubiquitination in plant immunity. Mol. Plant Pathol. 18:1313-1330.

CHAPTER II

SUMOylation is required for fungal development and pathogenicity in the rice blast fungus, *Magnaporthe oryzae*

This chapter was published in Molecular Plant Pathology.

Lim, Y-J. et al. (2018) *Mol. Plant Pathol.* 19:9.

ABSTRACT

Among the various post-translational modifications (PTMs), SUMOylation is a conserved process of attaching small ubiquitin-related modifier (SUMO) to protein substrate in eukaryotes. This process regulates many important biological mechanisms including transcriptional regulation, protein stabilization, cell cycle, DNA repair, and pathogenesis. However, the functional role of SUMOylation is not well understood in plant pathogenic fungi including the model fungal pathogen, *Magnaporthe oryzae*. In this study, we elucidated the roles of four SUMOylation-associated genes that encode one SUMO protein (MoSMT3), two E1 enzymes (MoAOS1 and MoUBA2), and one E2 enzyme (MoUBC9) in fungal development and pathogenicity. Western blot assays showed that SUMO modification was abolished in all deletion mutants. MoAOS1 and MoUBA2 mainly localized in the nucleus, whereas MoSMT3 and MoUBC9 localized in both the nucleus and cytoplasm. However, the four SUMOylation-associated proteins predominantly localized in the nucleus under oxidative stress condition. Deletion mutants for each of the four genes were viable, but showed significant defects in mycelial growth, conidiation, septum formation, conidial germination, appressorium formation, and pathogenicity. Several proteins responsible for conidiation were predicted to be SUMOylated, suggesting that conidiation is controlled at the post-translational level by SUMOylation. In addition to infection-related development, SUMOylation also played important roles in resistance to nutrient starvation, DNA damage, and oxidative stresses. Therefore, SUMOylation is required for infection-related fungal

development, stress responses, and pathogenicity in *M. oryzae*. This study provides new insight into the role of SUMOylation in the molecular mechanisms of pathogenesis of the rice blast fungus and other plant pathogens.

INTRODUCTION

Post-translational modifications (PTMs) regulate diverse biological processes by attaching specific proteins or functional groups to various substrates (Gill, 2004). PTMs include diverse protein modifying processes that are widely conserved in eukaryotic organisms (Watts, 2013). In fungal plant pathogens, the most comprehensively studied PTM is phosphorylation, which is essential for appressorium formation (Dean, 1997; Flaishman *et al.*, 1995; Kang *et al.*, 1999). Methylation in fungi has also been studied as post-translational epigenetic modifications (Jeon *et al.*, 2015; Martienssen and Colot, 2001). Ubiquitination is a major mechanism of protein degradation in eukaryotic organisms (Liu and Xue, 2011) and has been actively studied in various fungi, including plant pathogens (Guo *et al.*, 2015; Oh *et al.*, 2012; Prakash *et al.*, 2016). In contrast, in depth studies of SUMOylation, which has components different from those of ubiquitination, are limited to the model fungus *Saccharomyces cerevisiae* and human fungal pathogens (Denison *et al.*, 2005; Leach *et al.*, 2011; Park *et al.*, 2011).

SUMOylation attaches small ubiquitin-related modifier (SUMO) to substrate proteins. This process has several important biological roles, including in transcriptional regulation, protein localization and stability, cell cycle, DNA repair, and stress resistance (Alonso *et al.*, 2015; Johnson and Blobel, 1999; Lomeli and Vazquez, 2011). The main components of SUMOylation other than SUMO are SUMO-activating enzymes (E1), SUMO-conjugating enzyme (E2), SUMO ligases (E3), and SUMO proteases. In the SUMOylation process, the SUMO precursor is

cleaved by SUMO protease (hydrolase) to reveal the diglycine motif at its C-terminal end and become a mature form (Hickey *et al.*, 2012). SUMO is then activated by formation of a thioester bond between a cysteine residue of E1 and a glycine residue of SUMO. SUMO is transferred from E1 to a cysteine residue of E2 by a thioester bond (Desterro *et al.*, 1999; Johnson and Blobel, 1997). E3 facilitates formation of an isopeptide bond between a glycine residue of SUMO and lysine residues of the consensus motif ΨKXE/D (Ψ and X represent a hydrophobic amino acid and any amino acid, respectively) or a non-consensus motif on the substrate (Tatham *et al.*, 2001). This isopeptide bond is cleaved by SUMO protease (isopeptidase) (Hickey *et al*., 2012). SUMO is then recycled for use in SUMOylation (Dohmen, 2004; Lomeli and Vazquez, 2011; Sriramachandran and Dohmen, 2014). This process is similar to ubiquitination, but E1 acts as a heterodimer and E3 is not essential for attaching SUMO to substrates (Gill, 2004; Müller *et al.*, 2001; Saracco *et al.*, 2007).

SUMOylation regulates the inflammatory response in mammals, flowering time and resistance to abiotic stress in plants, and sporulation and virulence in fungi (Dohmen, 2004; Gujjula *et al.*, 2016; Harting *et al.*, 2013; Leach *et al*., 2011; Raorane *et al.*, 2013; Wong *et al.*, 2008). In *S. cerevisiae*, SMT3 plays a role as SUMO; AOS1 and UBA2 for E1 SUMO-activating enzymes; UBC9 for E2 SUMO-conjugating enzyme; SIZ1, SIZ2, CST9, and MMS21 for E3 SUMO ligases; and ULP1, ULP2, and WSS1 for SUMO proteases (Mullen *et al.*, 2010; Pasupala *et al.*, 2012). Among the SUMOylation components, SMT3, AOS1, UBA2, UBC9, MMS21, and ULP1 are essential for viability (Johnson and Blobel, 1999). However, in other fungal species, such as *Schizosaccharomyces pombe*, *Aspergillus nidulans*, *A. flavus* and *Candida albicans,* SUMO is not essential for viability (Leach *et al*.,

2011; Nie *et al.*, 2016; Tanaka *et al*., 1999; Wong *et al*., 2008). Despite these functional studies, the functional roles of the SUMOylation pathway in plant pathogenic fungi are unclear.

Magnaporthe oryzae is an ascomycete plant pathogen that causes rice blast disease, which is associated with a considerable socioeconomic burden (Kim *et al.*, 2009). *M. oryzae* is an important model organism for studying plant-fungal pathogen interactions because the host and fungal genomes have been sequenced and their genomes are now applicable to molecular biological studies (Dean *et al.*, 2005; Goff *et al*., 2002; Valent, 1990). The disease cycle starts when a conidium (asexual spore) attaches to a hydrophobic surface of the host plant, and germinates and forms an appressorium, a specialized infection structure, from the tip of the germ tube. The appressorium penetrates the host surface by exerting a pressure of > 8 MPa (Ebbole, 2007). After colonizing the host plant, secondary inoculum is produced by conidiogenesis (Goh *et al.*, 2011). The secondary inoculum is a key factor for epidemics as *M. oryzae* is a polycyclic pathogen (Kim *et al*., 2009). A better understanding of SUMOylation in the rice blast fungus will provide new insights into infection-related fungal development.

In this study, we identified the components of SUMOylation among ubiquitin-like modifiers (UBLs) by phylogenetic analysis and determined their functions in *M. oryzae*. The SUMOylation machinery was conserved in diverse fungal phyla. Deletion of the four genes encoding SUMO, two E1, and E2 enzymes exhibited pleiotropic phenotypes including conidiation, septum formation, sensitivity to stress, and pathogenicity. Further analysis indicated that infection-related fungal development and pathogenicity was regulated by SUMOylation. This study will

improve our understanding of SUMOylation in the rice blast pathogen and other plant pathogenic fungi.

MATERIALS AND METHODS

I. Identification of SUMOylation machinery in fungi

SUMOylation components in fungi and model organisms were identified by whole protein BLAST search of the *S. cerevisiae* SUMO (SMT3), E1 (AOS1 and UBA2), E2 (UBC9), E3 (SIZ1, SIZ2, MMS21 and CST9), and SUMO-protease (ULP1, ULP2, and WSS1) sequences using an e-value of $1e^{-5}$. The fungal proteome datasets used were Fungal Genome Gold Standard from CFGP 2.0 (Choi *et al.*, 2013), the model organisms were from Ensembl (Aken *et al.*, 2016), and the *S. cerevisiae* query proteins were from SGD (Cherry, 2015). A domain analysis was performed using InterProScan-5.25-64.0 software to eliminate sequences without characterized domains. The domain sequences were retrieved and aligned by MAFFT software (Katoh and Standley, 2013) and sparsely aligned regions were trimmed using trimAl software (Capella-Gutierrez *et al.*, 2009). For phylogenetic analysis, the best protein evolution model for each component alignment was determined and phylogenetic trees were constructed using RAxML v8.2 software with 1,000 bootstraps (Stamatakis, 2014).

II. Targeted gene deletion and complementation

M. oryzae KJ201 (wild type) was obtained from the Center for Fungal Genetic Resources (CFGR) at Seoul National University, Seoul, Korea (Table 1). Protoplasts were generated from mycelia grown in liquid complete medium (CM) at 25°C for 3

d. The upstream (1.0–1.5 kb) and downstream (1.0–1.5 kb) flanking regions of each SUMOylation-associated gene (*MoSMT3*, *MoAos1*, *MoUba2*, and *MoUbc9*) were amplified from the genomic DNA (gDNA) of the wild type (Table 2). The 1.4-kb hygromycin B phosphotransferase gene (HPH) cassette was amplified from pBCATPH (Yun, 1998). Constructs were produced by double-joint PCR using these three amplicons (upstream flanking, downstream flanking, and HPH cassette) for targeted gene deletion. Targeted gene deletion mutants were generated by transforming the constructs into protoplasts using PEG. The targeted gene deletion mutants were selected on TB3 agar supplemented with 200 ppm hygromycin B, and screened by PCR analysis of mycelia using the ORF primers. To generate the double gene deletion mutant, a 1.2 kb geneticin resistance cassette was amplified from pII99 (Lee *et al*., 2003), and transformed into Δ*Moaos1* protoplasts. To produce complementation strains, constructs containing each ORF and promoter were amplified using upstream forward and downstream reverse primers for the gDNA of the wild type. The complemented strains were generated by co-transforming these constructs and a geneticin cassette into protoplasts of the single gene deletion mutants. The complemented strains were selected on TB3 agar supplemented with 800 ppm geneticin, and screened by PCR of mycelia using the ORF primers. All strains used in this study have been deposited in the Center for Fungal Genetic Resources (http://genebank.snu.ac.kr) at Seoul National University, Korea.

Table 1. List of strains used in this study

Strain	Description	Source
KJ201	*M. oryzae*, wild type strain	CFGR
Δ*Mosmt3*	*M. oryzae*, *SMT3* deletion mutant	This study
*Mosmt3*c	*M. oryzae*, genetic complementation strain of the Δ*Mosmt3*	This study
Δ*Moaos1*	*M. oryzae*, *AOS1* deletion mutant	This study
Moaos1c	*M. oryzae*, genetic complementation strain of the Δ*Moaos1*	This study
Δ*Mouba2*	*M. oryzae*, *UBA2* deletion mutant	This study
*Mouba2*c	*M. oryzae*, genetic complementation strain of the Δ*Mouba2*	This study
Δ*Moaos1*Δ*Mouba2*	*M. oryzae*, *UBA2* deletion mutant of the Δ*Moaos1*	This study
Δ*Moubc9*	*M. oryzae*, *UBC9* deletion mutant	This study
*Moubc9*c	*M. oryzae*, genetic complementation strain of the Δ*Moubc9*	This study
Mav203	Two hybrid yeast strain (MATα, *leu*2-3,112, *trp*1-901, *his*3Δ200, *ade*2-101, *gal*4Δ, *gal*80Δ, *SPAL*10*::URA*3, *GAL*1::*lacZ*, *HIS*3UAS GAL1*::HIS*3*@LYS* 2, *can*1R, *cyh*2R)	Invitrogen

Table 2. Primer sequence used in this study

Name	Sequence 5'→3'
MGG_01669_5'flnk_F	GGTTACCCTCTAGAGAGTCCTG
MGG_01669_5'flnk_R	CCTCCACTAGCTCCAGCCAAGCCCGTTGGTGTAGTCTCTCTACC
MGG_01669_3'flnk_F	GTTGGTGTCGATGTCAGCTCCGGAGTTCGTCCCGGTATGGGTATTG
MGG_01669_3'flnk_R	CCAACCAGGGTAGGATAAGGG
MGG_01669_nested_F	GGGTTCAGGTCCAGTATAGAGC
MGG_01669_nested_R	ACTTAGGTACCACGGACAGC
MGG_01669_qRT_F	CAGGCTCCCATTCAAAACACC
MGG_01669_qRT_R	CGTTGCTGCTATCCACAGC
MGG_06733_5'flnk_F	GGAGAAGAAAGTCGACCCAGTG
MGG_06733_5'flnk_R	CCTCCACTAGCTCCAGCCAAGCCGACAGCCCTAACGGACTGAAG
MGG_06733_3'flnk_F	GTTGGTGTCGATGTCAGCTCCGGAGCACCTCTTATCGTACAGCTCTCG
MGG_06733_3'flnk_R	GAATGCTCACCTCAACGCTGCT
MGG_06733_nested_F	GCGTTTGGGACTGAACCCT
MGG_06733_nested_R	GAGCATAAGATACCTGCGGCAA
MGG_06733_qRT_F	GATTTATCACGCGCCACTCTCG
MGG_06733_qRT_R	GTTCGGTCAGCAGTTTTGGCAAG
MGG_00970_5'flnk_F	CTGGAGCTGCTTGGCAAATTCATC
MGG_00970_5'flnk_R	CCTCCACTAGCTCCAGCCAAGCCGCTTACGGACTGGATGGTC
MGG_00970_3'flnk_F	GTTGGTGTCGATGTCAGCTCCGGAGCCAGAAATCGAGTTGGCTCTC
MGG_00970_3'flnk_R	GTTGGGGTAGATCCAATTGGTGATGG
MGG_00970_nested_F	GAGCTTTACTGCCGAGAACTC
MGG_00970_nested_R	GAACAGCGCACAGGCTTTCTC
MGG_00970_qRT_F	CTGTTCCATCCCAACGTCTACC
MGG_00970_qRT_R	GGTTGTATGCGTCTGCCTGAG
MGG_05737_5'flnk_F	CCTCATCAATGTCATCGGCCTTC

MGG_05737_5'flnk_R	CCTCCACTAGCTCCAGCCAAGCCCAGAGGCGCAAAGTGAAAGGC
MGG_05737_3'flnk_F	GTTGGTGTCGATGTCAGCTCCGGAGCGAGACATTCAGTCAGTTTGGG
MGG_05737_3'flnk_R	GCTGAAGTTTGAGAGGGTTGG
MGG_05737_nested_F	AGAGTCGCGGAGCAAGACTATTC
MGG_05737_nested_R	CGTGTGTTGTTTGTGCCAATCTCG
MGG_05737_qRT_F	GGTGACGGACAACAATAACGAG
MGG_05737_qRT_R	GGTGACGGACAACAATAACGAG
Hyg_F	GGCTTGGCTGGAGCTAGTGGAGG
Hyg_R	CTCCGGAGCTGACATCGACACCAAC
01669_Y2H_F_attB	AAAAAGCAGGCTTAATGCAGGACTCAATGACAGC
01669_Y2H_R_attB	AGAAAGCTGGGTACAAGCCCATATAATTACTGTCC
06733_Y2H_F_attB	AAAAAGCAGGCTTAATGGCGACAAATCCCGAGTC
06733_Y2H_R_attB	AGAAAGCTGGGTACTCTCAATCCTCGTCGTCTG
05737_promoter_F_EcoRI	GAATTCCAACTAGCCTTGATGACG
05737_promoter_R_Sal I	GTCGACTATGGAAGTGGATTGTCTCG
05737_F_HA_Sal I	GTCGACATGTACCCATACGATGTTCCAGATTACGCTATGTCGGATCGCGA
05737_R_Apa I	GGGCCCTTAAGCACCACCAACCTG
01669_EF1α_F	CCCAATCTTCAAAATGCAGGACTCAATGACAGC
01669_attb_R	AGAAAGCTGGGTACTGTCCAAGGGTCATGTC
06733_EF1α_F	CCCAATCTTCAAAATGGCGACAAATCCCGAGTC
06733_attb_R	AGAAAGCTGGGTAATCCTCGTCGTCTGAAATGAC
00970_EF1α_F	CCCAATCTTCAAAATGTCTCTCAGCCAGAACCG
00970_attb_R	AGAAAGCTGGGTAAGGGGCTGGGTTCTCCCT
EF1α_Xba I_F	TCTAGACGGTACCTATAGGGCGAA
EF1α_R	TTTGAAGATTGGGTTCCTTTTG
RFP_EF1α_F	CCCAATCTTCAAAATGGCCTCCTCCGAGGAC
RFP_Hind III_R	AAGCTTGGCGCCGGTGGAGT
05737_Hind III_F	AAGCTTATGTCGGATCGCGAGAAC

05737 R	TTAAGCACCACCAACCTGCTC
Trpc terminator_05737_F	GGTGGTGCTTAAGATCCACTTAACGTTACTG
Trpc terminator_Xho I_R	CTCGAGAAGAAGGATTACCTCTAAAC
attb_F	GGGGACAAGTTTGTACAAAAAAGCAGGCT
attb_R	GGGGACCACTTTGTACAAGAAAGCTGGGT
pDEST22_AD_F	TATAACGCGTTTGGAATCACT
pDEST22,32_AD,BD_R	AGCCGACAACCTTGATTGGAGAC
pDEST32_BD_F	AACCGAAGTGCGCCAAGTGTCTG
COS1_qRT_F	TGCACCACGATCCCAGAGA
COS1_qRT_R	GCGATGTTGTGCCGTTGTTCC
COM1_qRT_F	GCCAGAGGTCCGCTATCAAA
COM1_qRT_R	CGGGATCTCGTCACTGGATT
CON7_qRT_F	TAAGGAGATCCGCAAAGAGT
CON7_qRT_R	TAGCGTTGTAGTCGGGGAGT
HOX2_qRT_F	TGGGGTTCTGCAGCCATGTT
HOX2_qRT_R	GTCCCGTGGTGTTACGTTCTGG

III. Southern blotting and RT-PCR

The wild type and the deletion mutants were cultured in liquid CM at 25°C for 3 d to extract gDNA and total RNA and extraction of the gDNA and total RNA as described previously (Kong *et al*., 2015). The gDNA was digested at 37°C with restriction enzymes, separated on a 1% agarose gel, and transferred to a nitrocellulose membrane. The membrane was hybridized with p32-labeled probe generated using a Random Primers DNA Labeling System kit (Invitrogen, USA), and exposed to X-ray film. Total RNA (5 μg) was reverse-transcribed to complementary DNA (cDNA) using an ImProm-II Reverse Transcription System kit (Promega, USA), and subjected to qRT-PCR using 50 ng of cDNA, 3 μL of primers, and 5 μL of SYBR Green PCR Master Mix in a Rotor-Gene Q 2plex (Qiagen, Germany). Transcript levels were quantified by RT-PCR using 100 ng of cDNA, 3 μL of primers, and 10 μL of 2X master mix using in a C1000 thermal cycler (Bio-Rad, USA).

IV. Mycelial growth, conidiation, and appressorium formation

All strains were cultured in modified complete agar medium (CMA) at 25°C for 9 d for assessment of mycelial growth and colony morphology (Iyer and Chattoo, 2003). Conidia were collected from cultures on V8 agar after incubation for 7 d and conidiation was measured under a microscope using a hemacytometer. To assess conidial germination and appressorium formation, 70 μL of conidial suspensions (3 $\times 10^4$/mL) was dropped on a hydrophobic cover glass at 25°C. Conidial germination and appressorium formation were evaluated under a microscope after incubation for

2, 8, and 24 h. Conidiogenesis and conidial adhesion assays were performed as described previously (Goh *et al*., 2011; Lau and Hamer, 1998). These experiments were performed in triplicate for three times.

Morphology of conidia was observed using at least 100 conidia. Hyphae from conidia were incubated with Calcofluor white (CFW, 10 μg/mL, Sigma Aldrich, USA) at 25℃ for 5 min to stain septa, and visualized using a fluorescence microscope (Carl Zeiss, Oberkochen, Germany). Cell length was measured using ImageJ software. These experiments were performed in triplicate for three times.

V. Cytorrhysis and plasmolysis assays

Conidial suspensions (3×10^4/mL) was incubated on a hydrophobic cover glass at 25℃ for 48 h. The sterilized distilled water (SDW) was removed, and the appressoria were treated with glycerol (1, 3, and 5 M) or PEG (400, 1,000, 3,350, and 8,000 Da). At least 100 collapsed and plasmolyzed appressoria were counted under a microscope. These experiments were performed in triplicate for three times.

VI. Sensitivity assessment to stress conditions

Minimal agar medium (MMA) was used to test sensitivity to nutrient starvation stress (Choi *et al*., 2015). To assess sensitivity to DNA damage stress, CMA was supplemented with 10 mM hydroxy urea (HU, DNA synthesis inhibitor) and 0.05% methyl methanesulfonate (MMS, DNA alkylating agent). For oxidative stress, CMA was supplemented with 5 mM H_2O_2 and 3 mM methyl viologen (MV). The wild type, deletion mutants, and complemented strains were cultured in triplicate under the

above five stress conditions and CMA (control) at 25°C for 9 d.

VII. Pathogenicity tests

A pathogenicity test was performed using the susceptible rice cultivar, Nakdongbyeo. For spray inoculation assays, 10 mL of conidia suspension (5×10^4/mL, containing 250 ppm Tween 20) was inoculated onto 4-week-old rice seedlings. Inoculated rice plants were incubated at 25°C for 1 d at a relative humidity (RH) of 100% in the dark and then at 28°C for 5–6 d in a growth chamber. For sheath inoculation assays, conidia suspension (2×10^4/mL) was inoculated onto sheaths of 6-week-old rice seedlings, which was then incubated at 25°C for 24 or 48 h. At least 50 infection sites were observed under a microscope. These experiments were performed with triplicate for three times.

VIII. Western blot

The promoter of *MoSmt3* (*Eco*RI-*Sal*I) and HA-fused *MoSmt3* (*Sal*I-*Apa*I) were TA cloned into pGEMT-easy (Promega, USA) (Table 2). The cloned vectors were digested with the corresponding restriction enzymes and ligated into pCB1004 (Wang *et al*., 1999). The pCB1004:native promoter:HA:SMT3 (pHA-SMT3) and geneticin resistance cassette were co-transformed into the wild type and the single gene deletion mutants. Transformants were cultured in liquid CM at 25°C for 3 d to harvest mycelia. Proteins were extracted using 600 μL of PRO-PREP protein extraction solution (Intron Biotechnology, Korea). Proteins (75 μg) were separated on a 4–20% gradient SDS-PAGE gel (Bio-Rad, USA) and transferred to an Immun-

Blot LF PVDF membrane using transfer buffer (20% methanol [v/v], 0.25 M Tris, and 2 M glycine). The membrane was probed with an anti-HA antibody (1:1,000, Bethyl, USA) and anti-ubiquitin antibody (P4D1) (1:1,000, Cell Signaling Technology, USA) using a Pierce Fast Western Blot Kit and ECL Substrate (Pierce Biotechnology, Rockford, IL, USA). An anti-actin antibody (1:1000, Cell Signaling Technology, USA) was used as the loading control. The probed membrane was exposed to x-ray film.

IX. Yeast two-hybrid assay

The coding sequences of MoAOS1 and MoUBA2 were amplified from cDNA of the wild type (Table 2). A yeast two-hybrid (Y2H) assay was performed using the ProQuest Two-Hybrid System kit (Invitrogen, USA). The coding sequence of MoAOS1 and MoUBA2 was inserted into both pDEST22 and pDEST32 using a Gateway system. The MaV203 yeast strain was cultured in YPAD liquid medium at 30°C until an optical density at 600 nm of 0.4 was reached (Table 1). Yeast competent cells were generated using lithium acetate (LiAc). Next, 1 μg of *MoAOS1* and *MoUBA2* inserted vectors, 100 μg of denatured salmon sperm DNA, and 100 μL of competent cells were co-transformed using LiAc and PEG. The control plasmids (pEXP22RalGDS-wt, pEXP22RalGDS-m1, and pEXP22RalGDS-m2) were co-transformed with pEXP32Krev1 using the same method and selected on SC-Leu/Trp (SC-LT) agar. Selected co-transformants were confirmed by amplifying the inserted coding sequence. Interaction of MoAOS1 and MoUBA2 was confirmed on SC-Leu/Trp/His + 25 mM 3-amino-1,2,4-triazole (SC-LTH + 3AT) agar and validated

by X-gal assay.

X. Intracellular localization

The EF1α promoter (originated from *Fusarium verticillioides*) was amplified from YL1320. The coding sequences of MoSMT3, MoAOS1, MoUBA2, and MoUBC9 were amplified from the cDNA of the wild type. Fusion constructs of the EF1α promoter and each coding sequence were generated using double-joint PCR and fused in pFPL-rh containing the coding sequence of mRFP. Next, the coding sequence of mRFP was conjugated to the C-terminal coding sequence. The C-terminus of SMT3 is cleaved upon reaching maturity. Therefore, another plasmid was generated to observethe localization of SMT3. mRFP and the TrpC terminator were amplified from pFPL-rh and pBCATPH. EF1α promoter:mRFP (*Xba*I-*Hin*dIII) and SMT3:TrpC terminator (*Hin*dIII-*Xho*I) fusion constructs were generated using double-joint PCR and TA-cloned into pGEMT-easy. The cloned vectors were digested with the corresponding restriction enzymes and fused in pCB1004. The pFPL-rh:EF1α promoter:AOS1 (pLOCAL01669), pFPL-rh:EF1α promoter:UBA2 (pLOCAL06733), pFPL-rh:EF1α promoter:UBC9 (pLOCAL00970), and pCB1004:EF1α promoter:mRFP:SMT3:TrpC terminator (pLOCAL05737) constructs were co-transformed with a geneticin resistance cassette into all of the deletion mutants. Localization of MoSMT3, MoAOS1, MoUBA2, and MoUBC9 in conidia and developmental stage including conidial germination and appressorium formation was observed using a fluorescence microscope (Carl Zeiss, Oberkochen, Germany). Conidia were incubated in Hoechst33342 solution (10 mg/mL, Invitrogen,

USA) at 25°C for 30 min to stain nuclei.

RESULTS

I. Phylogenetic analysis of UBLs in fungi

We identified *S. cerevisiae* SUMOylation homologs in fungi by protein BLAST and Pfam domain analysis. The domain analysis of *S. cerevisiae* showed that SMT3 possessed a SUMO domain (PF11976), AOS1 and UBC2 possessed a ThiF domain (PF00899), UBC9 contained a ubiquitin-conjugating domain (PF00179), and the E3 enzymes possessed various zinc finger domains (PF02891 and PF14634) (Table 3). Proteins with those domains were identified from the selected model organisms and fungal species. This retrieved not only SUMOylation-associated proteins, but all UBLs including for neddylation and urmylation (Figure 1A and Table 4). Fungi had relatively fewer UBLs than animal and plant. For SUMO, only one gene was widely conserved in most fungal species, but some had more than one polyphyletic gene (Figure 2). Unlike SUMO, E1 enzymes were divided into six clades with specific functions annotated based on *S. cerevisiae* proteins, including UBA1 for ubiquitination, UBA3 for neddylation, UBA4 for urmylation, the two SUMOylation clades (AOS1 and UBA2), and one clade with unknown function (Figure 1B and Figure 2B). UBC9 showed the highest diversity, but its homologs were well conserved in Ascomycetes (Figure 2C). SIZ2 homologs were identified in all classes, but SIZ1 was identified in only fungi and animals, and MMS21 only in fungi and oomycota (Figure 2D and 2E). CST9 was found only in *S. cerevisiae*. CST9 homologs were also found in *Allomyces macrogynus* and *Candida albicans* by BLAST, but these lacked the E3 ligase zinc-RING finger domain (PF14634). ULP1

and ULP2 were also detected in all classes, but WSS1 was absent from animals (Figure 2F and 2G). Unlike the SIZ1 and SIZ2 homologs, which were polyphyletic, the fungal ULP1 and ULP2 homologs were monophyletic (Figure 2D and 2F). In *M. oryzae*, the domains of all SUMOylation components showed ≥ 42% sequence similarity with corresponding *S. cerevisiae* components (Table 5). The homologs of *M. oryzae* SUMOylation components with the highest levels of similarity were named after the *S. cerevisiae* genes.

Table 3. Domains of *S. cerevisiae* SUMOylation components

Class	Protein	Length	Pfam ID	Pfam description	Start	End
SUMO	SMT3	101	PF11976	Ubiquitin-2 like Rad60 SUMO-like	24	91
E1	AOS1	347	PF00899	ThiF family	16	331
	UBA2	636	PF00899	ThiF family	9	437
			PF10585	Ubiquitin-activating enzyme active site	280	363
E2	UBC9	157	PF00179	Ubiquitin-conjugating enzyme	8	148
E3	SIZ1	904	PF02891	MIZ/SP-RING zinc finger	357	405
			PF02037	SAP domain	35	68
			PF14324	PINIT domain	175	312
	SIZ2	726	PF02891	MIZ/SP-RING zinc finger	334	382
			PF02037	SAP domain	44	77
			PF14324	PINIT domain	155	289
	MMS21	267	PF11789	Zinc-finger of the MIZ type in Nse subunit	171	227

	CST9	482	PF14634	zinc-RING finger domain	54	92
Protease	ULP1	621	PF02902	Ulp1 protease family, C-terminal catalytic domain	447	613
	ULP2	1034	PF02902	Ulp1 protease family, C-terminal catalytic domain	456	674
	WSS1	269	PF08325	WLM domain	27	220

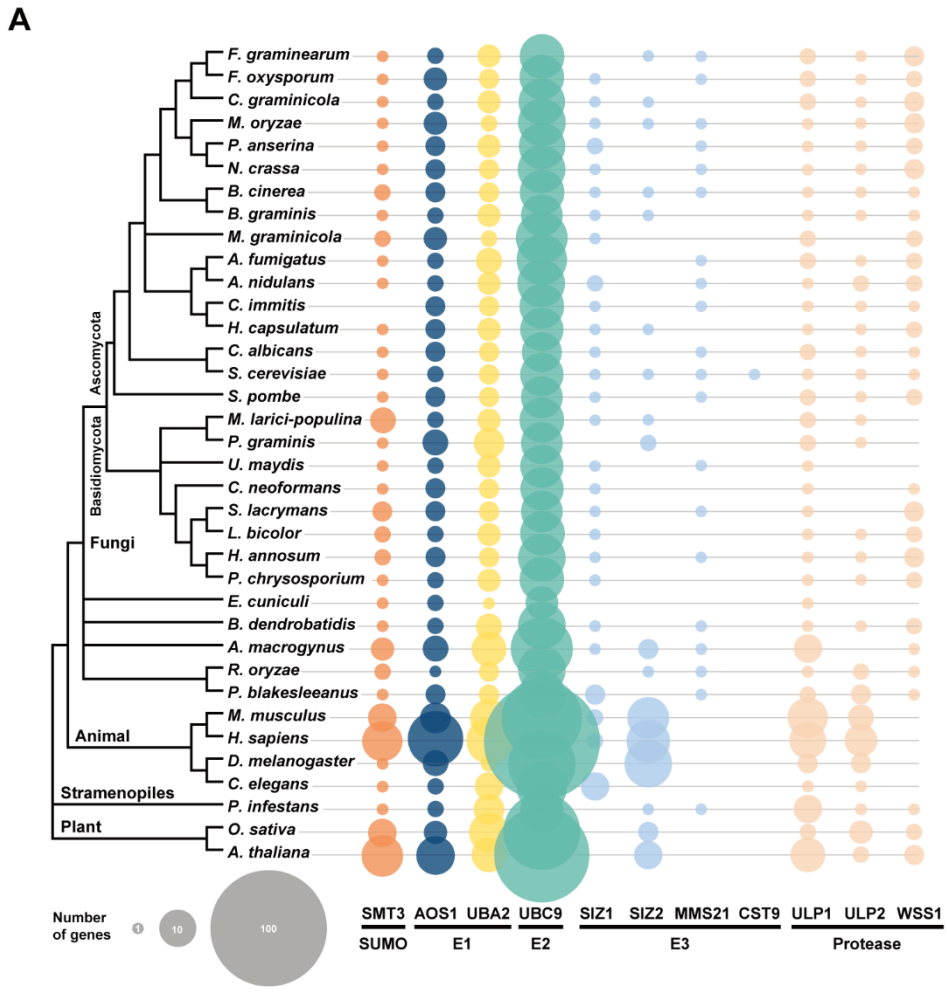
A
F. graminearum
F. oxysporum
C. graminicola
M. oryzae
P. anserina
N. crassa
B. cinerea
B. graminis
M. graminicola
A. fumigatus
A. nidulans
C. immitis
H. capsulatum
C. albicans
S. cerevisiae
S. pombe
M. larici-populina
P. graminis
U. maydis
C. neoformans
S. lacrymans
L. bicolor
H. annosum
P. chrysosporium
E. cuniculi
B. dendrobatidis
A. macrogynus
R. oryzae
P. blakesleeanus
M. musculus
H. sapiens
D. melanogaster
C. elegans
P. infestans
O. sativa
A. thaliana
Ascomycota
Basidiomycota
Fungi
Animal
Stramenopiles
Plant
Number of genes
1
10
100
SMT3
AOS1
UBA2
UBC9
SIZ1
SIZ2
MMS21
CST9
ULP1
ULP2
WSS1
SUMO
E1
E2
E3
Protease

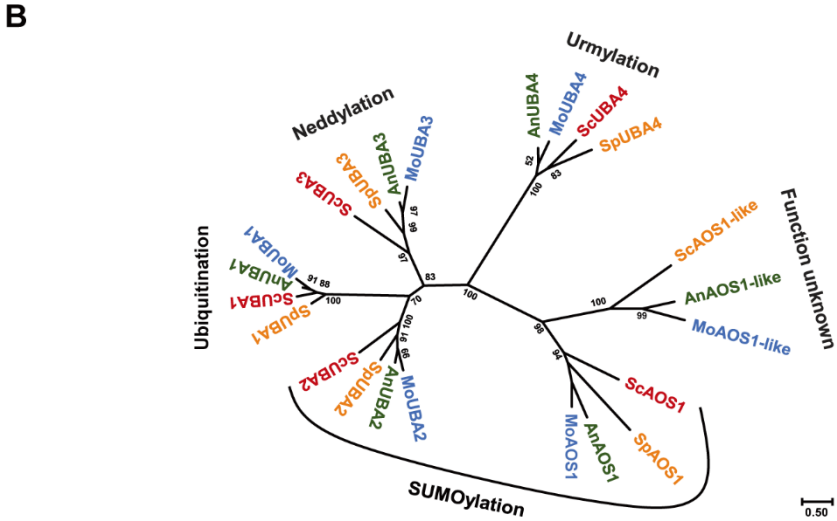
B
Urmylation
AnUBA4
MoUBA4
ScUBA4
SpUBA4
Neddylation
AnUBA3
MoUBA3
ScUBA3
SpUBA3
Ubiquitination
AnUBA1
MoUBA1
ScUBA1
SpUBA1
AnUBA2
MoUBA2
ScUBA2
SpUBA2
Function unknown
ScAOS1-like
AnAOS1-like
MoAOS1-like
ScAOS1
AnAOS1
MoAOS1
SpAOS1
SUMOylation
0.50

Figure 1. Yeast homologs of UBLs in fungi. (A) A schematic species tree of the Fungal Genome Gold Standard from CFGP (http://cfgp.riceblast.snu.ac.kr) and model organisms was constructed based on the NCBI taxonomy. The number of yeast homologs in each species is represented by the areas of the circles. (B) Unrooted E1 domain tree of *M. oryzae* (Mo), *A. nidulans* (An), *S. pombe* (Sp), and *S. cerevisiae* (Sc). The tree was constructed by the maximum-likelihood method with 1,000 bootstrappings.

Table 4. The number of *S. cerevisiae* homologs of SUMOylation components in the selected species

Kingdom	Phylum	Species	SUMO	E1		E2	E3				Protease		
			SMT3	AOS1	UBA2	UBC9	SIZ1	SIZ2	MMS21	CST9	ULP1	ULP2	WSS1
Fungi	Ascomycota	*Fusarium graminearum*	1	2	4	15	0	1	1	0	2	1	3
Fungi	Ascomycota	*Fusarium oxysporum*	1	4	3	15	1	0	1	0	2	1	2
Fungi	Ascomycota	*Colletotrichum graminicola*	1	2	4	16	1	1	0	0	2	1	3
Fungi	Ascomycota	*Magnaporthe oryzae*	1	4	2	17	1	1	1	0	1	1	3
Fungi	Ascomycota	*Podospora anserina*	1	3	4	16	2	0	1	0	1	1	2
Fungi	Ascomycota	*Neurospora crassa*	1	3	3	17	1	0	1	0	1	1	3
Fungi	Ascomycota	*Botrytis cinerea*	2	3	3	15	1	1	1	0	1	1	1
Fungi	Ascomycota	*Blumeria graminis*	1	2	4	13	1	1	0	0	1	1	1
Fungi	Ascomycota	*Mycosphaerella graminicola*	2	4	2	20	1	0	0	0	2	0	2
Fungi	Ascomycota	*Aspergillus fumigatus*	1	2	5	19	0	0	1	0	2	1	2
Fungi	Ascomycota	*Aspergillus nidulans*	1	2	4	17	2	0	1	0	1	2	2
Fungi	Ascomycota	*Coccidioides immitis*	0	3	3	15	1	0	1	0	1	1	1
Fungi	Ascomycota	*Histoplasma capsulatum*	1	3	4	14	1	1	0	0	1	1	2
Fungi	Ascomycota	*Candida albicans*	1	3	3	12	1	0	1	0	2	1	1

Fungi	Ascomycota	*Saccharomyces cerevisiae*	1	2	3	14	1	1	1	1	1	1	1
Fungi	Ascomycota	*Schizosaccharomyces pombe*	1	3	3	13	1	0	1	0	2	1	2
Fungi	Basidiomycota	*Melampsora laricis-populina*	5	2	4	15	1	1	0	0	2	1	0
Fungi	Basidiomycota	*Puccinia graminis*	1	5	7	13	0	2	0	0	2	1	1
Fungi	Basidiomycota	*Ustilago maydis*	1	2	4	14	1	0	1	0	1	0	0
Fungi	Basidiomycota	*Cryptococcus neoformans*	1	3	3	14	1	0	0	0	1	0	1
Fungi	Basidiomycota	*Serpula lacrymans*	3	3	3	13	1	0	1	0	1	0	3
Fungi	Basidiomycota	*Laccaria bicolor*	2	2	4	15	1	0	0	0	1	1	2
Fungi	Basidiomycota	*Heterobasidion annosum*	2	3	3	17	1	0	1	0	1	1	3
Fungi	Basidiomycota	*Phanerochaete chrysosporium*	1	2	4	15	1	0	0	0	1	1	2
Fungi	Microsporidia	*Encephalitozoon cuniculi*	1	2	1	8	0	0	0	0	1	0	0
Fungi	Chytridiomycota	*Batrachochytrium dendrobatidis*	1	2	5	17	1	0	1	0	1	1	2
Fungi	Blastocladiomycota	*Allomyces macrogynus*	4	5	9	29	1	3	1	0	6	0	1
Fungi	Mucoromycota	*Rhizopus oryzae*	2	1	3	17	0	1	1	0	1	2	1
Fungi	Mucoromycota	*Phycomyces blakesleeanus*	1	3	3	16	3	0	1	0	2	3	1
Animal	Chordata	*Mus musculus*	6	7	11	48	2	13	0	0	12	5	0
Animal	Chordata	*Homo sapiens*	12	23	16	101	2	14	0	0	10	8	0

Animal	Arthropoda	*Drosophila melanogaster*	1	5	2	34	0	17	0	0	3	3	0
Animal	Nematoda	*Caenorhabditis elegans*	1	2	6	19	6	0	0	0	1	1	0
Stramenopiles	Oomycota	*Phytophthora infestans*	1	2	7	14	0	1	1	0	6	1	1
Plant	Streptophyta	*Oryza sativa*	6	4	12	44	0	3	0	0	2	4	2
Plant	Streptophyta	*Arabidopsis thaliana*	13	11	9	68	0	6	0	0	9	2	3

A

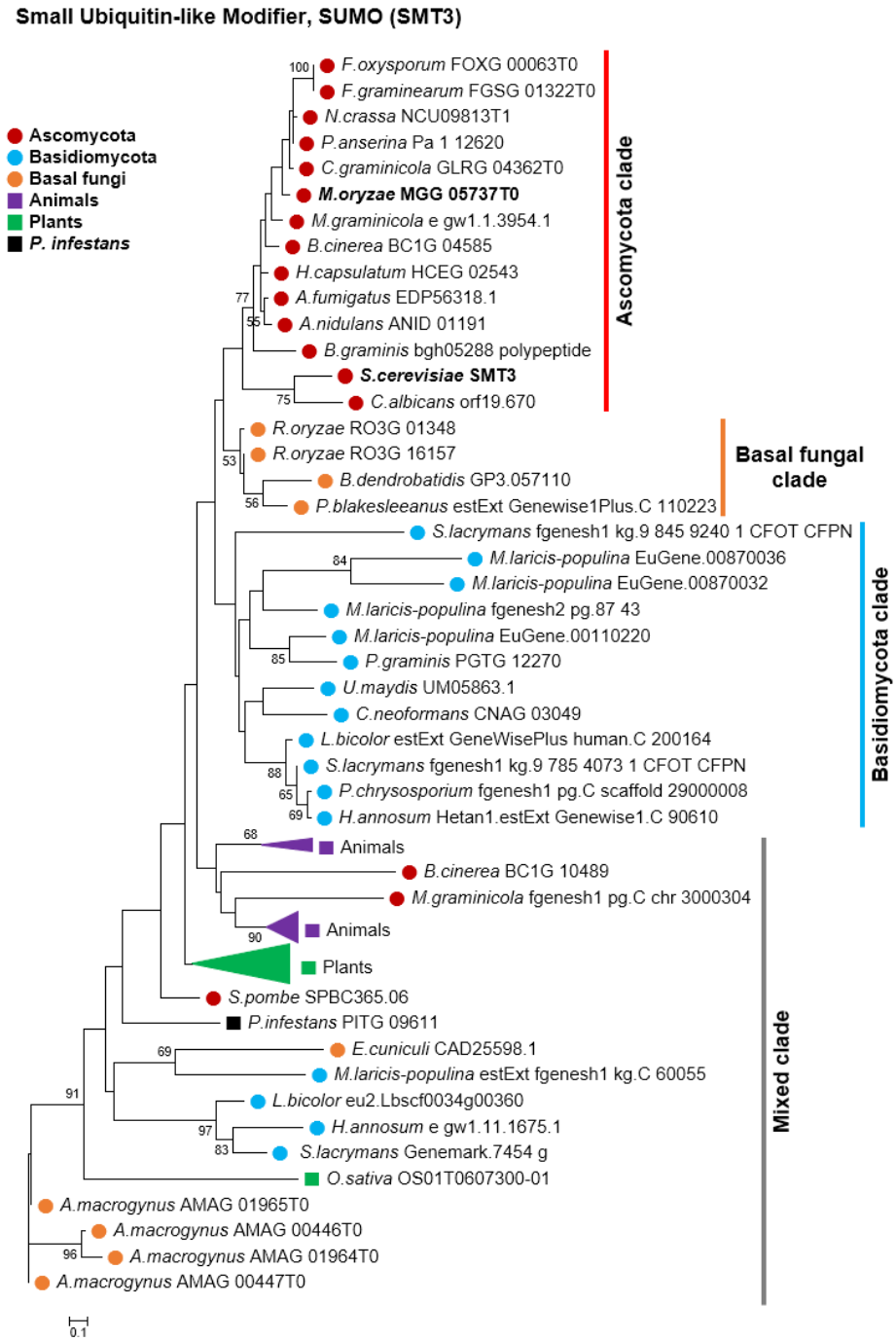
Small Ubiquitin-like Modifier, SUMO (SMT3)
Ascomycota
Basidiomycota
Basal fungi
Animals
Plants
P. infestans
F.oxysporum FOXG 00063T0
F.graminearum FGSG 01322T0
N.crassa NCU09813T1
P.anserina Pa 1 12620
C.graminicola GLRG 04362T0
M.oryzae MGG 05737T0
M.graminicola e gw1.1.3954.1
B.cinerea BC1G 04585
H.capsulatum HCEG 02543
A.fumigatus EDP56318.1
A.nidulans ANID 01191
B.graminis bgh05288 polypeptide
S.cerevisiae SMT3
C.albicans orf19.670
Ascomycota clade
R.oryzae RO3G 01348
R.oryzae RO3G 16157
B.dendrobatidis GP3.057110
P.blakesleeanus estExt Genewise1Plus.C 110223
Basal fungal clade
S.lacrymans fgenesh1 kg.9 845 9240 1 CFOT CFPN
M.laricis-populina EuGene.00870036
M.laricis-populina EuGene.00870032
M.laricis-populina fgenesh2 pg.87 43
M.laricis-populina EuGene.00110220
P.graminis PGTG 12270
U.maydis UM05863.1
C.neoformans CNAG 03049
L.bicolor estExt GeneWisePlus human.C 200164
S.lacrymans fgenesh1 kg.9 785 4073 1 CFOT CFPN
P.chrysosporium fgenesh1 pg.C scaffold 29000008
H.annosum Hetan1.estExt Genewise1.C 90610
Basidiomycota clade
Animals
B.cinerea BC1G 10489
M.graminicola fgenesh1 pg.C chr 3000304
Animals
Plants
S.pombe SPBC365.06
P.infestans PITG 09611
E.cuniculi CAD25598.1
M.laricis-populina estExt fgenesh1 kg.C 60055
L.bicolor eu2.Lbscf0034g00360
H.annosum e gw1.11.1675.1
S.lacrymans Genemark.7454 g
O.sativa OS01T0607300-01
A.macrogynus AMAG 01965T0
A.macrogynus AMAG 00446T0
A.macrogynus AMAG 01964T0
A.macrogynus AMAG 00447T0
Mixed clade
0.1

B

Ubiquitin-activating enzyme, E1 (AOS1 and UBA2)

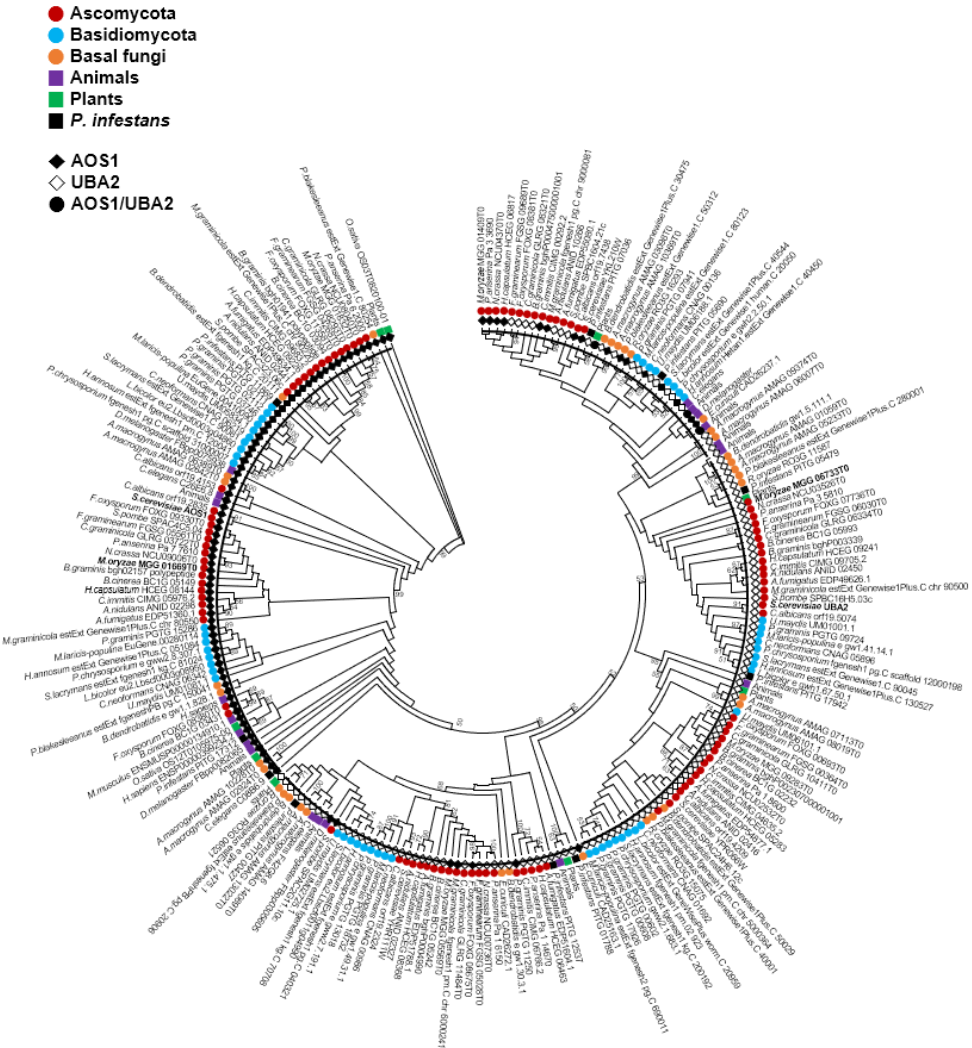

C


Ubiquitin-conjugating enzyme, E2 (UBC9)
Ascomycota
Basidiomycota
Basal fungi
Animals
Plants
P. infestans

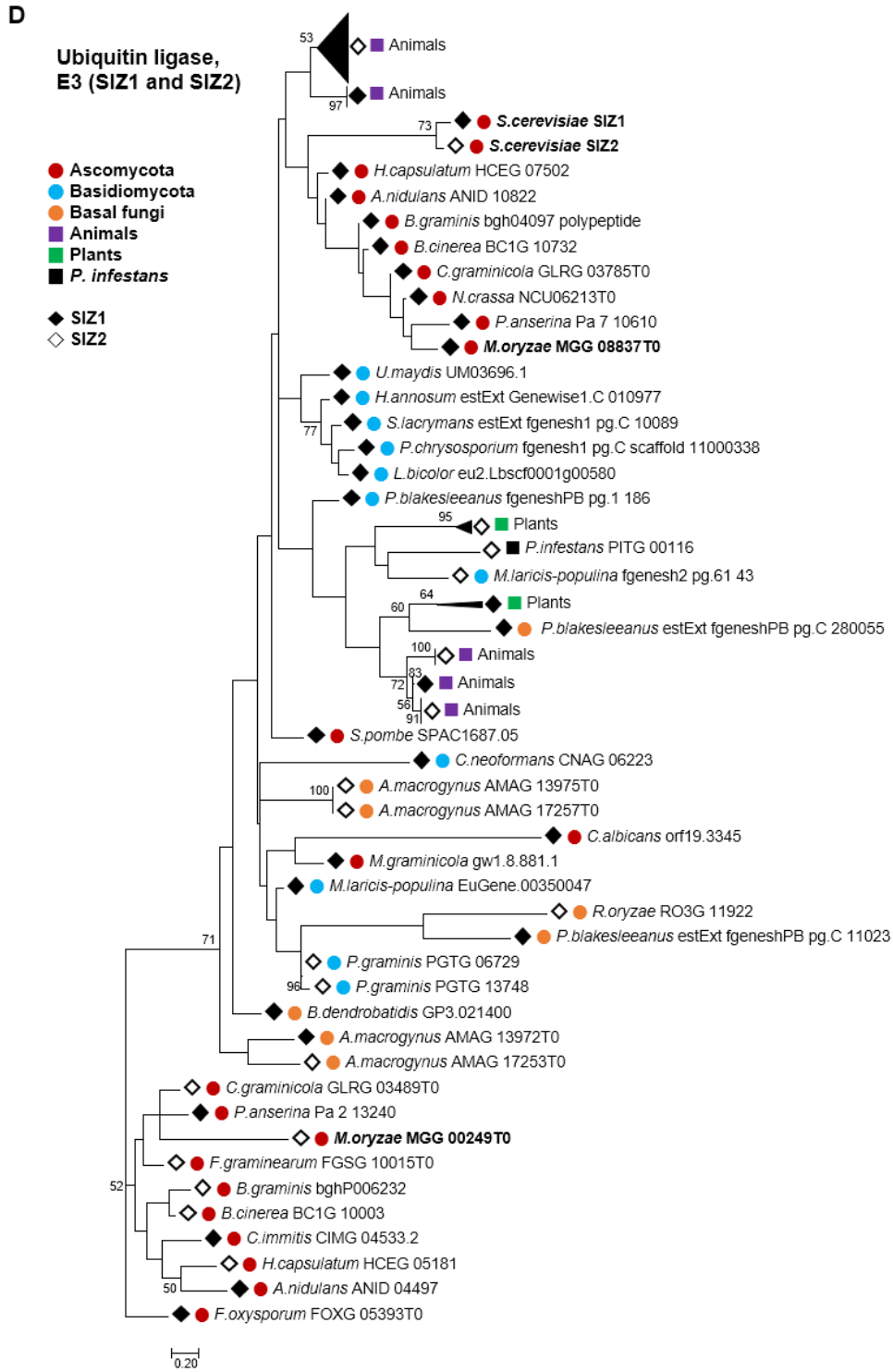
D
Ubiquitin ligase,
E3 (SIZ1 and SIZ2)
Ascomycota
Basidiomycota
Basal fungi
Animals
Plants
P. infestans
SIZ1
SIZ2
Animals
Animals
S.cerevisiae SIZ1
S.cerevisiae SIZ2
H.capsulatum HCEG 07502
A.nidulans ANID 10822
B.graminis bgh04097 polypeptide
B.cinerea BC1G 10732
C.graminicola GLRG 03785T0
N.crassa NCU06213T0
P.anserina Pa 7 10610
M.oryzae MGG 08837T0
U.maydis UM03696.1
H.annosum estExt Genewise1.C 010977
S.lacrymans estExt fgenesh1 pg.C 10089
P.chrysosporium fgenesh1 pg.C scaffold 11000338
L.bicolor eu2.Lbscf0001g00580
P.blakesleeanus fgeneshPB pg.1 186
Plants
P.infestans PITG 00116
M.laricis-populina fgenesh2 pg.61 43
Plants
P.blakesleeanus estExt fgeneshPB pg.C 280055
Animals
Animals
Animals
S.pombe SPAC1687.05
C.neoformans CNAG 06223
A.macrogynus AMAG 13975T0
A.macrogynus AMAG 17257T0
C.albicans orf19.3345
M.graminicola gw1.8.881.1
M.laricis-populina EuGene.00350047
R.oryzae RO3G 11922
P.blakesleeanus estExt fgeneshPB pg.C 11023
P.graminis PGTG 06729
P.graminis PGTG 13748
B.dendrobatidis GP3.021400
A.macrogynus AMAG 13972T0
A.macrogynus AMAG 17253T0
C.graminicola GLRG 03489T0
P.anserina Pa 2 13240
M.oryzae MGG 00249T0
F.graminearum FGSG 10015T0
B.graminis bghP006232
B.cinerea BC1G 10003
C.immitis CIMG 04533.2
H.capsulatum HCEG 05181
A.nidulans ANID 04497
F.oxysporum FOXG 05393T0
0.20

E

Ubiquitin ligase, E3 (MMS21)

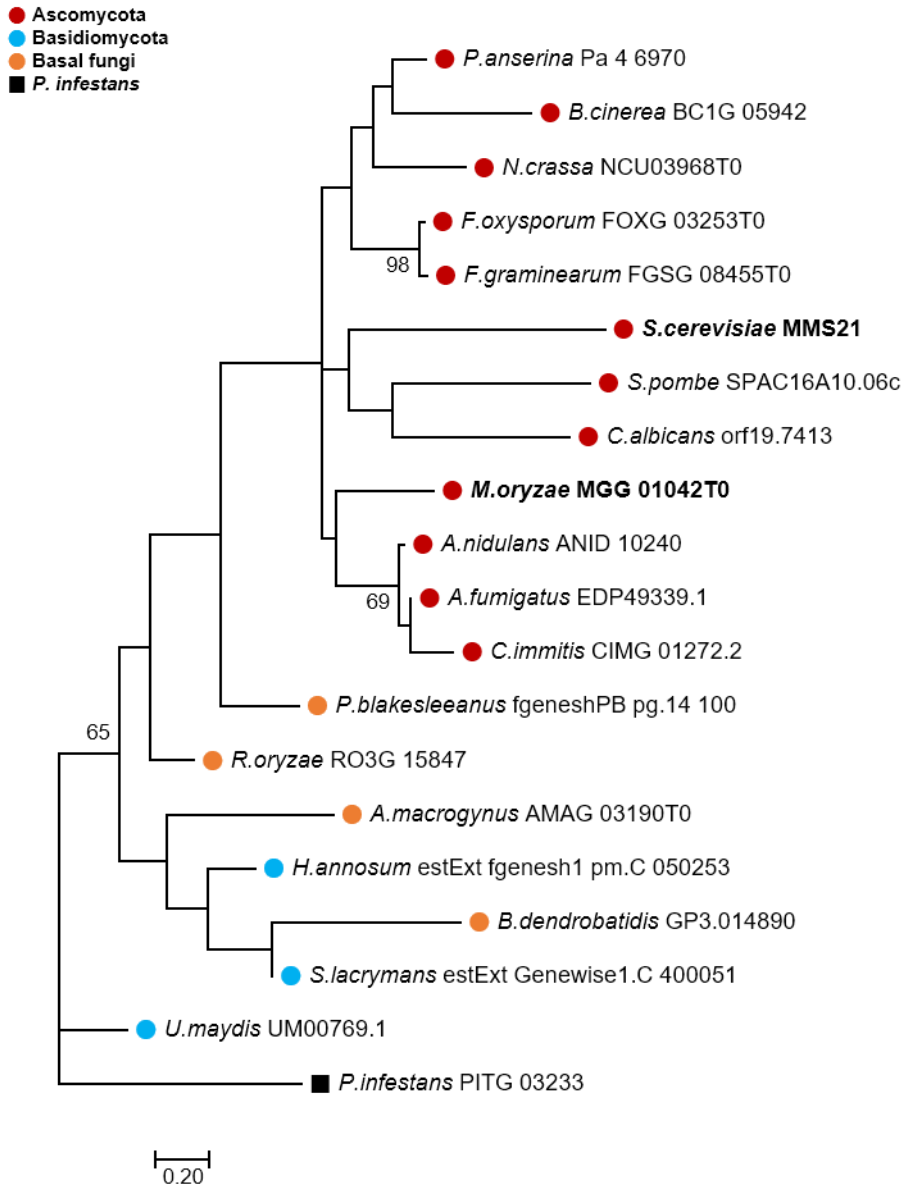

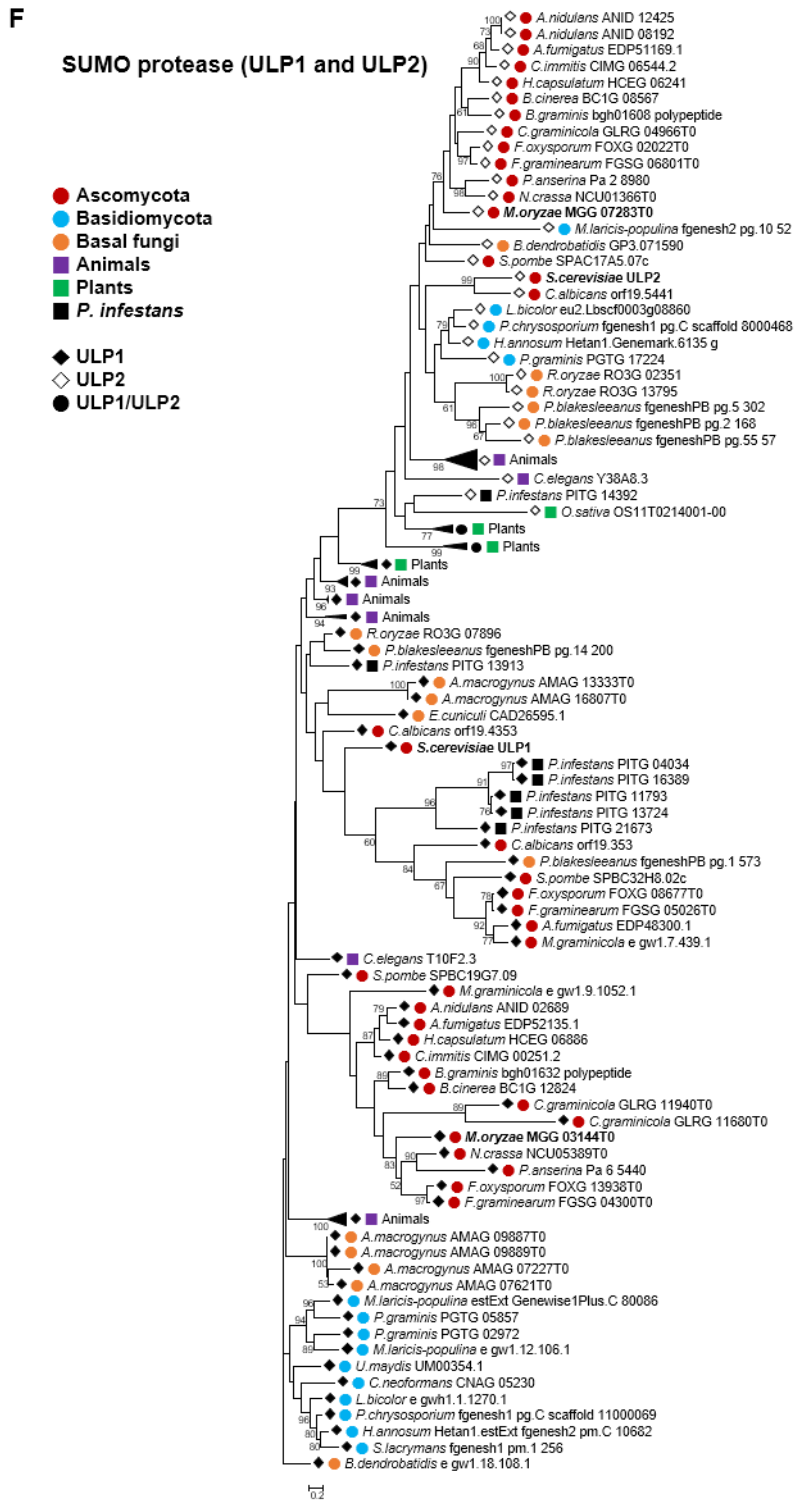
F
SUMO protease (ULP1 and ULP2)
Ascomycota
Basidiomycota
Basal fungi
Animals
Plants
P. infestans
ULP1
ULP2
ULP1/ULP2
A.nidulans ANID 12425
A.nidulans ANID 08192
A.fumigatus EDP51169.1
C.immitis CIMG 06544.2
H.capsulatum HCEG 06241
B.cinerea BC1G 08567
B.graminis bgh01608 polypeptide
C.graminicola GLRG 04966T0
F.oxysporum FOXG 02022T0
F.graminearum FGSG 06801T0
P.anserina Pa 2 8980
N.crassa NCU01366T0
M.oryzae MGG 07283T0
M.laricis-populina fgenesh2 pg.10 52
B.dendrobatidis GP3.071590
S.pombe SPAC17A5.07c
S.cerevisiae ULP2
C.albicans orf19.5441
L.bicolor eu2.Lbscf0003g08860
P.chrysosporium fgenesh1 pg.C scaffold 8000468
H.annosum Hetan1.Genemark.6135 g
P.graminis PGTG 17224
R.oryzae RO3G 02351
R.oryzae RO3G 13795
P.blakesleeanus fgeneshPB pg.5 302
P.blakesleeanus fgeneshPB pg.2 168
P.blakesleeanus fgeneshPB pg.55 57
Animals
C.elegans Y38A8.3
P.infestans PITG 14392
O.sativa OS11T0214001-00
Plants
Plants
Plants
Animals
Animals
Animals
R.oryzae RO3G 07896
P.blakesleeanus fgeneshPB pg.14 200
P.infestans PITG 13913
A.macrogynus AMAG 13333T0
A.macrogynus AMAG 16807T0
E.cuniculi CAD26595.1
C.albicans orf19.4353
S.cerevisiae ULP1
P.infestans PITG 04034
P.infestans PITG 16389
P.infestans PITG 11793
P.infestans PITG 13724
P.infestans PITG 21673
C.albicans orf19.353
P.blakesleeanus fgeneshPB pg.1 573
S.pombe SPBC32H8.02c
F.oxysporum FOXG 08677T0
F.graminearum FGSG 05026T0
A.fumigatus EDP48300.1
M.graminicola e gw1.7.439.1
C.elegans T10F2.3
S.pombe SPBC19G7.09
M.graminicola e gw1.9.1052.1
A.nidulans ANID 02689
A.fumigatus EDP52135.1
H.capsulatum HCEG 06886
C.immitis CIMG 00251.2
B.graminis bgh01632 polypeptide
B.cinerea BC1G 12824
C.graminicola GLRG 11940T0
C.graminicola GLRG 11680T0
M.oryzae MGG 03144T0
N.crassa NCU05389T0
P.anserina Pa 6 5440
F.oxysporum FOXG 13938T0
F.graminearum FGSG 04300T0
Animals
A.macrogynus AMAG 09887T0
A.macrogynus AMAG 09889T0
A.macrogynus AMAG 07227T0
A.macrogynus AMAG 07621T0
M.laricis-populina estExt Genewise1Plus.C 80086
P.graminis PGTG 05857
P.graminis PGTG 02972
M.laricis-populina e gw1.12.106.1
U.maydis UM00354.1
C.neoformans CNAG 05230
L.bicolor e gwh1.1.1270.1
P.chrysosporium fgenesh1 pg.C scaffold 11000069
H.annosum Hetan1.estExt fgenesh2 pm.C 10682
S.lacrymans fgenesh1 pm.1 256
B.dendrobatidis e gw1.18.108.1
0.2

G

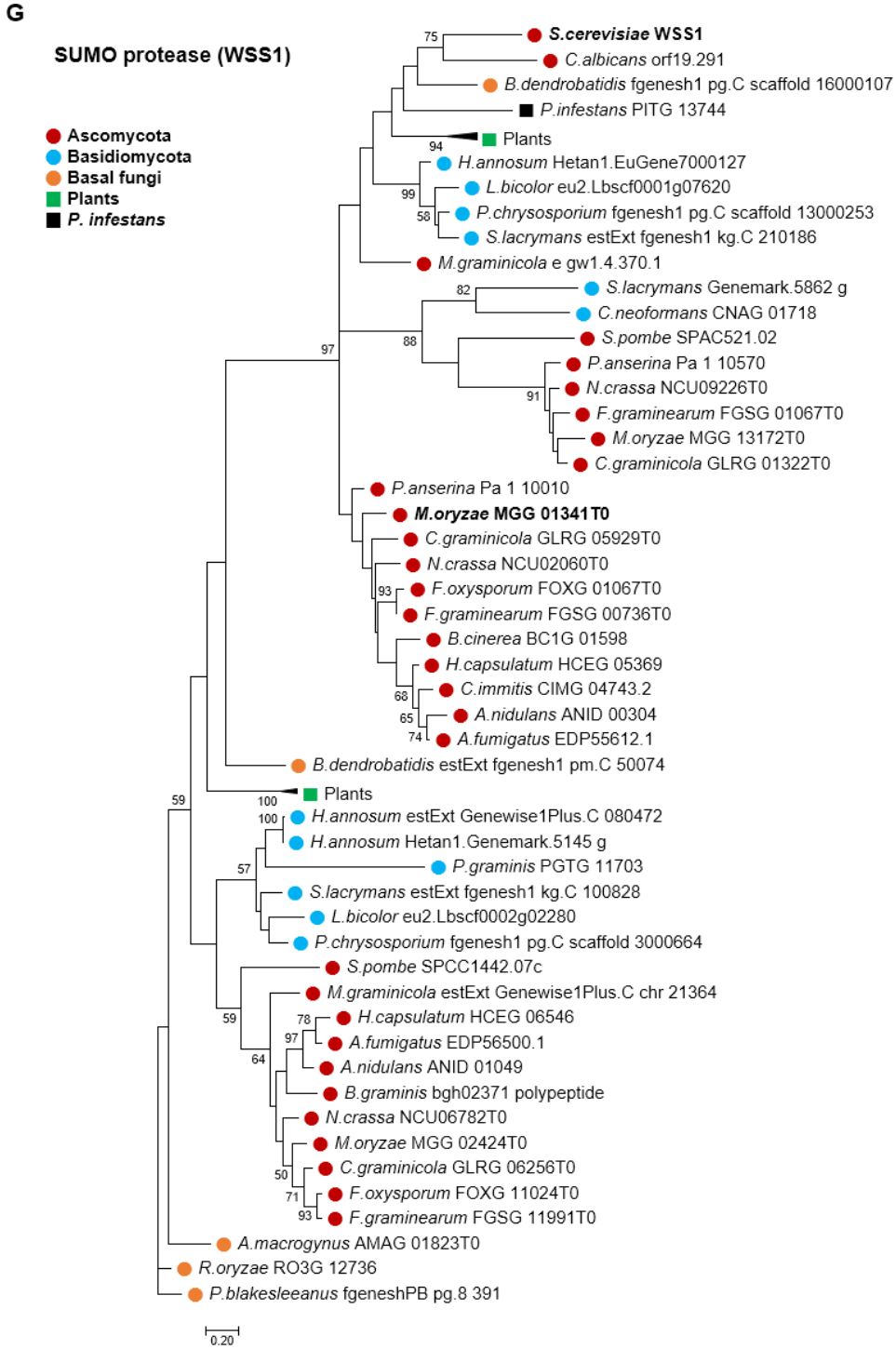
SUMO protease (WSS1)
Ascomycota
Basidiomycota
Basal fungi
Plants
P. infestans
S.cerevisiae WSS1
C.albicans orf19.291
B.dendrobatidis fgenesh1 pg.C scaffold 16000107
P.infestans PITG 13744
Plants
H.annosum Hetan1.EuGene7000127
L.bicolor eu2.Lbscf0001g07620
P.chrysosporium fgenesh1 pg.C scaffold 13000253
S.lacrymans estExt fgenesh1 kg.C 210186
M.graminicola e gw1.4.370.1
S.lacrymans Genemark.5862 g
C.neoformans CNAG 01718
S.pombe SPAC521.02
P.anserina Pa 1 10570
N.crassa NCU09226T0
F.graminearum FGSG 01067T0
M.oryzae MGG 13172T0
C.graminicola GLRG 01322T0
P.anserina Pa 1 10010
M.oryzae MGG 01341T0
C.graminicola GLRG 05929T0
N.crassa NCU02060T0
F.oxysporum FOXG 01067T0
F.graminearum FGSG 00736T0
B.cinerea BC1G 01598
H.capsulatum HCEG 05369
C.immitis CIMG 04743.2
A.nidulans ANID 00304
A.fumigatus EDP55612.1
B.dendrobatidis estExt fgenesh1 pm.C 50074
Plants
H.annosum estExt Genewise1Plus.C 080472
H.annosum Hetan1.Genemark.5145 g
P.graminis PGTG 11703
S.lacrymans estExt fgenesh1 kg.C 100828
L.bicolor eu2.Lbscf0002g02280
P.chrysosporium fgenesh1 pg.C scaffold 3000664
S.pombe SPCC1442.07c
M.graminicola estExt Genewise1Plus.C chr 21364
H.capsulatum HCEG 06546
A.fumigatus EDP56500.1
A.nidulans ANID 01049
B.graminis bgh02371 polypeptide
N.crassa NCU06782T0
M.oryzae MGG 02424T0
C.graminicola GLRG 06256T0
F.oxysporum FOXG 11024T0
F.graminearum FGSG 11991T0
A.macrogynus AMAG 01823T0
R.oryzae RO3G 12736
P.blakesleeanus fgeneshPB pg.8 391
0.20

Figure 2. Phylogenetic trees of SUMOylation components in fungi and model organisms. Phylogenetic trees of SUMOylation components in fungi and model organisms that are homologous to *S. cerevisiae* SUMOylation components were constructed by the maximum-likelihood method with 1,000 bootstraps and the LG or BLOSUM62 protein substitution method. The sequences used for alignments were (A) PF11976 for SUMO, SMT3; (B) PF00899 for E1, AOS1, and UBA2; (C) PF00179 for E2, UBC9; (D) PF02891 for E3, SIZ1, and SIZ2; (E) PF11789 for E3, MMS21; (F) PF02902 for protease, ULP1, and ULP2; and (G) PF08325 for protease and WSS1. Clades that contained more than three species of the same fungal phylum, animal, and plant are shown without genus/species names. The yeast components are marked with star and *M. oryzae* homologs are shown in bold. Only bootstrap values > 50% are shown.

Table 5. The closest *S. cerevisiae* homologs of SUMOylation components in *M. oryzae*

Class	*S. cerevisiae* protein	*M. oryzae* accession	Seq. similarity (%)
SUMO	SMT3	MGG_05737	77
E1	AOS1	MGG_01669	60
		MGG_01832	48
		MGG_01409	37
		MGG_05569	51
	UBA2	MGG_06733	58*
		MGG_09283	61
E2	UBC9	MGG_00970	81
		MGG_04081	55
		MGG_06562	54
		MGG_01756	52
		MGG_00103	50
		MGG_03728	49
		MGG_02568	62
		MGG_05478	50
		MGG_01807	49
		MGG_00600	49
		MGG_00180	54
		MGG_14071	46
		MGG_14266	52
		MGG_04388	49
		MGG_09913	47
		MGG_09977	47
		MGG_02446	49
E3	SIZ1	MGG_08837	53
	SIZ2	MGG_00249	42
	MMS21	MGG_01042	62
	CST9	-	-
Protease	ULP1	MGG_03144	45
	ULP2	MGG_07283	52
	WSS1	MGG_01341	52
		MGG_13172	49
		MGG_02424	47

The closest yeast homologs are highlighted in grey.

* It has larger sequence coverage.

II. SUMO-activation and -conjugation enzymes are essential for SUMOylation in *M. oryzae*

To confirm that the identified SUMOylation-associated genes are important for SUMOylation in *M. oryzae*, we generated targeted deletion mutants in the genes encoding SUMO (MoSMT3), E1 (MoAOS1 and MoUBA2) and E2 (MoUBC9) by double-joint PCR and homologous recombination. The single gene deletion mutants were generated by inserting a hygromycin resistance cassette, and a targeted double gene deletion mutant was generated by inserting a geneticin resistance cassette into the single gene deletion mutants. Deletion of the target genes was confirmed by Southern blotting and qRT-PCR (Figure 3). In previous studies, the levels of SUMO-modified substrates increased upon exposure to high temperature, nutrient, DNA damage, and oxidative stresses (Leach *et al*., 2011; Lewicki *et al.*, 2015). Therefore, thermal stress was applied to the wild type and to Δ*Moaos1*, Δ*Mouba2*, and Δ*Moubc9*. A plasmid (pHA-SMT3) was constructed by fusing MoSMT3 with an HA-tag and the native promoter of *MoSMT3*, and was transformed into the wild type and the single gene deletion mutants. The phenotypes of the deletion mutants and the wild type were unaffected by transformation. This suggests that HA-tagged MoSMT3 did not affect any other biological processes. Western blotting indicated that SUMOylation in the wild type was dramatically greater during mycelial growth and conidiation at high temperatures than at 25°C (Figure 4A and Figure 5). Oxidative stress (100 mM H_2O_2) also increased the level of SUMOylation (Figure 6)**.** However, the levels of SUMOylated proteins in the deletion mutants significantly decreased at high temperatures (Figure 4A). These results indicate that MoSMT3

acts as SUMO, and that MoAOS1, MoUBA2, and MoUBC9 are indispensable for SUMOylation in *M. oryzae*. Ubiquitination-associated components were included in the predicted SUMOylation machineries (Table 4). In contrast, deletion of MoSMT3, MoAOS1, MoUBA2, and MoUBC9 did not affect the level of ubiquitination, suggesting that they are specific to SUMOylation (Figure 7).

Interaction of the AOS1 and UBA2 subunits of E1 heterodimers is required for SUMO activation in eukaryotic organisms, including human, *Arabidopsis thaliana*, and *S. cerevisiae* (Gill, 2004). To determine whether MoAOS1 and MoUBA2 interact as heterodimers, we performed a yeast two-hybrid (Y2H) assay. AOS1 and UBA2 were cloned into both AD and BD vectors. After co-transformation, MoAOS1/MoUBA2 and MoUBA2/MoAOS1 were selected on SC-Leu/Trp medium and confirmed by PCR amplification. AOS1 and UBA2 strongly interacted on SC-Leu/Trp/His + 25 mM 3-amino-1,2,4-triazole (3AT) medium. The interactions of MoAOS1 and MoUBA2 were confirmed by X-gal assay (Figure 4B). These results indicate that MoAOS1 and MoUBA2 are subunits of the E1 activating enzyme complex, similar to ScAOS1 and ScUBA2.

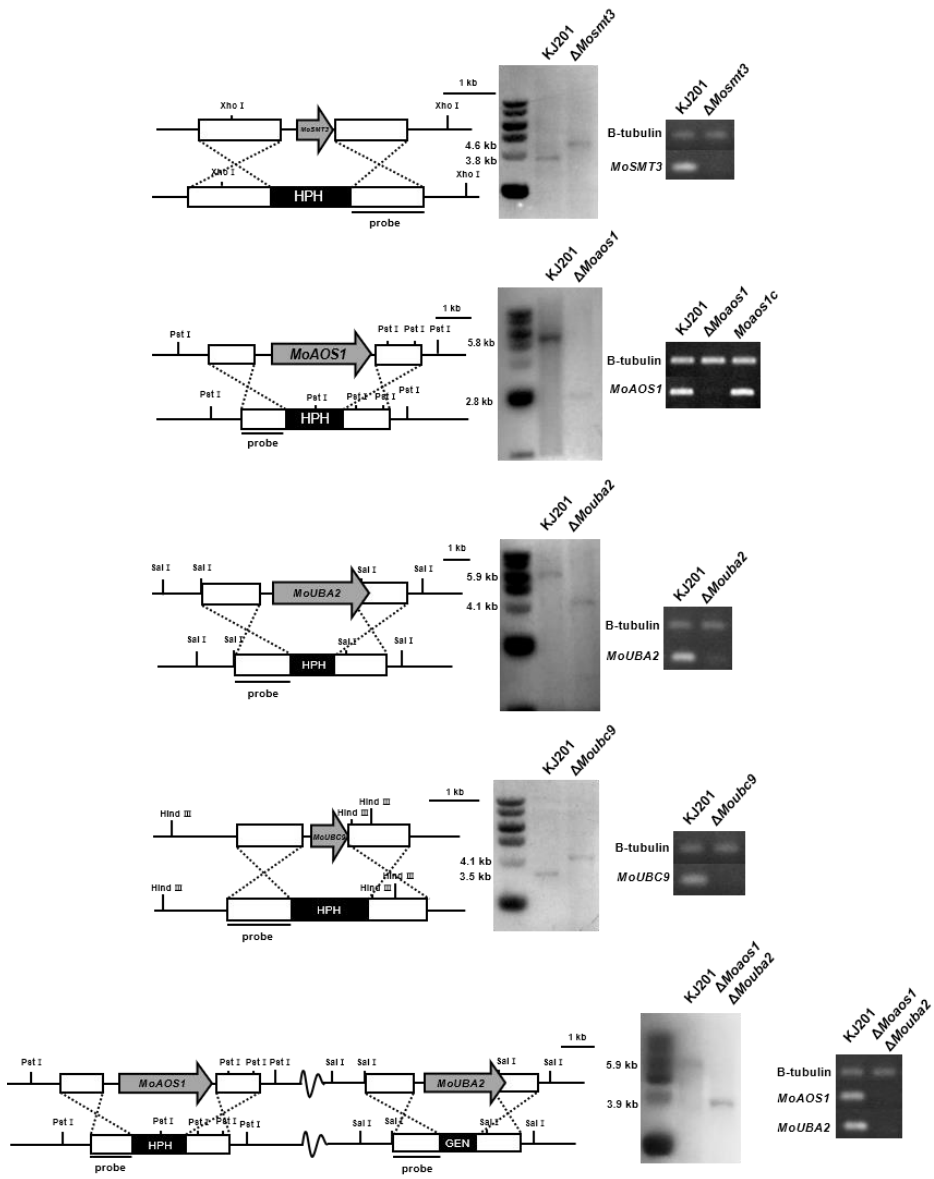

Figure 3. Southern blot analysis and RT-PCR of the deletion mutants. Genomic DNA of wild type and deletion mutants was extracted and digested with *Pst*I, *Sal*I, *Hin*dIII, or *Xho*I. The upstream or downstream construct of each gene was used as a probe for Southern blot analysis. Complementary DNA was synthesized from total RNA. β-tubulin was used for normalization.

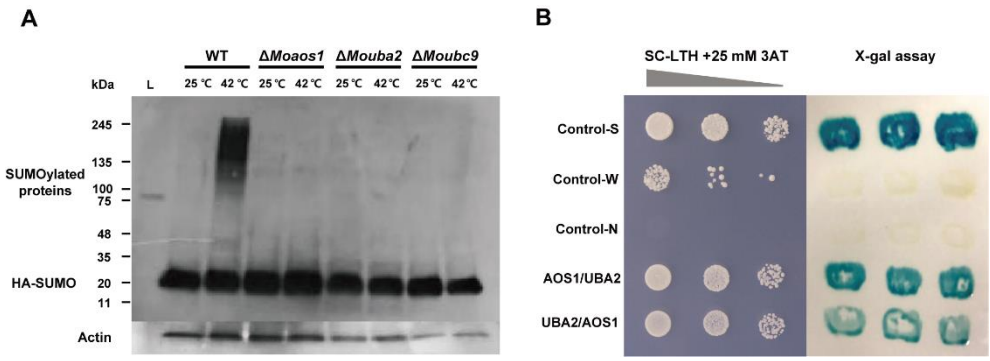

Figure 4. SUMOylated proteins in wild type, Δ*Moaos1*, Δ*Mouba2*, and Δ*Moubc9*, and yeast two-hybrid (Y2H) assay of MoAOS1 and MoUBA2. (A) Protein extracts from the wild type and deletion mutants were separated on SDS-PAGE and subjected to western blotting using an anti-HA antibody. (B) Y2H assay of the interaction of MoAOS1 and MoUBA2 (Control-S, strong interaction; Control-W, weak interaction; Control-N, no interaction).

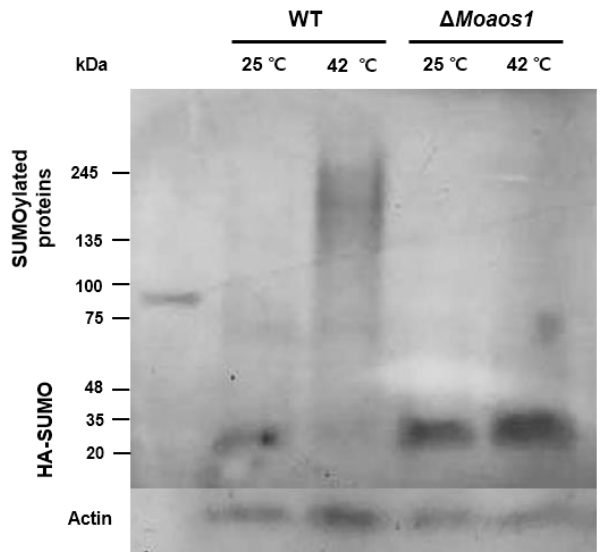

Figure 5. SUMOylation in wild type and Δ*Moaos1* during conidiation. Protein extract from the wild type during conidiation was separated on SDS-PAGE and subjected to Western analysis using an anti-HA antibody.

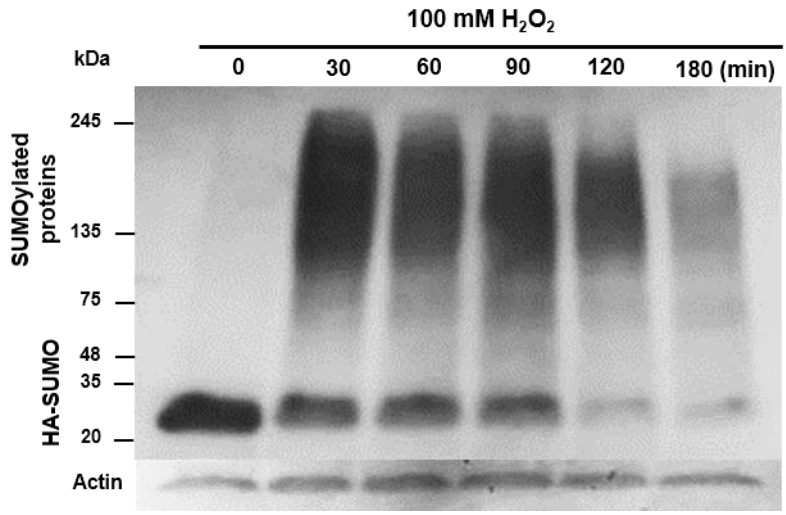

Figure 6. SUMOylated proteins in wild type under oxidative stress. Protein extract from the wild type treated with oxidative stress (100 mM H_2O_2) was separated on SDS-PAGE and subjected to Western blot analysis using an anti-HA antibody.

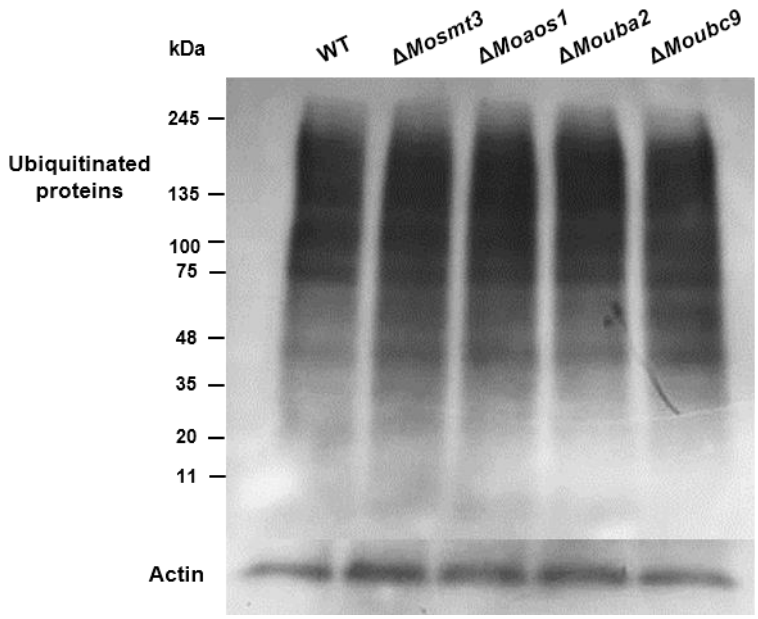

Figure 7. Ubiquitination in the wild type, Δ*Mosmt3,* Δ*Moaos1*, Δ*Mouba2* and Δ*Moubc9*. Protein extracts of wild type, Δ*Mosmt3,* Δ*Moaos1*, Δ*Mouba2* and Δ*Moubc9* were separated on SDS-PAGE, and subjected to Western blot analysis using an anti-ubiquitin (P4D1) antibody. Ubiquitination was not affected in all of the deletion mutants.

III. The SUMOylation machinery is essential for fungal development

To assess the biological function of SUMOylation in *M. oryzae*, we generated five Δ*Mosmt3*, two Δ*Moaos1*, two Δ*Mouba2*, eight Δ*Moaos1*Δ*Mouba2* and three ΔMoubc9 as explained above. The phenotype of each deletion mutant were same. We also generated complemented strains for all deletion mutants. In comparison to the wild type, all deletion mutants had significant defects in mycelial growth, conidia size, conidiation, conidial germination, and appressorium formation (Table 6). Mycelial growth of the deletion mutants reduced by 10~25% compared to the wild type (Table 6). The number of conidia was counted to quantitatively confirm the production of conidia. All of the deletion mutants produced 4~8 × 10^4/mL conidia, which was markedly lower than the wild type (4.8 × 10^5/mL) (Figure 8A). To identify the reason for reduced conidia formation, we observed conidiophores under a microscope. In the wild type, conidia were produced in a sympodial pattern on the conidiophores, but the deletion mutants produced none, one, or two conidia on the conidiophores (Figure 8B). To further assess the defects in conidiation, the expression levels of conidiation-related genes (*Cos1*, *Com1*, *Con7*, and *Hox2*) were examined in the wild type and the deletion mutants (Kim *et al*., 2009; Odenbach *et al.*, 2007; Yang *et al.*, 2010; Zhou *et al.*, 2009). However, the expression levels of *Cos1*, *Com1*, *Con7*, and *Hox2* did not differ between the wild type and the deletion mutants (Figure 8C).

In the wild type, 95% conidial germination and 92% appressorium formation

were observed on a hydrophobic surface after 2 and 8 h of incubation, respectively. In contrast, the frequencies of conidial germination and appressorium formation were 69~79% and 65~71% in the deletion mutants at 2 and 8 h, respectively (Figure 9). However, following incubation for a further 24 h, 84~89% of the deletion mutant conidia germinated and 70~77% of germ tubes formed appressoria (Table 7). Thus, we performed a conidia adhesion test to assess the cause of the delayed conidial germination and appressorium formation. Compared to the wild type (91%), conidia of the deletion mutants (54~76%) ineffectively attached to the hydrophobic surface of gelbond film. These results suggest ineffective conidial adhesion to be responsible for delayed conidial germination and appressorium formation in the deletion mutants. These pleiotropic phenotypes were recovered in the complemented strains (Figure 10, Table 6 and Table 7).

Table 6. Developmental phenotypes of the wild type, deletion mutants and complemented strains

Strain	Growth (mm)	Conidiation (10^4/ml)	Conidial size		Conidial germination (%)	Appressorium formation (%)
			Length (μm)	Width (μm)		
KJ201	61.5±0.4	48.3±3.8	31.1±3.2	9.8±1.6	95.3±0.6	92.3±1.2
Δ*Mosmt3*	45.9±3.3***	4.2±1.3***	26.5±3.7***	8.9±1.4	70.3±6.8***	70.7±0.6***
Mosmt3c[a]	62.4±2.0	43.7±4.2	30.5±3.0	8.7±1.0	92.3±0.6	90.0±1.0
Δ*Moaos1*	53.3±1.5***	8.4±0.5***	26.0±4.3***	9.1±1.6	75.7±3.1***	65.7±3.5***
Moaos1c	59.2±2.3	44.7±10.3	29.2±2.8	9.0±1.1	94.3±0.6	90.7±1.5
Δ*Mouba2*	53.3±0.5***	7.2±0.2***	25.7±5.1***	9.7±1.6	76.3±1.5***	71.3±4.7***
Mouba2c	60.2±1.2	39.7±5.7	29.1±2.9	8.3±1.0	95.3±1.2	93.0±4.4
Δ*Moaos1*Δ*Mouba2*	55.2±0.3***	8.2±0.9***	25.3±4.3***	8.3±1.1	69.3±2.5***	66.7±2.1***
Δ*Moubc9*	51.5±1.0***	4.3±0.3***	26.1±4.6***	8.9±1.2	69.0±3.6***	72.0±1.7***
Moubc9c	58.6±1.5	49.3±7.0	29.7±3.0	9.1±1.0	94.7±1.5	92.0±1.0

The significance was statistically determined by *t*-test with ***$p < 0.001$.

[a]Complemented strains were named after the gene name with c

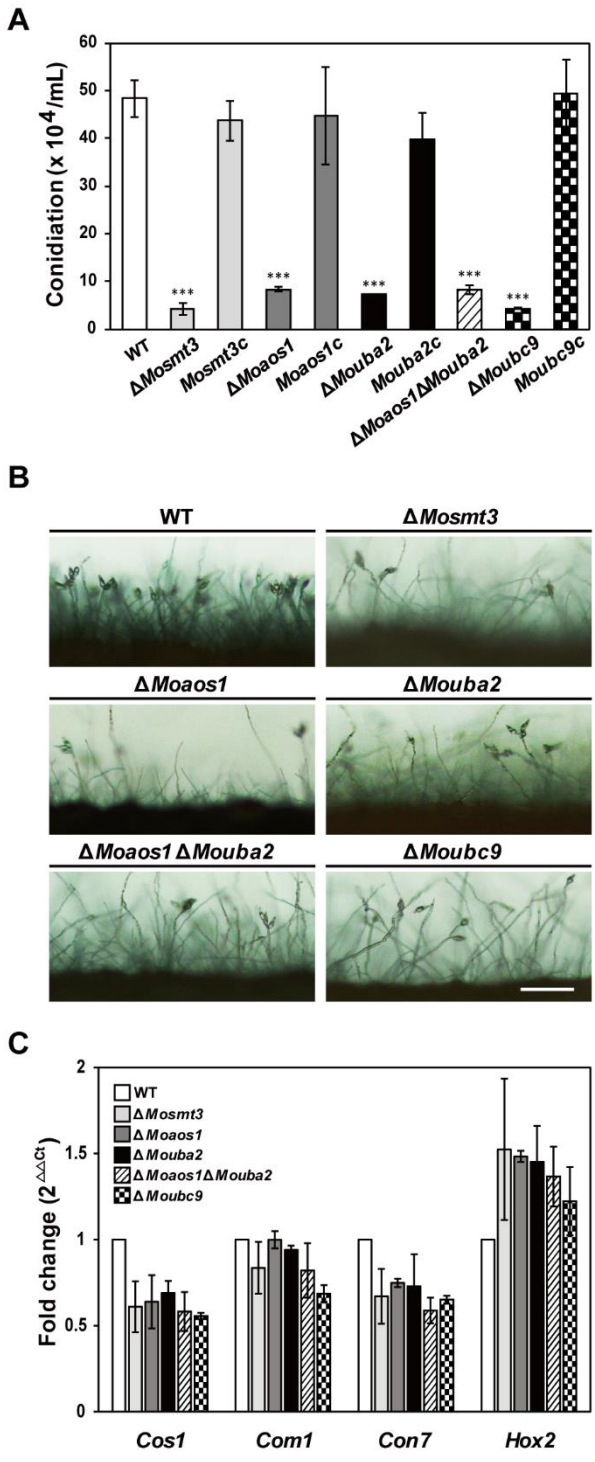
A
Conidiation (x 10^4/mL)
60
50
40
30
20
10
0
***
WT
ΔMosmt3
Mosmt3c
ΔMoaos1
Moaos1c
ΔMouba2
Mouba2c
ΔMoaos1ΔMouba2
ΔMoubc9
Moubc9c
B
WT
ΔMosmt3
ΔMoaos1
ΔMouba2
ΔMoaos1ΔMouba2
ΔMoubc9
C
Fold change (2^-ΔΔCt)
2
1.5
1
0.5
0
WT
ΔMosmt3
ΔMoaos1
ΔMouba2
ΔMoaos1ΔMouba2
ΔMoubc9
Cos1
Com1
Con7
Hox2

Figure 8. Conidiation of the wild type, Δ*Mosmt3*, Δ*Moaos1*, Δ*Mouba2*, and Δ*Moubc9* in *M. oryzae*. (A) Conidia of the wild type, deletion mutants, and complemented strains were collected from V8 agar after incubation for 7 d. Significance was determined by *t*-test (***$p < 0.001$). (B) Conidiogenesis on conidiophores was observed under a microscope. Scale bar, 100 μm. (C) Expression of conidiation-related genes during conidiation was quantified by qRT-PCR.

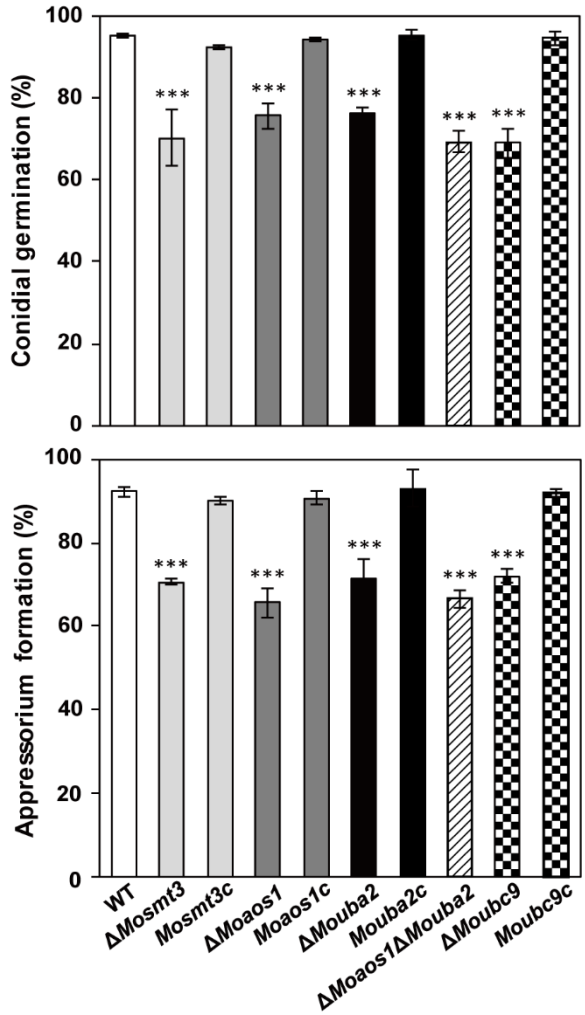

Figure 9. Conidial germination and appressorium formation of the wild type, Δ*Mosmt3*, Δ*Moaos1*, Δ*Mouba2*, and Δ*Moubc9* in *M. oryzae*. Percentage of conidial germination and appressorium formation on a hydrophobic surface after incubation for 2 and 8 h, respectively. Significance was determined by *t*-test (***$p < 0.001$).

Table 7. Conidial germination and appressorium formation of the wild type, deletion mutants and complemented strains after incubation for 2 h, 8 h and 24 h

Strain	Germination			Appressorium formation	
	2 h (%)	8 h (%)	24 h (%)	8 h (%)	24 h (%)
KJ201	95.3±0.6	95.7±2.5	96.3±1.2	92.3±1.2	94.3±0.6
Δ*Mosmt3*	70.3±6.8***	80.7±4.0**	89.3±2.1**	70.7±0.6***	77.3±3.1**
Mosmt3c	92.3±0.6	93.0±0.0	94.0±2.6	90.0±1.0	93.7±2.1
Δ*Moaos1*	75.7±3.1***	81.0±4.6**	85.7±3.5**	65.7±3.5***	72.7±2.5***
Moaos1c	94.3±0.6	95.7±2.1	96.0±1.0	90.7±1.5	93.0±1.0
Δ*Mouba2*	76.3±1.5***	87.3±8.7**	88.0±1.0**	71.3±4.7***	76.7±2.5***
Mouba2c	95.3±1.2	96.7±1.5	97.0±1.0	93.0±4.4	93.7±1.2
Δ*Moaos1*Δ*Mouba2*	69.3±2.5***	81.3±2.1**	84.0±2.6**	66.7±2.1***	70.0±1.7***
Δ*Moubc9*	69.0±3.6***	85.0±2.0**	87.7±2.3**	72.0±1.7***	73.7±4.2***
Moubc9c	94.7±1.5	95.7±1.2	96.0±1.0	92.0±1.0	93.0±1.7

The significance was statistically determined by *t*-test with $^{**}p < 0.05$ and $^{***}p < 0.001$.

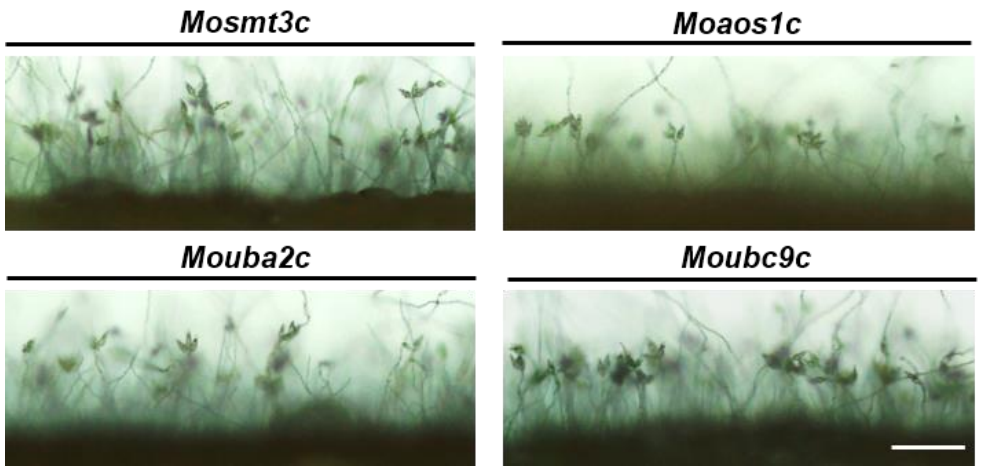

Figure 10. Defective conidiogenesis was recovered in complemented strains. Conidiogenesis on conidiophores was observed under a microscope. Scale bar, 100 μm.

IV. SUMOylation-associated genes are involved in septum formation

To examine the roles of SUMOylation-associated genes in septum formation in *M. oryzae*, conidia septa were observed under a microscope. In the wild type, most conidia (93%) had three cells, compared to 58~64% in the deletion mutants, in which 23~28% and 11~18% had two and one cell, respectively (Figure 11A). Moreover, conidia of the deletion mutants significantly shorter than those of the wild type (Table 6). The abnormal conidia morphology was recovered in the complemented strains (Figure 11A and Table 6). Hyphal growth of the deletion mutants was observed under a microscope after staining with Calcofluor white (CFW). In contrast to the wild type (60 μm), the cell length of hyphae between two septa was markedly shorter in the deletion mutants (45~50 μm) (Figure 11B and 11C). These results suggest that SUMOylation-associated genes are involved in septum formation of conidia and hyphae in *M. oryzae*.

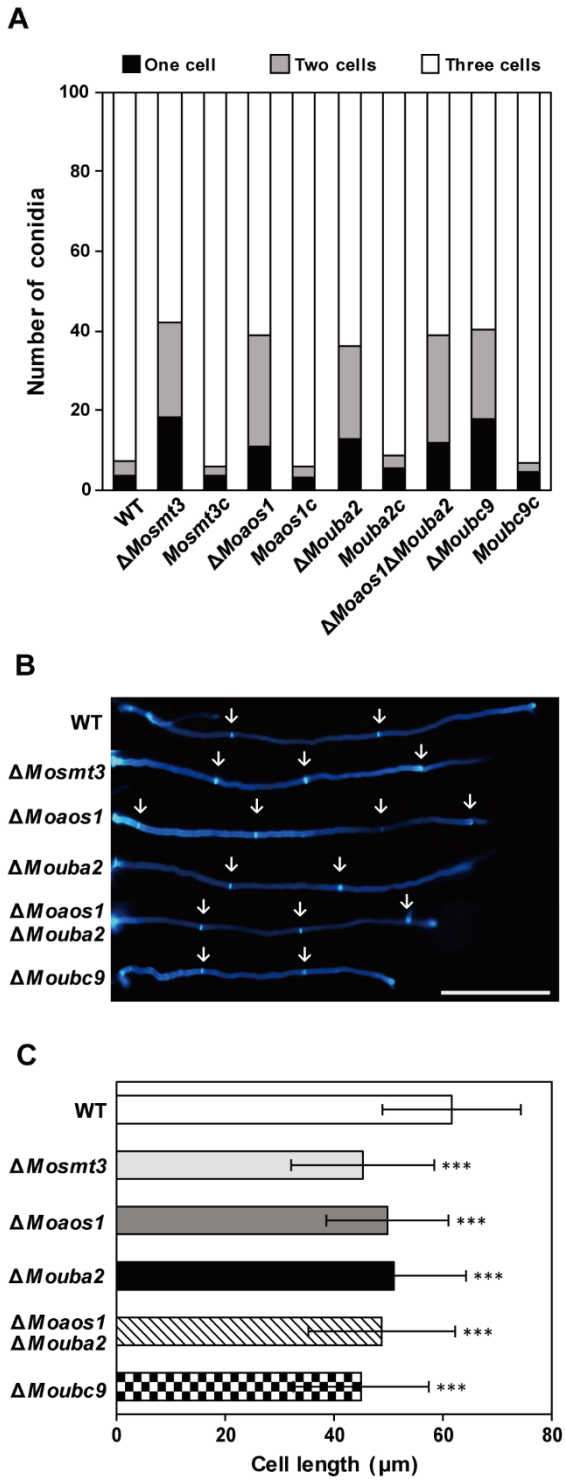
A
One cell
Two cells
Three cells
Number of conidia
100
80
60
40
20
0
WT
ΔMosmt3
Mosmt3c
ΔMoaos1
Moaos1c
ΔMouba2
Mouba2c
ΔMoaos1ΔMouba2
ΔMoubc9
Moubc9c
B
WT
ΔMosmt3
ΔMoaos1
ΔMouba2
ΔMoaos1
ΔMouba2
ΔMoubc9
C
WT
ΔMosmt3
ΔMoaos1
ΔMouba2
ΔMoaos1
ΔMouba2
ΔMoubc9
***
***
***
***
***
0
20
40
60
80
Cell length (μm)

Figure 11. Number of cells in conidia and cell length in hyphae. (A) Percentage of conidia with one, two, or three cells in the wild type, deletion mutants, and complemented strains. (B) Hyphae were stained with Calcofluor white (CFW) and observed under a fluorescence microscope. White arrows indicate septa of hyphae; scale bar, 200 μm. (C) Cell length of hyphae was measured using ImageJ. Significance was determined by *t*-test (***$p < 0.001$).

V. The SUMOylation components are important for stress tolerance

SUMO deletion mutants of *S. pombe* and *A. nidulans* are sensitive to heat and DNA damage stresses (Tanaka *et al.*, 1999; Wong *et al*., 2008). To investigate the role of SUMOylation-associated genes in stress resistance in *M. oryzae*, we measured mycelial growth after culturing the wild type and the deletion mutants to the following stresses: minimal agar medium (MMA) for nutrient starvation stress, 10 mM hydroxyurea and 0.05% methyl methanesulfonate for DNA damage stress, and 5 mM H_2O_2 and 3 mM methyl viologen for oxidative stress (Figure 12). The sensitivity of Δ*Mosmt3*, Δ*Moaos1*, Δ*Mouba2*, and Δ*Moaos1*Δ*Mouba2*, but not Δ*Moubc9*, to the nutrient starvation and oxidative stresses was greater than that of the wild type (Figure 13A, 13B and Figure 12). The sensitivity of all of the deletion mutants to DNA damage stress was also higher than that of the wild type (Figure 13A, 13B and Figure 12). These sensitivities to stress conditions were recovered in the complemented strains (Figure 12). These results indicate that SUMOylation components are involved in stress resistance.

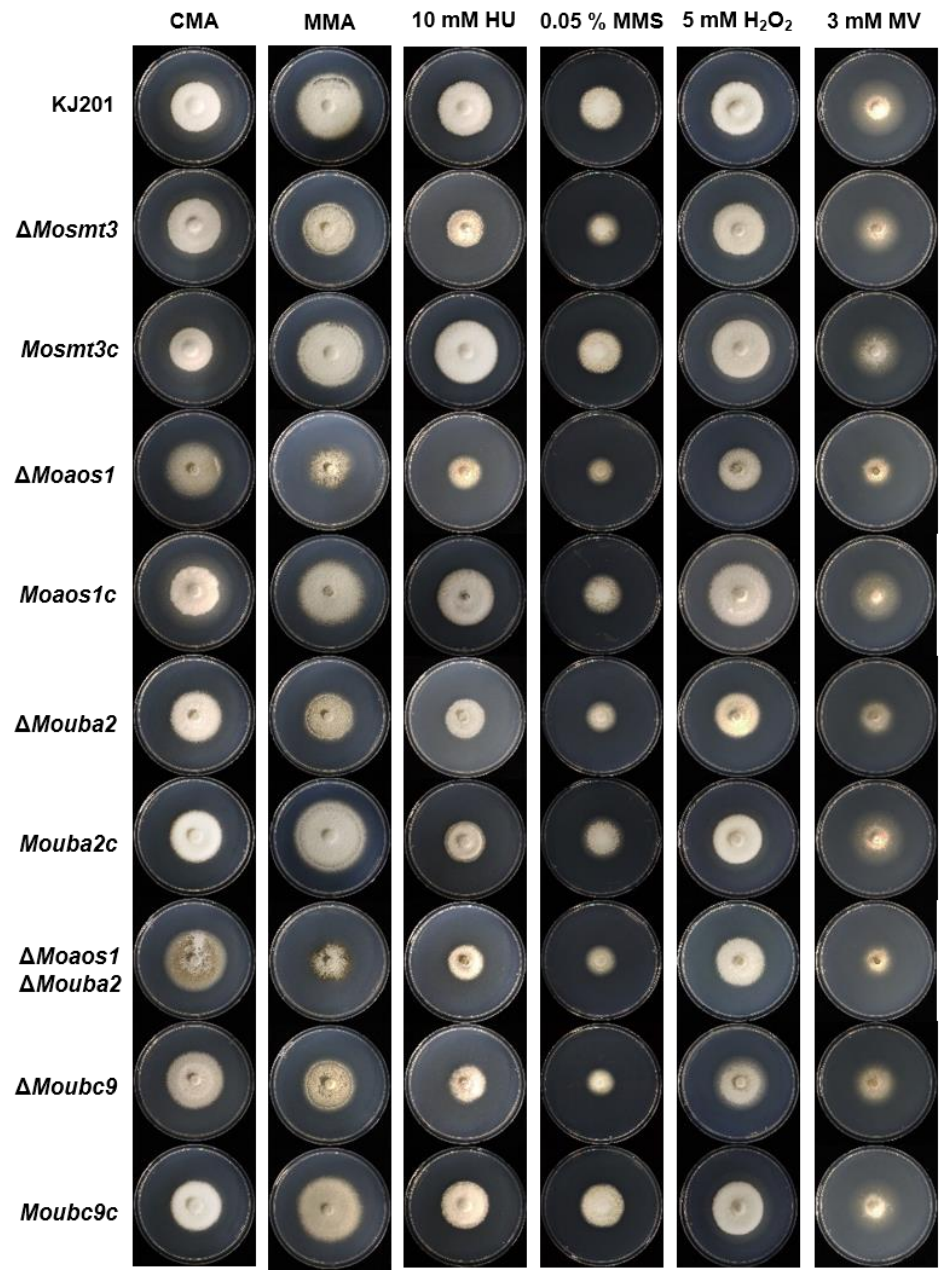

Figure 12. Mycelial growth and morphology under stress conditions. Strains were inoculated on nutrient starvation stress (MMA), DNA damage stress (10 mM hydroxyurea and 0.05% methyl methanesulfonate), and oxidative stress (5 mM H_2O_2 and 3 mM methyl viologen). Mycelial growth was measured 9 d after inoculation.

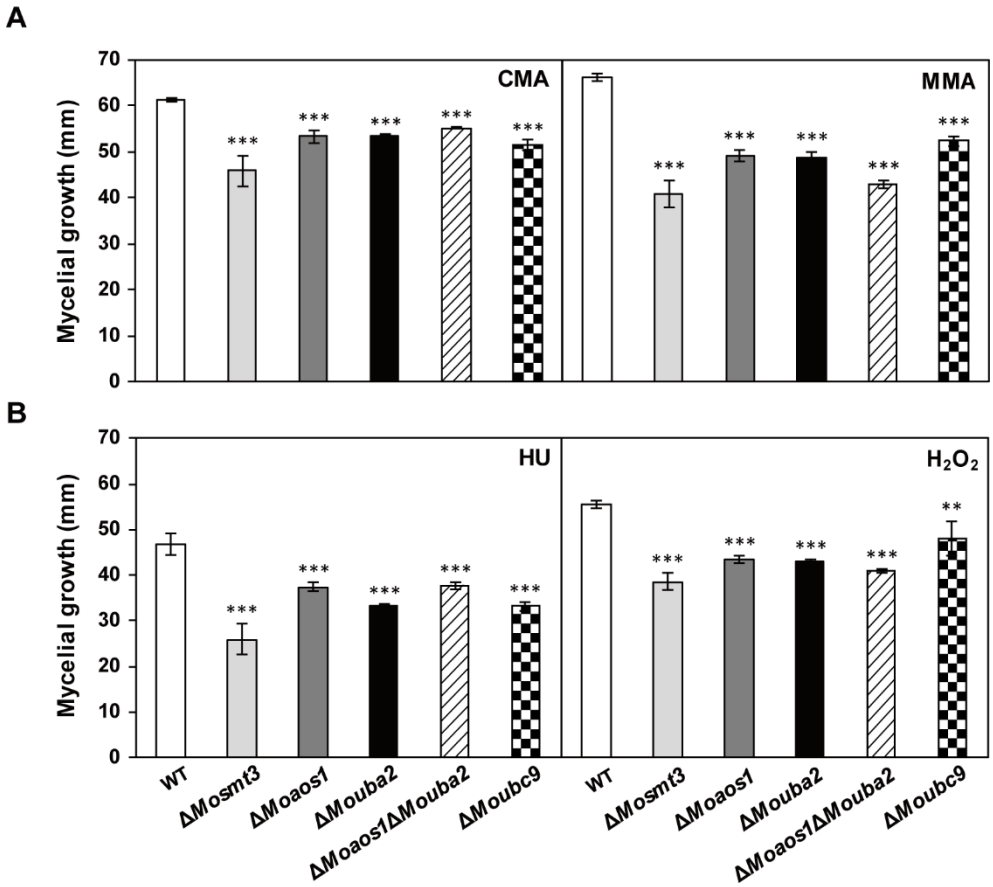

Figure 13. Mycelial growth under stress conditions. (A) Nutrient starvation stress on MMA and CMA. (B) DNA damage and oxidative stress on CMA containing 10 mM hydroxyurea and 5 mM H_2O_2, respectively. Significance was determined by *t*-test (**$p < 0.05$ and ***$p < 0.001$).

VI. SUMO, E1, and E2 are required for functional appressoria and fungal pathogenicity

SUMOylation is necessary for virulence in *C. glabrata*, an opportunistic pathogen of bloodstream infections (BSIs) (Gujjula *et al*., 2016). To investigate whether SUMOylation is required for the pathogenicity of *M. oryzae*, we performed spray and sheath inoculation assays. Conidial suspensions (5×10^4/mL) of the wild type and deletion mutants were sprayed onto 4-week-old rice plants of cultivar Nakdongbyeo. The wild type induced typical lesions, but the deletion mutants showed smaller and fewer lesions (Figure 14A). The disease lesion type was evaluated based on lesion sizes (Valent *et al*., 1991). In the wild type and complemented strains, disease lesion type was 4, but disease lesion type of deletion mutants was 1.5~2. The reduced pathogenicity of the deletion mutants was recovered in the complemented strains (Figure 14A). Penetration sites of appressoria were observed in rice sheath cells at 24 hours post-inoculation (hpi) under a microscope. In comparison to wild type, collapsed appressoria were frequently observed in the rice sheath cells inoculated by the deletion mutants. In the wild type, 62% of appressoria penetrated host cells, compared to 1~10% in the deletion mutants. In particular, the penetration function of Δ*Moaos1*Δ*Mouba2* reduced to the greatest extent (Figure 15A and 15B). These results suggest that the reduced pathogenicity was due to defective appressoria penetration. Therefore, we performed a cytorrhysis test to estimate the turgor pressure in appressoria. Matured appressoria of the wild type and deletion mutants were treated with glycerol solution (1, 3, and 5 M). In the wild type, the number of collapsed appressoria increased from 49% to 74% with

increasing glycerol concentration. However, the Δ*Mosmt3*, Δ*Mouba2*, Δ*Moaos1*Δ*Mouba2*, and Δ*Moubc9* mutants showed fewer collapsed appressoria than the wild type. (Figure 15C). These data suggest that the turgor pressure in appressoria of the deletion mutants was not less than that of the wild type. Therefore, to determine the cell wall integrity of appressoria, we performed plasmolysis assay using polyethylene glycol (PEG) of different molecular sizes. This showed that the plasmolysis to cytorrhysis ratios of the deletion mutants did not differ significantly from that of the wild type (data not shown).

Next, we performed a sheath inoculation assay to evaluate the cause of restricted lesion development on rice cells. Growth of invasive hyphae (IH) at 48 hpi was classified into three types: Type I for IH restricted to the primary infection cell, Type II for IH growth to adjacent cells, and Type III for extensive growth of IH to over adjacent cells. While 82% of the IH from the appressoria of the wild type were Type II and III, the corresponding values in the deletion mutants were only 31~43% (Figure 16B). Remarkably, IH growth significantly reduced in Δ*Moaos1*Δ*Mouba2* compared to the single gene deletion mutants (Figure 14B and 16B). The reduced penetration rate and invasive growth was recovered in the complemented strains (Figure 16A and 17). These results indicate that SUMOylation is important for functional appressoria and the pathogenicity of *M. oryzae*.

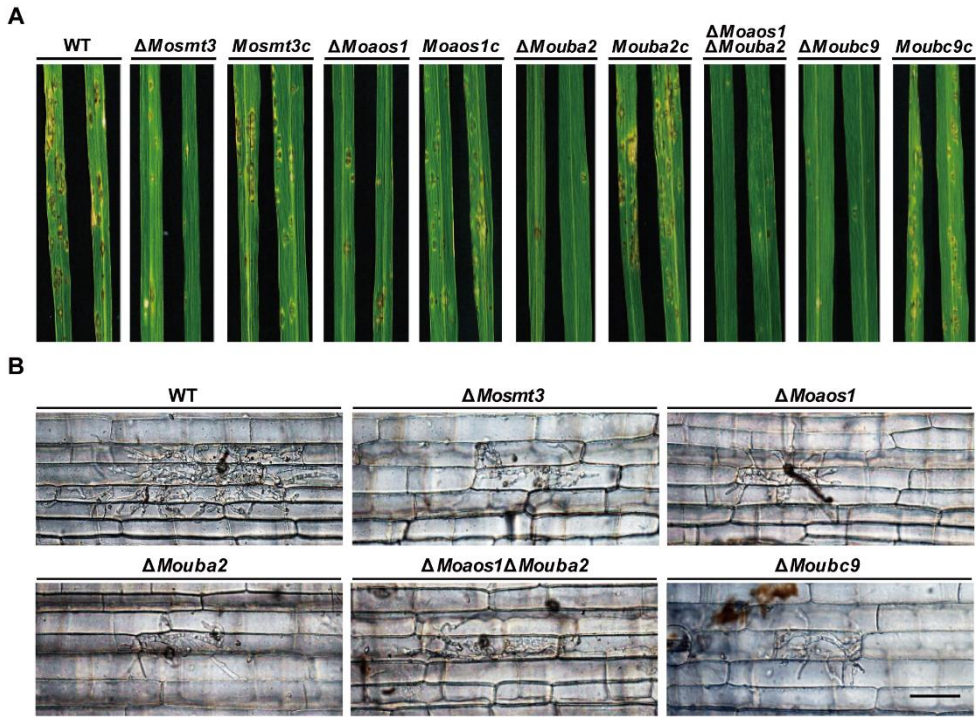

Figure 14. Pathogenicity assays by spray and sheath inoculation. (A) Conidial suspensions (5×10^4/mL) were sprayed onto 4-week-old rice seedlings, and lesions were observed at 6 dpi. (B) Conidial suspensions (2×10^4/mL) were inoculated onto rice sheath cells. Invasive hyphae (IH) growth was observed under a microscope at 48 hpi. Scale bar, 50 μm.

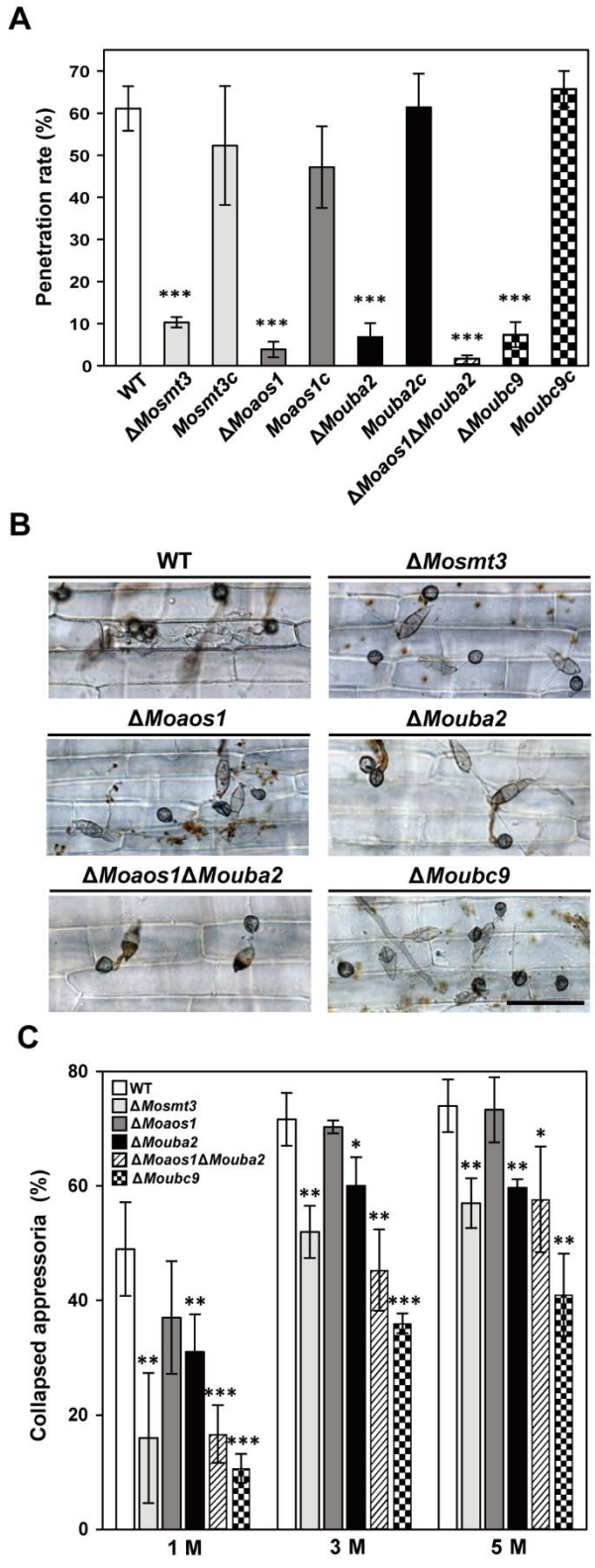
A
Penetration rate (%)
70
60
50
40
30
20
10
0
***
WT
ΔMosmt3
Mosmt3c
ΔMoaos1
Moaos1c
ΔMouba2
Mouba2c
ΔMoaos1ΔMouba2
ΔMoubc9
Moubc9c
B
WT
ΔMosmt3
ΔMoaos1
ΔMouba2
ΔMoaos1ΔMouba2
ΔMoubc9
C
Collapsed appressoria (%)
80
60
40
20
0
WT
ΔMosmt3
ΔMoaos1
ΔMouba2
ΔMoaos1ΔMouba2
ΔMoubc9
**
***
*
1 M
3 M
5 M

Figure 15. Penetration function of appressoria. (A and B) Rate of penetration of rice sheath cells by appressoria at 24 hpi. Scale bar, 50 μm. (C) The number of collapsed appressoria after treatment with 1, 3, and 5 M glycerol. Significance was determined by *t*-test (*$p < 0.01$, **$p < 0.05$ and ***$p < 0.001$).

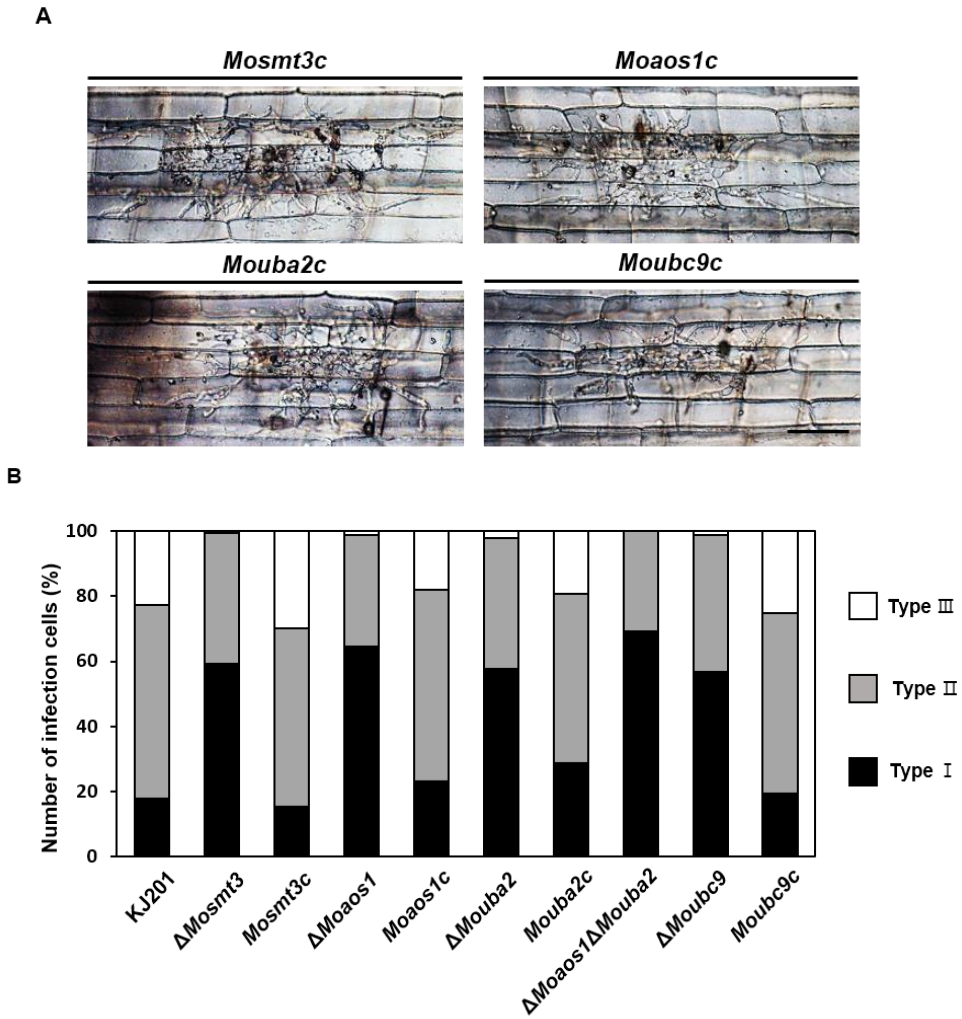

Figure 16. Invasive hyphae (IH) growth in the complemented strains. (A) Conidial suspensions (2×10^4/mL) of the complemented strains were inoculated onto 6-week-old rice sheath cells. IH growth was observed under a microscope at 48 hpi. Scale bar, 50 μm. (B) Growth of IH into neighboring cells was classified into three types: Type I for IH restricted to the primary infection cell; Type II for IH growth to adjacent cells; Type III for extensive growth of IH to over adjacent cells.

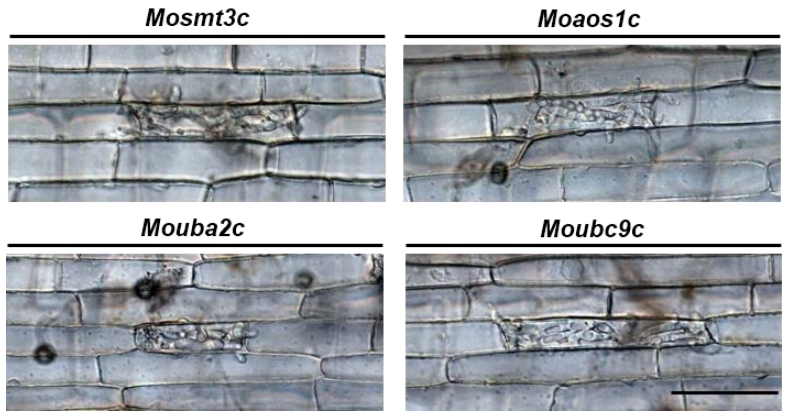

Figure 17. Penetration assay of the complemented strains. Conidial suspensions (2×10^4/mL) of the complemented strains were inoculated onto 6-week-old rice sheath cells. Penetration by appressoria at 24 hpi was observed under a microscope. Scale bar, 50 μm.

VII. SUMOylation-associated proteins are localized to the nucleus and cytoplasm

Most SUMOylation components are localized to the nucleus, and to a lesser extent the cytoplasm (Gill, 2004; Gillies *et al.*, 2016; Truong *et al.*, 2012). To observe the localization of SUMOylation components, we transformed the deletion mutants with plasmids containing monomeric red fluorescent protein (mRFP) fused with MoSMT3, MoAOS1, MoUBA2, or MoUBC9. Intracellular localization of MoSMT3, MoAOS1, MoUBA2, and MoUBC9 was observed under a fluorescence microscope. MoAOS1 and MoUBA2 largely localized to the nucleus, but MoSMT3 and MoUBC9 were present in the nucleus and cytoplasm (Figure 18A and 19). However, all four SUMOylation components predominantly localized in nucleus under oxidative stress condition (100 mM H_2O_2) (Figure 18B).

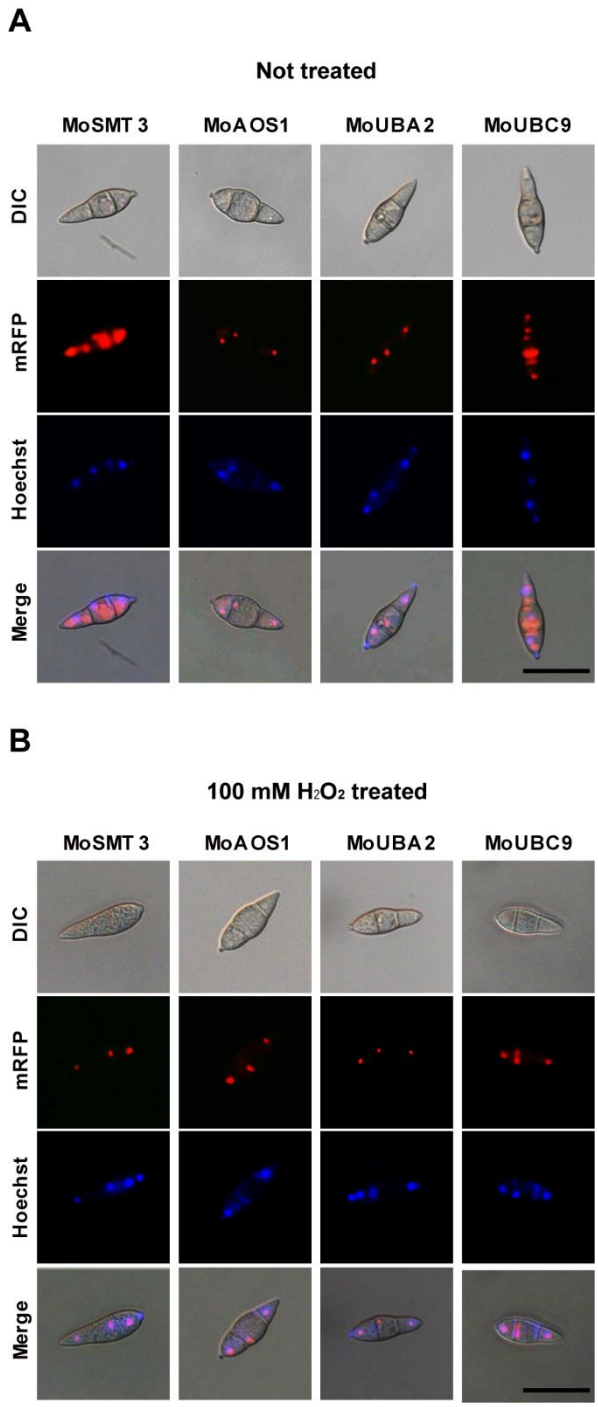
A
Not treated
MoSMT 3
MoAOS1
MoUBA 2
MoUBC9
DIC
mRFP
Hoechst
Merge
B
100 mM H2O2 treated
MoSMT 3
MoAOS1
MoUBA 2
MoUBC9
DIC
mRFP
Hoechst
Merge

Figure 18. Intracellular localization of SUMOylation components in *M. oryzae*. (A) MoAOS1 and MoUBA2 localized predominantly in the nucleus, but MoSMT3 and MoUBC9 localized to both the nucleus and the cytoplasm. Nuclei were stained with Hoechst 33342. Scale bar, 25 μm. (B) The four SUMOylation components predominantly localized in nucleus under oxidative stress condition (100 mM H_2O_2). Scale bar, 25 μm.

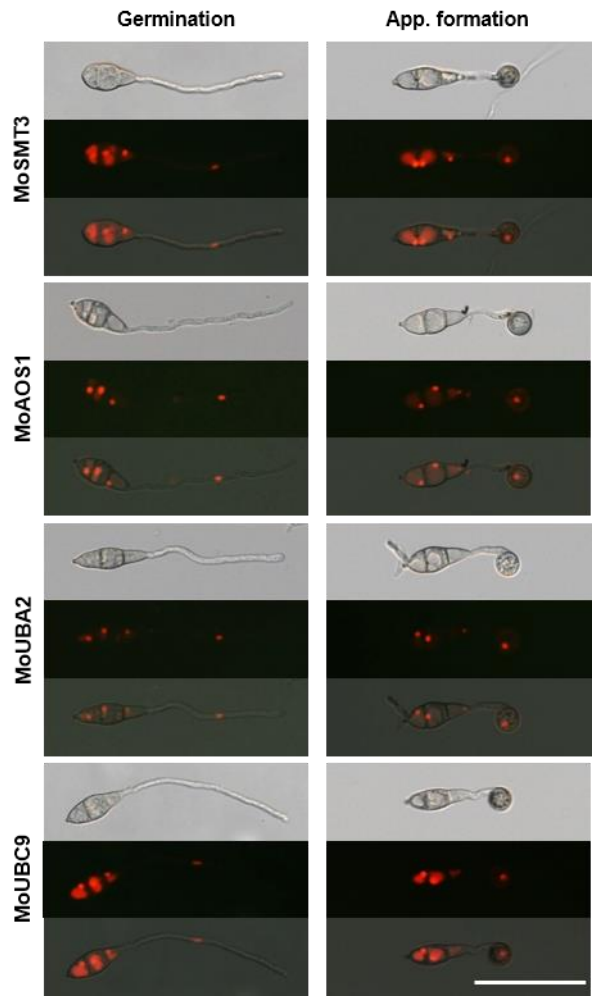

Figure 19. Intracellular localization of SUMOylation components during conidial germination and appressorium formation. MoAOS1, MoUBA2, MoSMT3 and MoUBC9 predominantly localized in nuclei during conidial germination and appressorium formation. Scale bar, 50 μm.

DISCUSSION

Since the discovery of SUMO in *S. cerevisiae* in 1995, SUMOylation has been investigated for over 20 years in other model organisms (Broday *et al.*, 2004; Ihara *et al.*, 2008; Meluh and Koshland, 1995; Nacerddine *et al.*, 2005; Nowak and Hammerschmidt, 2006; Nie *et al.*, 2009; Park *et al*., 2011). However, the machinery and functional roles of SUMOylation in plant pathogenic fungi are unclear. Recent advances in genome sequencing and molecular tools enable identification and functional characterization of SUMOylation components. We comprehensively analyzed SUMOylation in the model fungal plant pathogen, *M. oryzae*.

I. The SUMOylation machinery in fungi differs from other UBLs

Understanding of the function of SUMOylation machinery is limited to model species. Unlike ubiquitination, SUMOylation does not involve protein degradation, but instead enhances protein stability (Müller *et al*., 2001). A previous study on ubiquitination in *M. oryzae* identified SUMO, E1, and E2 enzymes as ubiquitination components using a domain search method (Oh *et al*., 2012). However, SUMOylation and other PTMs in yeast utilize different machineries (Johnson *et al*., 1997; Müller *et al*., 2001). Our phylogenetic analysis showed that MoAOS1 and MoUBA2 are clearly separated from the other E1 UBLs. The ubiquitin E2 enzyme (MGG_01756) in *M. oryzae* (Shi *et al.*, 2016) was either not grouped with MoUBC9 and ScUBC9, therefore, ubiquitination-related proteins formed their own clade. In

addition, the *MoSTM3, MoAOS1, MoUBA2,* and *MoUBC9* deletion mutants exhibited normal ubiquitination. Although all UBLs have the same ubiquitin-like domains, their diverse functions may be due to differences in their sequence. For example, the three-dimensional structure of human SUMO protein (12 kDa) is similar to that of ubiquitin (8.5 kDa) despite their 18% sequence similarity, and SUMO has an additional 15 amino acids at its N-terminal end (Melchior, 2000; Müller *et al*., 2001). Overall, our data indicated that SUMOylation components are not involved in ubiquitination, instead being involved in a unique PTM.

II. SUMOylation does not affect viability, but is essential for development of *M. oryzae*

S. cerevisiae deletion mutants, Δ*smt3*, Δ*aos1*, Δ*uba2*, and Δ*ubc9* were nonviable (Schwarz *et al.*, 1998). However, deletion of *MoSmt3*, *MoAos1*, *MoUba2*, and *MoUbc9* did not affect the viability of *M. oryzae*. SUMO deletion mutants of *A. nidulans*, *A. flavus*, *C. albicans*, and *S. pombe* were also viable (Leach *et al*., 2011; Nie *et al.*, 2016; Shayeghi *et al.*, 1997; Tanaka *et al*., 1999; Wong *et al*., 2008). Although fungi with deletions of SUMOylation-associated genes are viable, they are defective in development. This phenomenon may be, in part, due to presence of structural paralogs of the SUMOylation-associated proteins. Our phylogenetic analysis showed that the AOS1 clade contains only one protein in *S. cerevisiae*, but two proteins in other fungal species, such as *M. oryzae*, *A. nidulans*, and *S. pombe*. This additional gene may have the same functions as the AOS1 for SUMOylation. However, this speculation does not fully support the viability of other SUMOylation defective mutants of *M. oryzae* such as Δ*M osmt3*. Alternatively, this may be

explained by ‘centrality-lethality’ rule (Jeong *et al*., 2001). Further study is required to understand non-lethality of SUMOylation defective mutants including in fungi *M. oryzae*.

Like the other mutants of SUMOylation components in other organisms (Gujjula *et al*., 2016; Leach *et al*., 2011; Nie *et al*., 2016; Wong *et al*., 2008), Δ*Mosmt3*, Δ*Moaos1*, Δ*Mouba2*, Δ*Moaos1*Δ*Mouba2*, and Δ*Moubc9* showed significantly reduced mycelial growth, conidiation, conidial germination, appressorium formation, stress resistance, and pathogenicity. Deletion of the SUMOylation-associated genes was not lethal, unlike in *S. cerevisiae* and *C. glabrata* (Gujjula *et al*., 2016; Schwarz *et al*., 1998), but deletion of even one of these genes almost abolished SUMOylation in *M. oryzae*. These data indicate that all SUMOylation components are indispensable for SUMOylation. The pleiotrophic phenotypes of the deletion mutants may be due to dysfunction of SUMOylation, because SUMOylated proteins play roles in chromatin organization, transcriptional regulation, RNA biosynthesis, and ribosome biogenesis (Nie *et al.*, 2015).

III. SUMOylation is involved in conidiation

Conidiation is a key factor in outbreak of rice blast epidemics (Kim *et al*., 2009). In this study, conidiation was defective in the SUMOylation-associated gene deletion mutants. However, the expression of conidiation-related genes (*Cos1*, *Com1*, *Con7*, and *Hox2*) reported by others (Kim *et al*., 2009; Odenbach *et al*., 2007; Yang *et al*., 2010; Zhou *et al*., 2009), not significantly increased or decreased in the deletion mutants. These data suggest that conidiation is regulated not only at the transcriptional level, but also at the post-translational level. This is supported by the

fact that SUMO acts as a stabilizer of transcription factors (Rosonina *et al.*, 2017). Subsequent identification of SUMOylated motifs in conidiation-related genes further supports the hypothesis that modification of conidiation-related genes by SUMO controls conidiation in *M. oryzae.* Similar conidiation phenotypes were reported in SUMOylation mutants of *A. nidulans* and *A. flavus* (Nie *et al*., 2016; Wong *et al*., 2008). These results suggest that SUMOylation is crucial for conidiation in filamentous fungi.

IV. SUMOylation provides new insight into the function of appressoria and pathogenicity

In this study, spray inoculation of the deletion mutants resulted in generation of fewer and smaller lesions. The rates of penetration by appressoria of the deletion mutants significantly reduced, suggesting dysfunctionality of appressoria. A cytorrhysis assay indicated that the turgor pressure generation in the appressoria of deletion mutants were abnormal, but not less than the wild type. Furthermore, ratios of plasmolysis to cytorrhysis, indicating the cell wall integrity, were not significantly different between the deletion mutants and wild type. Re-modelling of actin cytoskeleton, along with turgor pressure and cell wall integrity, has been reported as another important factor for appressoria function (Dagdas *et al*., 2012). Deletion mutants of septin GTPase had defect in penetration and pathogenicity due to abnormal assembly of actin cytoskeleton in *M. oryzae* (Gupta *et al*., 2015). These septin proteins, MoSEP3, MoSEP4, MoSEP5 and MoSEP6, are predicted to be SUMOylated according to GPS-SUMO 2.0 (Zhao *et al*., 2014). These suggest that SUMOylation may affect other factors such as re-modelling of the actin cytoskeleton

rather than turgor generation and cell wall integrity of appressoria.

IH growth of the deletion mutants was significantly lower than that of the wild type. This may be due to the role of SUMOylation conferring tolerance to oxidative stress induced by plant (Feligioni and Nisticò, 2013). The fact that the degree of inhibition of mycelial growth of the deletion mutants by oxidative stress was greater than the wild type. Further study should evaluate the mechanism by which SUMOylation affects oxidative stress resistance and IH growth.

In this study, we found that the SUMOylation machinery differs from that involved in ubiquitination, and evaluated the roles of SUMOylation-associated genes in infection-related development, the stress response, and pathogenicity of *M. oryzae*. These findings provide not only new insight into SUMOylation as a unique PTM in fungi, but will also facilitate decipherment of the mechanisms of pathogenesis of *M. oryzae* and other fungal plant pathogens.

LITERATURE CITED

Aken, B. L., Ayling, S., Barrell, D., Clarke, L., Curwen, V., Fairley, S., Banet, J. F., Billis, K., Girón, C. G., Howe, T. H. K., Kähäri, A., Kokocinski, F., Martin, F. J., Murphy, D. N., Nag, R., Ruffier, M., Schuster, M., Tang, Y. A., Vogel J.-H., White, S., Zadissa, A., Flicek, P. and Searle, S. M. J. 2016. The Ensembl gene annotation system. Database (Oxford). 2016.

Alonso, A., Greenlee, M., Matts, J., Kline, J., Davis, K. J. and Miller, R. K. 2015. Emerging roles of sumoylation in the regulation of actin, microtubules, intermediate filaments, and septins. Cytoskeleton. 72:305-339.

Broday, L., Kolotuev, I., Didier, C., Bhoumik, A., Gupta, B. P., Sternberg, P. W., Podbilewicz, B. and Ronai, Z. 2004. The small ubiquitin-like modifier (SUMO) is required for gonadal and uterine-vulval morphogenesis in *Caenorhabditis elegans*. Genes Dev. 18:2380-2391.

Capella-Gutierrez, S., Silla-Martinez, J. M. and Gabaldon, T. 2009. trimAl: a tool for automated alignment trimming in large-scale phylogenetic analyses. Bioinformatics. 25:1972-1973.

Cherry, J. M. 2015. The *Saccharomyces* genome database: a tool for discovery. Cold Spring Harb Protoc. pdb top083840.

Choi, J., Cheong, K., Jung, K., Jeon, J., Lee, G.-W., Kang, S., Kim, S., Lee, Y.-W. and Lee, Y.-H. 2013. CFGP 2.0: a versatile web-based platform for supporting comparative and evolutionary genomics of fungi and oomycetes. Nucleic Acids Res. 41:D714-719.

Choi, J., Chung, H., Lee, G.-W., Koh, S.-K., Chae, S.-K. and Lee, Y.-H. 2015. Genome-wide analysis of hypoxia-responsive genes in the rice blast fungus, *Magnaporthe oryzae*. PloS ONE. 10:e0134939.

Dagdas, Y. F., Yoshino, K., Dagdas, G., Ryder, L. S., Bielska, E., Steinberg, G. and Talbot, N. J. 2012. Septin-mediated plant cell invasion by the rice blast fungus, *Magnaporthe oryzae*. Science. 336:1590-1595.

Dean, R. A. 1997. Signal pathways and appressorium morphogenesis. Annu. Rev. Phytopathol. 35:211-234.

Dean, R. A., Talbot, N. J., Ebbole, D. J., Farman, M. L., Mitchell, T. K., Orbach, M. J., Thon, M., Kulkarni, R., Xu, J.-R., Pan, H., Read, N. D., Lee, Y.-H., Carbone, I., Brown, D., Oh, Y., Donofrio, N., Jeong, J. S., Soanes, D. M., Djonovic, S., Kolomiets, E., Rehmeyer, C., Li, W., Harding, M., Kim, S., Lebrun, M.-H., Bohnert, H., Coughlan, S., Butler, J., Calvo, S., Ma, L.-J., Nicole, R., Purcell, S., Nusbaum, C., Galagan, J. E. and Birren, B. W. 2005. The genome sequence of the rice blast fungus *Magnaporthe grisea*. Nature. 434:980.

Denison, C., Rudner, A. D., Gerber, S. A., Bakalarski, C. E., Moazed, D. and Gygi, S. P. 2005. A proteomic strategy for gaining insights into protein sumoylation in yeast. Mol. Cell. Proteomics. 4:246-254.

Desterro, J. M., Rodriguez, M. S., Kemp, G. D. and Hay, R. T. 1999. Identification of the enzyme required for activation of the small ubiquitin-like protein SUMO-1. J. Bio. Chem. 274:10618-10624.

Dohmen, R. J. 2004. SUMO protein modification. Biochim. Biophys. Acta. 1695:113-131.

Ebbole, D. J. 2007. *Magnaporthe* as a model for understanding host-pathogen interactions. Annu. Rev. Phytopathol. 45:437-456.

Feligioni, M. and Nisticò, R. 2013. SUMO: a (oxidative) stressed protein. Neuromol. Med. 15:707-719.

Flaishman, M., Hwang, C.-S. and Kolattukudy, P. 1995. Involvement of protein phosphorylation in the induction of appressorium formation in *Colletotrichum gloeosporioides* by its host surface wax and ethylene. Physiol. Mol. Plant Pathol. 47:103-117.

Gill, G. 2004. SUMO and ubiquitin in the nucleus: different functions, similar mechanisms? Genes Dev. 18:2046-2059.

Gillies, J., Hickey, C. M., Su, D., Wu, Z., Peng, J. and Hochstrasser, M. 2016. SUMO pathway modulation of regulatory protein binding at the ribosomal DNA locus in *Saccharomyces cerevisiae*. Genetics. 202:1377-1394.

Goff, S. A., Ricke, D., Lan, T. H., Presting, G., Wang, R., Dunn, M., Glazebrook, J., Sessions, A., Oeller, P., Varma, H., Hadley, D., Hutchison, D., Martin, C., Katagiri, F., Lange, B. M., Moughamer, T., Xia, Y., Budworth, P., Zhong, J., Miquel, T., Paszkowski, U., Zhang, S., Colbert, M., Sun, W. L., Chen, L., Cooper, B., Park, S., Wood, T. C., Mao, L., Quail, P., Wing, R., Dean, R., Yu, Y., Zharkikh, A., Shen, R., Sahasrabudhe, S., Thomas, A., Cannings, R., Gutin, A., Pruss, D., Reid, J., Tavtigian, S., Mitchell, J., Eldredge, G., Scholl, T., Miller, R. M., Bhatnagar, S., Adey, N., Rubano, T., Tusneem, N., Robinson, R., Feldhaus, J., Macalma, T., Oliphant, A. and Briggs, S. 2002. A draft sequence of the rice genome (*Oryza sativa L*. ssp. *japonica*). Science. 296:92-100.

Goh, J., Jeon, J., Kim, K. S., Park, J., Park, S.-Y. and Lee, Y.-H. 2011. The PEX7-mediated peroxisomal import system is required for fungal development and pathogenicity in *Magnaporthe oryzae*. PLoS ONE. 6:e28220.

Goh, J., Kim, K. S., Park, J., Jeon, J., Park, S.-Y. and Lee, Y.-H. 2011. The cell cycle gene *MoCDC15* regulates hyphal growth, asexual development and plant infection in the rice blast pathogen *Magnaporthe oryzae*. Fungal Genet. Biol. 48:784-792.

Gujjula, R., Veeraiah, S., Kumar, K., Thakur, S. S., Mishra, K. and Kaur, R. 2016. Identification of components of the SUMOylation machinery in *Candida glabrata*: role of the deSUMOylation peptidase *CgUlp2* in virulence. J. Biol. Chem. 291:19573-19589.

Guo, M., Gao, F., Zhu, X., Nie, X., Pan, Y. and Gao, Z. 2015. MoGrr1, a novel F-box protein, is involved in conidiogenesis and cell wall integrity and is critical for the full virulence of *Magnaporthe oryzae*. Appl. Microbiol. Biotechnol. 99:8075-8088.

Gupta, Y. K., Dagdas, Y. F., Martinez-Rocha, A. L., Kershaw, M. J., Littlejohn, G. R., Ryder, L. S., Sklenar, J., Menke, F. and Talbot, N. J. 2015. Septin-dependent assembly of the exocyst is essential for plant infection by *Magnaporthe oryzae*. The Plant Cell. 27:3277-3289.

Harting, R., Bayram, Ö., Laubinger, K., Valerius, O. and Braus, G. H. 2013. Interplay of the fungal sumoylation network for control of multicellular development. Mol. Microbiol. 90:1125-1145.

Hickey, C. M., Wilson, N. R. and Hochstrasser, M. 2012. Function and regulation of SUMO proteases. Nat. Rev. Mol. Cell Biol. 13:755-766.

Ihara, M., Stein, P. and Schultz, R. M. 2008. UBE2I (UBC9), a SUMO-conjugating enzyme, localizes to nuclear speckles and stimulates transcription in mouse oocytes. Biol. Reprod. 79:906-913.

Iyer, G. and Chattoo, B. B. 2003. Purification and characterization of laccase from the rice blast fungus, *Magnaporthe grisea*. FEMS Microbiol. Lett. 227:121-126.

Jeon, J., Choi, J., Lee, G.-W., Park, S.-Y., Huh, A., Dean, R. A., and Lee, Y.-H. 2015. Genome-wide profiling of DNA methylation provides insights into epigenetic regulation of fungal development in a plant pathogenic fungus, *Magnaporthe oryzae*. Sci. Rep. 5:1-11.

Jeong, H., Mason, S. P., Barabási, A. L. and Oltvai, Z. N. 2001. Lethality and centrality in protein networks. Nature. 411:41.

Johnson, E. S. and Blobel, G. 1997. Ubc9p is the conjugating enzyme for the ubiquitin-like protein Smt3p. J. Biol. Chem. 272:26799-26802.

Johnson, E. S. and Blobel, G. 1999. Cell cycle–regulated attachment of the ubiquitin-related protein SUMO to the yeast septins. J. Cell Biol. 147:981-994.

Johnson, E. S., Schwienhorst, I., Dohmen, R. J. and Blobel, G. 1997. The ubiquitin-like protein Smt3p is activated for conjugation to other proteins by an Aos1p/Uba2p heterodimer. EMBO J. 16:5509-5519.

Kang, S. H., Khang, C. H. and Lee, Y.-H. 1999. Regulation of cAMP-dependent protein kinase during appressorium formation in *Magnaporthe grisea*. FEMS Microbiol. Lett. 170:419-423.

Katoh, K. and Standley, D. M. 2013. MAFFT multiple sequence alignment software

version 7: improvements in performance and usability. Mol. Biol. Evol. 30:772-780.

Kim, S., Park, S.-Y., Kim, K. S., Rho, H.-S., Chi, M.-H., Choi, J., Park, J., Kong, S., Park, J., Goh, J. and Lee, Y.-H. 2009. Homeobox transcription factors are required for conidiation and appressorium development in the rice blast fungus *Magnaporthe oryzae*. PLoS Genet. 5:e1000757.

Kong, S., Park, S.-Y. and Lee, Y.-H. 2015. Systematic characterization of the bZIP transcription factor gene family in the rice blast fungus, *Magnaporthe oryzae*. Environ. Microbiol. 17:1425-1443.

Lau, G. W. and Hamer, J. E. 1998. Acropetal: a genetic locus required for conidiophore architecture and pathogenicity in the rice blast fungus. Fungal Genet. Biol. 24:228-239.

Leach, M. D., Stead, D. A., Argo, E. and Brown, A. J. 2011. Identification of sumoylation targets, combined with inactivation of SMT3, reveals the impact of sumoylation upon growth, morphology, and stress resistance in the pathogen *Candida albicans*. Mol. Bio. Cell. 22:687-702.

Lee, J., Lee, T., Lee, Y.-W., Yun, S.-H.. and Turgeon, B. G. 2003. Shifting fungal reproductive mode by manipulation of mating type genes: obligatory heterothallism of *Gibberella zeae*. Mol. Microbiol. 50:145-152.

Lewicki, M. C., Srikumar, T., Johnson, E. and Raught, B. 2015. The *S. cerevisiae* SUMO stress response is a conjugation-deconjugation cycle that targets the transcription machinery. J. Proteom. 118:39-48.

Liu, T.-B. and Xue, C. 2011. The ubiquitin-proteasome system and F-box proteins in

pathogenic fungi. Mycobiology. 39:243-248.

Lomeli, H. and Vazquez, M. 2011. Emerging roles of the SUMO pathway in development. Cell. Mol. Life Sci. 68:4045-4064.

Martienssen, R. A. and Colot, V. 2001. DNA methylation and epigenetic inheritance in plants and filamentous fungi. Science. 293:1070-1074.

Melchior, F. 2000. SUMO-nonclassical ubiquitin. Annu. Rev. Cell Dev. Biol. 16:591-626.

Meluh, P. B. and Koshland, D. 1995. Evidence that the MIF2 gene of Saccharomyces cerevisiae encodes a centromere protein with homology to the mammalian centromere protein CENP-C. Mol. Biol. Cell. 6:793-807.

Müller, S., Hoege, C., Pyrowolakis, G. and Jentsch, S. 2001. SUMO, ubiquitin's mysterious cousin. Nat. Rev. Mol. Cell Biol. 2:202.

Mullen, J. R., Chen, C. F. and Brill, S. J. 2010. Wss1 is a SUMO-dependent isopeptidase that interacts genetically with the Slx5-Slx8 SUMO-targeted ubiquitin ligase. Mol. Cell Biol. 30:3737-3748.

Nacerddine, K., Lehembre, F., Bhaumik, M., Artus, J., Cohen-Tannoudji, M., Babinet, C., Pandolfi, P. P. and Dejean, A. 2005. The SUMO pathway is essential for nuclear integrity and chromosome segregation in mice. Dev. Cell. 9:769-779.

Nie, M., Vashisht, A. A., Wohlschlegel, J. A. and Boddy, M. N. 2015. High confidence fission yeast SUMO conjugates identified by tandem denaturing affinity purification. Sci. Rep. 5:1-8.

Nie, M., Xie, Y., Loo, J. A. and Courey, A. J. 2009. Genetic and proteomic evidence for roles of Drosophila SUMO in cell cycle control, Ras signaling, and early

pattern formation. PloS ONE. 4:e5905.

Nie, X., Yu, S., Qiu, M., Wang, X., Wang, Y., Bai, Y., Zhang, F. and Wang, S. 2016. *Aspergillus flavus* SUMO contributes to fungal virulence and toxin attributes. J. Agric. Food Chem. 64:6772-6782.

Nowak, M. and Hammerschmidt, M. 2006. Ubc9 regulates mitosis and cell survival during zebrafish development. Mol. Biol. Cell. 17:5324-5336.

Odenbach, D., Breth, B., Thines, E., Weber, R. W., Anke, H. and Foster, A. J. 2007. The transcription factor Con7p is a central regulator of infection-related morphogenesis in the rice blast fungus *Magnaporthe grisea*. Mol. Microbiol. 64:293-307.

Oh, Y., Franck, W. L., Han, S.-O., Shows, A., Gokce, E., Muddiman, D. C. and Dean, R. A. 2012. Polyubiquitin is required for growth, development and pathogenicity in the rice blast fungus *Magnaporthe oryzae*. PloS ONE. 7:e42868.

Park, H. J., Kim, W. Y., Park, H. C., Lee, S. Y., Bohnert, H. J. and Yun, D. J. 2011. SUMO and SUMOylation in plants. Mol. Cells. 32:305-316.

Pasupala, N., Easwaran, S., Hannan, A., Shore, D. and Mishra, K. 2012. The SUMO E3 ligase Siz2 exerts a locus-dependent effect on gene silencing in *Saccharomyces cerevisiae*. Eukaryot. Cell. 11:452-462.

Prakash, C., Manjrekar, J. and Chattoo, B. B. 2016. Skp1, a component of E3 ubiquitin ligase, is necessary for growth, sporulation, development and pathogenicity in rice blast fungus (*Magnaporthe oryzae*). Mol. Plant Pathol. 17:903-919.

Raorane, M. L., Mutte, S. K., Varadarajan, A. R., Pabuayon, I. M. and Kohli, A. 2013.

Protein SUMOylation and plant abiotic stress signaling: in silico case study of rice RLKs, heat-shock and Ca^{2+}-binding proteins. Plant Cell Rep. 32:1053-1065.

Rosonina, E., Akhter, A., Dou, Y., Babu, J. and Sri Theivakadadcham, V. S. 2017. Regulation of transcription factors by sumoylation. Transcription. 8:220-231

Saracco, S. A., Miller, M. J., Kurepa, J. and Vierstra, R. D. 2007. Genetic analysis of SUMOylation in *Arabidopsis*: conjugation of SUMO1 and SUMO2 to nuclear proteins is essential. Plant Physiol. 145:119-134.

Schwarz, S. E., Matuschewski, K., Liakopoulos, D., Scheffner, M. and Jentsch, S. 1998. The ubiquitin-like proteins SMT3 and SUMO-1 are conjugated by the UBC9 E2 enzyme. Proc. Natl. Acad. Sci. U.S.A. 95:560-564.

Shayeghi, M., Doe, C. L., Tavassoli, M. and Watts, F. Z. 1997. Characterisation of *Schizosaccharomyces pombe* rad31, a UBA-related gene required for DNA damage tolerance. Nucleic Acids Res. 25:1162-1169.

Shi, H.-B., Chen, G.-Q., Chen, Y.-P., Dong, B., Lu, J.-P., Liu, X.-H. and Lin F.-C. 2016. MoRad6-mediated ubiquitination pathways are essential for development and pathogenicity in *Magnaporthe oryzae*. Environ. Microbiol. 18:4170-4187.

Sriramachandran, A. M. and Dohmen, R. J. 2014. SUMO-targeted ubiquitin ligases. Biochim. Biophys. Acta. 1843:75-85.

Stamatakis, A. 2014. RAxML version 8: a tool for phylogenetic analysis and post-analysis of large phylogenies. Bioinformatics. 30:1312-1313.

Tanaka, K., Nishide, J., Okazaki, K., Kato, H., Niwa, O., Nakagawa, T., Matsuda, H., Kawamukai, M. and Murakami, Y. 1999. Characterization of a fission yeast

SUMO-1 homologue, pmt3p, required for multiple nuclear events, including the control of telomere length and chromosome segregation. Mol. Cell. Biol. 19:8660-8672.

Tatham, M. H., Jaffray, E., Vaughan, O. A., Desterro, J. M., Botting, C. H., Naismith, J. H. and Hay, R. T. 2001. Polymeric chains of SUMO-2 and SUMO-3 are conjugated to protein substrates by SAE1/SAE2 and Ubc9. J. Biol. Chem. 276:35368-35374.

Truong, K., Lee, T. D., Li, B. and Chen, Y. 2012. Sumoylation of SAE2 C terminus regulates SAE nuclear localization. J. Biol. Chem. 287:42611-42619.

Valent, B. 1990. Rice blast as a model system for plant pathology. Phytopathology. 80:33-36.

Valent, B., Farrall, L. and Chumley, F. G. 1991. *Magnaporthe grisea* genes for pathogenicity and virulence identified through a series of backcrosses. Genetics. 127:87-101.

Wang, H. L., Kim, S. H., Siu, H. and Breuil, C. 1999. Transformation of sapstaining fungi with hygromycin B resistance plasmids pAN 7-1 and pCB1004. Mycol. Res. 103:77-80.

Watts, F. Z. 2013. Starting and stopping SUMOylation. What regulates the regulator? Chromosoma. 122:451-463.

Wong, K. H., Todd, R. B., Oakley, B. R., Oakley, C. E., Hynes, M. J. and Davis, M. A. 2008. Sumoylation in *Aspergillus nidulans*: sumO inactivation, overexpression and live-cell imaging. Fungal Genet. Biol. 45:728-737.

Yang, J., Zhao, X., Sun, J., Kang, Z., Ding, S., Xu, J.-R. and Peng, Y. L. 2010. A

novel protein Com1 is required for normal conidium morphology and full virulence in *Magnaporthe oryzae*. Mol. Plant Microbe Interact. 23:112-123.

Yun, S.-H. 1998. Molecular genetics and manipulation of pathogenicity and mating determinants in *Mycosphaerella zeae-maydis* and *Cochliobolus heterostrophus*. Cornell University, Jan.

Zhao, Q., Xie, Y., Zheng, Y., Jiang, S., Liu, W., Mu, W., Liu, Z., Zhao, Y., Xue, Y. nad Ren, J. 2014. GPS-SUMO: a tool for the prediction of sumoylation sites and SUMO-interaction motifs. Nucleic Acids Res. 42:W325-W330.

Zhao, X., Mehrabi, R. and Xu, J.-R. 2007. Mitogen-activated protein kinase pathways and fungal pathogenesis. Eukaryot. Cell. 6:1701-1714.

Zhou, Z., Li, G., Lin, C. and He, C. 2009. Conidiophore stalk-less1 encodes a putative zinc-finger protein involved in the early stage of conidiation and mycelial infection in *Magnaporthe oryzae*. Mol. Plant Microbe Interact. 22:402-410.

CHAPTER III

F-box only and CUE proteins are crucial ubiquitination-associated components for conidiation and pathogenicity in the rice blast fungus, *Magnaporthe oryzae*

This chapter was published in Fungal Genetics and Biology.

Lim, Y.-J. and Lee, Y.-H. (2020) *Fungal Genet. and Biol*. 144:103473.

ABSTRACT

Ubiquitination, an important process in post-translational modification, regulates various mechanisms in eukaryotes including protein degradation and interaction, cell cycle, stress response, and pathogenicity. The Skp1/Cullin/F-box and the endoplasmic reticulum-associated degradation (ERAD) complexes, RING E3 ligase complexes, are involved in ubiquitin-mediated proteolysis and protein quality control. The F-box protein has FBXO (F-box only or others), FBXW (with WD40), and FBXL (with LRR) classes depending on which interaction domain is present on the C-terminus. The ubiquitin system component cue (CUE) protein is a key factor of ERAD. However, the biological roles of FBXO and CUE proteins are largely unknown in plant pathogenic fungi including *Magnaporthe oryzae*. To elucidate the roles of FBXO and CUE proteins in fungal development and pathogenicity, *MoFBX15* and *MoCUE1* were functionally characterized in *M. oryzae*. Two ubiquitination-associated genes were crucial for conidiation, alkaline stress tolerance, and pathogenicity in *M. oryzae*. In particular, *MoCUE1* was important for ER stress response and localization and translocation of cytoplasmic effectors. Moreover, ubiquitination and SUMOylation levels decreased and transcript levels of deSUMOylation-associated genes increased in Δ*Mofbx15* and Δ*Mocue1*. This study will provide not only comprehensive understanding of the role of ubiquitination but also new insights on crosstalk between ubiquitination and SUMOylation in rice blast fungus and other fungal pathogens.

INTRODUCTION

Post-translational modification (PTM) is essential for the regulation of diverse cellular processes including proteolysis, cell cycle, DNA repair, transcriptional regulation, protein interaction, and stabilization in eukaryotes (Oh et al., 2012). Among the PTMs, ubiquitination is necessary for protein quality control via the degradation of proteins through the ubiquitin-proteasome system (UPS) (Dielen et al., 2010). Ubiquitination is a reversible pathway that transfers ubiquitin to substrates through five main enzymes: E1 activating enzyme, E2 conjugating enzyme, E3 ligase, E4 ligase, and deubiquitinase (Müller et al., 2001). E3 ligase plays an important role in substrate specificity (Mathur et al., 2015). E3 ligase can be categorized into the RING-finger, homologous to E6AP C-terminus (HECT), and U-box classes. Among these, RING-finger is the major E3 ligase class (Kaneko et al., 2016), and the Skp1/Cullin/F-box (SCF) complex and endoplasmic reticulum-associated degradation (ERAD) are its most well-known complexes. The SCF complex is composed of four components: SKP1, CUL1, RING box protein 1 (RBX1), and F-box proteins (FBXs) (Kornitzer, 2006). The selectivity of substrates for proteasomal degradation is determined by FBXs. The F-box motif binds to SKP1 and the C-terminal motif binds to substrates in the FBX (Yu et al., 2007). FBXs include FBXO (F-box only or others), FBXW (with WD40), and FBXL (with leucine-rich repeats (LRRs)), which are classified according to the type of binding motif on the C-terminal (Nelson et al., 2013). ERAD is a crucial mechanism for ER stress responses (Smith et al., 2011). This mechanism adds ubiquitin to unfolded

proteins and translocates the ubiquitinated substrates into the cytosol for degradation via the UPS (Xie and Ng, 2010). ERAD has two main complexes including HRD1/DER3 and DOA10 (Smith et al., 2011). CUE1 is a common component of these complexes and is essential for recruiting an E2 conjugating enzyme (UBC7) and adding polyubiquitin chains to the substrates (Ruggiano et al., 2014; von Delbrück et al., 2016).

Studies of the model fungus *Saccharomyces cerevisiae* have shown that GRR1 and MET30 (FBXLs) are crucial for cell division and each protein is important for glucose uptake and sulfur metabolism, respectively (Jonkers and Rep, 2009; Thomas et al., 1995). CDC4 (FBXW) in *S. cerevisiae* and *Candida albicans* is essential to the cell cycle during G1 to S phases, dimorphic switching, temperature stress tolerance, amino-acid biosynthesis, and calcium sensing (Atir-Lande et al., 2005; Yochem and Byers, 1987). Both MFB1 (FBXO) and MDM30 (FBXO) are involved in growth on nonfermented carbon sources and mitochondrion morphology, but only MDM30 is essential to sporulation efficiency in *S. cerevisiae* (Dürr et al., 2006). In *S. cerevisiae*, Δ*cue1* exhibits defects in cold adaptation and sterol biosynthesis and is sensitive to ER stressors such as $NiCl_2$ and $NiSO_4$ (Luo et al., 2016). Unlike FBXL and FBXW, FBXO has not been studied extensively and the exact roles of the ERAD and its components including CUE1 are poorly understood in plant fungal pathogens including *Magnaporthe oryzae*.

SUMOylation, another PTM, regulates transcriptional regulation and protein stability in eukaryotes (Gill, 2004). As with ubiquitination, SUMOylation can be mediated through a sequential cascade with E1, E2, and E3 to form an isopeptide bond on lysine (K) residues of the substrates (Gill, 2004). Despite these similarities

between the two pathways, ubiquitination and SUMOylation have been studied as independent pathways because their sequence identity, protein structure, function, and participants differ (Gill, 2004). Ubiquitination and SUMOylation have been actively studied in rice blast fungus during the past decade (Guo et al., 2015; Lim et al., 2018; Liu et al., 2018; Oh et al., 2012; Prakash et al., 2016; Shi et al., 2016; Wang et al., 2018). Ubiquitination- and SUMOylation-associated components are indispensable for fungal development, stress response, and pathogenicity (Guo et al., 2015; Lim et al., 2018; Liu et al., 2018; Oh et al., 2012; Prakash et al., 2016; Shi et al., 2016; Wang et al., 2018). Recent studies have shown that ubiquitin and SUMO interact with each other in human and yeast (Lamoliatte et al., 2017; Parker and Ulrich, 2012); however, crosstalk between these pathways remains to be studied in *M. oryzae*.

M. oryzae is a destructive hemibiotrophic phytopathogen that causes rice blast disease and has recently been reported to causes severe wheat blast disease in South America and Bangladesh (Malaker et al., 2016; Pham et al., 2015). *M. oryzae* is a polycyclic pathogen that causes outbreaks of rice blast disease throughout the entire rice growth period, with the disease cycle then repeating (Kim and Lee, 2012). These diseases are associated with great socioeconomic damage worldwide (Kim et al., 2009). Since genome sequencing of *M. oryzae* was first completed in plant pathogenic fungi, *M. oryzae* has been studied as a model organism in the research field of host-pathogen interactions (Dean et al., 2005; Valent, 1990). When conidia, asexual spores, attach to the host surface and recognize signals such as hydrophobicity and cutin layer, they germinate and form a unique infection structure, appressorium. Appressoria are melanized and accumulate glycerol, *M. oryzae*

penetrates the host with enormous turgor pressure (>8 Mpa) (Mir et al., 2015). After successfully intruding into the host, *M. oryzae* colonizes the invaded cells by forming primary hyphae (PH) and differentiating into bulbous invasive hyphae (IH) (Mosquera et al., 2009). During the early infection stage, the biotrophic interfacial complex (BIC) appears on IH of *M. oryzae* and cytoplasmic effectors are accumulated in the BIC and translocated into the plant cell to regulate host immunity (Giraldo et al., 2013). After the rice blast fungus has colonizied in the host, conidiogenesis is occurred to form a secondary inoculum (Goh et al., 2011).

In this study, we determined the functional role of genes encoding F-box only and CUE proteins in *M. oryzae*. *MoFBX15* and *MoCUE1* were important for conidiation, alkaline stress tolerance, and pathogenicity. *MoCUE1* was especially central to ER stress response and essential for localization and translocation of PWL2 and Avr-Pita, cytoplasmic effectors. Ubiquitinated and SUMOylated proteins reduced in two deletion mutants. This study will provide novel perspective on the role of ubiquitination in pathogenicity and the crosstalk between ubiquitination and SUMOylation in *M. oryzae*.

MATERIALS AND METHODS

I. Multiple sequence alignment

To determine the number of FBXs, F-box, cyclin like domain (IPR001810) containing protein-encoding genes were retrieved from InterPro (http://www.ebi.ac.kr/interpro) and CFGP 2.0 database (http://cfgp.riceblast.snu.ac.kr) (Choi et al., 2012). Domain structures of F-box proteins were represented based on InterPro database. Protein sequences of CUE1 in *M. oryzae*, *S. cerevisiae*, *S. pombe*, and *H. sapiens* were retrieved from CFGP 2.0 database and aligned by MUSCLE tool of the MEGA v.10 software and T-COFFEE server.

II. Targeted gene deletion and complementation

Wild-type (WT), *M. oryzae* KJ201, was obtained from the Center for Fungal Genetic Resources (CFGR) at Seoul National University, Seoul, Korea. The WT was cultured in liquid complete medium (CM; 0.6% Yeast extract, 0.6% Tryptone, and 1% Sucrose (w/v)) at 25°C for 3 days with shaking for obtaining protoplasts. The upstream and downstream flanking regions of each *MoFBX15* and *MoCUE1* were amplified from genomic DNA (gDNA) of the WT. The hygromycin B phosphotransferase gene (HPH) cassette was amplified from pBCATPH (Kim et al., 2005). To perform the targeted gene deletion, constructs were produced by double joint polymerase chain reaction (PCR) using these three amplicons (upstream and downstream flanking and HPH cassette). Targeted gene deletion mutants were

generated and selected as previously described (Lim et al., 2018). To generate complemented strains, constructs including each promoter and open reading frame (ORF) were amplified from the gDNA of the WT. Geneticin resistance cassette was amplified from pII99 (Lee et al., 2003). The each complemented strains were generated by co-transforming these constructs and Geneticin cassette into each of protoplast of gene deletion mutants. The complemented strains were selected on TB3 agar medium (supplemented with 800 ppm Geneticin) and screened by mycelia PCR using ORF primers (Table 1). All strains used in this study have been deposited in the CFGR (http://genebank.snu.ac.kr) (Table 2).

Table 1. Primer sequences used in this study.

Name	Sequence 5'→3'
MGG_00768_5'flnk_F	TGTCATGCACCTCGCCGTAAG
MGG_00768_5'flnk_R	CCTCCACTAGCTCCAGCCAAGCCCAAGAAGCCTCCTCGAACGG
MGG_00768_3'flnk_F	GTTGGTGTCGATGTCAGCTCCGGAGTTCCGCGACAGACACTCTC
MGG_00768_3'flnk_R	CTCACTCGCCCTCTCTCGTA
MGG_00768_nested_F	CTGAAAGCGGAGACTGTGC
MGG_00768_nested_R	GTAGCCCGAGCCTGAGATAGAA
MGG_00768_qRT_F	GGGATTGATAGTGCCACCGAAT
MGG_00768_qRT_R	GTGGATGGAGGTTTGCACTGG
MGG_12163_5'flnk_F	CTGATTAACGGAACAGGCCGAT
MGG_12163_5'flnk_R	CCTCCACTAGCTCCAGCCAAGCCGTGTTGCGATTCGTTGTTCGC
MGG_12163_3'flnk_F	GTTGGTGTCGATGTCAGCTCCGGAGCGTAACGTTCTATGCCACACC
MGG_12163_3'flnk_R	CTGTCAATAACCGGGTCGTTC
MGG_12163_nested_F	TTCCGGTTGCCAGAGTGCTAC
MGG_12163_nested_R	CACACAAGTTATGGCCGAGTG
MGG_12163_qRT_F	TCCAGCCCGACCTGATTACAAG
MGG_12163_qRT_R	AGCAATCTTGGCCTCCATCTTC
Hyg_F	GGCTTGGCTGGAGCTAGTGGAGG
Hyg_R	CTCCGGAGCTGACATCGACACCAAC
HA_F	CCCATACGATGTTCCAGATTACG
COS1_qRT_F	TGCACCACGATCCCAGAGA
COS1_qRT_R	GCGATGTTGTGCCGTTTGTTCC
COM1_qRT_F	GCCAGAGGTCCGCTATCAAA
COM1_qRT_R	CGGGATCTCGTCACTGGATT
CON7_qRT_F	TAAGGAGATCCGCAAAGAGT
CON7_qRT_R	TAGCGTTGTAGTCGGGGAGT

HOX2_qRT_F	TGGGGTTCTGCAGCCATGTT
HOX2_qRT_R	GTCCCGTGGTGTTACGTTCTGG
ERR1_qRT_F	ACGATCCCAATGTTGACAC
ERR1_qRT_R	GGTACAGTCCCAGAGCAAAC
LHS1_qRT_F	ACCCAGTCCTTACCATCAAG
LHS1_qRT_R	CTATCTTAACCGGCTTGTCC
KAR2_qRT_F	AACGGTCTCGAGAACTATGC
KAR2_qRT_R	TCCTTCTGCTCCTCAAAATC
β-tubulin_F	ACAACTTCGTCTTCGGTCAG
β-tubulin_R	GTGATCTGGAAACCCTGGAG
MGG_12163_SacI_F	GAGCTCATGGCGAACGAGGAGATCAAC
MGG_12163_XbaI_R	TCTAGACTAGGAGCTGCCGGCGCCA

Table 2. List of strains used in this study as experimental materials.

Strain	Description	Source
KJ201	*M. oryzae*, wild type strain	CFGR
Δ*Mofbx15*	*M. oryzae*, *FBX15* deletion mutant	This study
*Mofbx15*c	*M. oryzae*, genetic complementation strain of the Δ*Mofbx15*	This study
Δ*Mocue1*	*M. oryzae*, *CUE1* deletion mutant	This study
Mocue1c	*M. oryzae*, genetic complementation strain of the Δ*Mocue1*	This study
BY4742	*S.cerevisiae*, haploid wild type strain (S288C isogenic yeast strain: MATalpha; his3D1; leu2D0; lys2D0; ura3D0)	Euroscarf
Y10850 (Δ*cue1*)	*S.cerevisiae*, *CUE1* deletion mutant (BY4742; MATα; ura3Δ0; leu2Δ0; his3Δ1; lys2Δ0; YMR264w::kanMX4)	Euroscarf
Δ*cue1*:*Mocue1*	*S.cerevisiae*, genetic complementation strain of the Δ*cue1*	This study

III. Yeast complementation assay

S. cerevisiae WT and Δ*cue1* strain, Y10000 and Y10850, were obtained from Euroscarf, Frankfurt, Germany. *MoCUE1* was amplified from cDNA of the WT and cloned into pYES2 yeast expression vector (Invitrogen, California, USA). pYES2:*Mocue1* was transformed in the Y10850 competent cells using LiAc/PEG (Lithium acetate/Polyethylene Glycol) method. Transformants were selected on synthetic-defined (SD)-Ura agar medium containing 2% Raffinose and were confirmed by PCR using primers for amplifying the *MoCUE1*. The WT, Δ*cue1*, and complemented strain of *S. cerevisiae* were cultured in liquid Yeast Extract-Peptone-Dextrose medium (YPD; 1% Yeast Extract, 2% Peptone, and 2% Raffinose (w/v)) for overnight at 30°C with shaking. And then cultured yeast cells were diluted to OD600 of 0.5 and serially diluted 10 fold to 10^{-4}. Diluted yeast cells were spot inoculated on YPD agar medium and each containing 2.5 mM $NiSO_4$ and 2.5 mM $NiCl_2$.

IV. Southern blot assay and qRT and RT-PCR

The WT and targeted gene deletion mutants were cultured in liquid CM at 25°C for 3 days with shaking to extract the gDNA and total RNA as previously described (Kong et al., 2015). The gDNA was digested at 37 °C with restriction enzyme, separated on 1 % Agarose gel and transferred to nitrocellulose membrane. The membrane was hybridized with p32-labeled probe that generated using a Random Primers DNA Labeling System kit (Invitrogen, California, USA). The hybridized membrane was exposed to X-ray film. To check the expression levels during the

conidiation stage, sterile membrane filter (Whatman, Maidstone, England) was placed on V8 agar medium and total RNA was extracted from the conidiating mycelia cultured on the membrane filter. To confirm the expression levels of unfolded protein response-related genes, total RNA was extracted from the mycelia that cultured in liquid CM at 25°C for 3 days and 30 min after containing 10 mM Dithiothreitol (DTT) and 10 μg/mL Tunicamycin (TM), respectively. The total RNA was reverse transcribed to complementary DNA (cDNA) and performed quantitative reverse transcription (qRT)-PCR using 50 ng cDNA in a Rotor-Gene Q 2plex no PC (Qiagen, Venlo, Netherlands) as previously described (Lim et al., 2018). Transcript levels were quantified by RT-PCR using 100 ng of cDNA in a C1000 thermal cycler (Bio-Rad, California, USA). β-tubulin coding gene was used to normalize.

V. Mycelial growth, conidiation, conidial germination and appressorium formation

To assess the mycelial growth and colony morphology, all of strains were cultured in modified complete agar medium (CMA; 1% Glucose, 0.2% Peptone, 0.1% Yeast extract, 1% Casamino acid, 0.6% $NaNO_3$, 0.05% KCl, 0.05% $MgSO_4$, 0.15% KH_2PO_4 (w/v), 0.1% Trace element (v/v), 0.1% Vitamin supplement (v/v) adjust pH 6.5) and minimal agar medium (MMA; 1% Glucose, 0.6% $NaNO_3$, 0.05% KCl, 0.05% $MgSO_4$, 0.15% KH_2PO_4 (w/v), 0.1% Trace element (v/v), 0.1% Vitamin supplement (v/v) adjust pH 6.5) at 25°C for 9 days. Conidia were cultured on V8 agar medium and collected after incubation for 7 days. Conidiation was measured under a microscope using a hemacytometer. To measure the percentage of conidial

germination and appressorium formation, 70 μl of conidia suspension (3×10^4 /mL) was dropped on hydrophobic cover glass and incubated at 25°C for 2 and 8 h. To observe the conidiogenesis, all of strains were cultured on oatmeal agar medium (OMA; 5% Oatmeal, 2.5% Agar (w/v)) at 25°C for 10 days and then after putting a cover glass on a cultured agar block incubated at 25°C for 1 day. These experiments were performed in triplicates.

VI. Pathogenicity tests

Pathogenicity tests were performed using the susceptible rice cultivar, Nakdongbyeo (*Oryzae sativa*). To perform spray inoculation assay, 10 mL of conidia suspension (5×10^4 /mL, supplemented with 250 ppm of Tween 20) was inoculated on 4-week-old rice. Inoculated rice was incubated at 25°C for 1 day in humid and dark chamber (100% relative humidity) and then incubated at 28°C for 5 days in growth chamber. For performing sheath inoculation assay, conidia suspension (2×10^4 /mL) was inoculated on sheath of 6-week-old of rice. Inoculated rice sheath was incubated at 25°C for 48 h. After then, invasive hyphal growth was observed under a microscope. These experiments were performed triplicates.

VII. Staining assay

Conidia were harvested from culture on V8 agar medium at 25°C for 7 days. Conidial suspension (3×10^4 /mL) was dropped on slide glass that was coated with water agar medium. To stain septa, Calcofluor white (CFW, 10 μg/mL, Sigma Aldrich, USA) was treated on conidial hyphae at 25°C for 5 min in dark condition.

After then, dye was washed several times using sterilized distilled water and stained hyphae were observed using fluorescence microscope (Carl Zeiss, Oberkochen, Germany). Cell length of at least 100 conidial hyphae was measured using ImageJ software. These experiments were performed in triplicate.

VIII. ER, oxidative, and alkaline stress response test

To assess response to stress, 2 mM DTT and 0.15 μg/mL TM for ER stress and 5 mM H_2O_2 for oxidative stress were added in CMA and CMA was adjusted to pH 8.0 for alkaline stress. The WT, deletion mutants, and complemented strains were cultured under ER stress, oxidative stress, and alkaline stress conditions at 25°C for 9 days. These experiments were performed in triplicate.

IX. Western blot assay

pCB1004:MoSMT3pro:HA:MoSMT3 (pHA-SMT3) was generated as previously described (Lim et al., 2018). To confirm SUMOylation levels in all of strains, pHA-SMT3 and Geneticin resistance cassette were co-transformed in the WT and deletion mutants. To harvest mycelia, transformed WT and deletion mutants were cultured in liquid CM at 25°C for 3 days with shaking. Proteins were extracted using PRO-PREP™ protein extraction solution (Intron Biotechnology, Korea). To observe each ubiquitination and SUMOylation levels, 35 μg and 75 μg of protein samples were separated on 4-20% gradient sodium dodecyl sulfate-polyacrylamide gel electrophoresis (SDS-PAGE) gel (BIO-RAD, California, USA) and transferred to Immun-Blot LF polyvinylidene fluoride (PVDF) membrane (BIO-RAD,

California, USA). The membrane was probed with anti-HA antibody (1:1000, BETHYL, Alabama, USA) and anti-ubiquitin antibody (1:1000, Cell Signaling Technology, Massachusetts, USA) as previously described (Lim et al., 2018). The anti-Actin antibody (1:1000, Cell Signaling Technology, Massachusetts, USA) was used as a loading control. The levels of ubiquitination and SUMOylation in WT and deletion mutants were measured by band intensity of Western blot using ImageJ software.

X. Localization of fungal effectors

To observe apoplastic effector (BAS4) and cytoplasmic effectors (PWL2 and Avr-Pita) localization, plasmids containing BAS4pro:BAS4:mRFP, PWL2pro:PWL2:eGFP:NLS: NCterm, or Avr-Pitapro:Avr-Pita:eGFP:NCterm were co-transformed with a geneticin resistance cassette into the WT, Δ*Mocue1*, and Δ*Mosmt3*, respectively. The *Mosmt3* deletion mutant was generated in the previous study (Lim et al., 2018). Localization of BAS4, PWL2, and Avr-Pita was observed at least 100 infected sites using a fluorescence microscope (Carl Zeiss, Oberkochen, Germany) at biotrophic IH growth stage (30-32 hour post inoculation (hpi)). Fluorescent intensity of the cytoplasmic effectors was measured using ImageJ software. These experiments were performed in triplicate.

RESULTS

I. Identification of F-box proteins and the multi-sequence alignment of CUE1

F-box proteins include F-box cyclin like domain (IPR001810) on the N-terminus (Xu et al., 2009). FBXs are classified into FBXO, FBXW, and FBXL classes depending on which substrate-binding motif is present on the FBX C-terminus (Nelson et al., 2013). Through InterPro term searching, we retrieved protein sequences of 43 FBXs in *M. oryzae* from the CFGP2.0 and InterPro databases. Among the 43 FBXs, 33 FBXOs, 7 FBXWs, and 3 FBXLs were included, and MoFBX15 (MGG_00768) was included within the FBXOs. On average, FBXW had seven WD40 repeats and FBXL had eight LRRs (Figure. 1A). To investigate the relationship between the presence of a substrate-binding motif and interspecies conservation, we performed BLAST MATRIX using the Fungal Genome Gold Standard dataset, obtained from CFGP 2.0 database. As results, FBXWs and FBXLs which include a substrate-binding motif, were conserved among species. However, most FBXOs including MoFBX15 were Ascomycota-specific or *M. oryzae*-specific FBXs (Figure. 2)**.** CUE1 of *S. cerevisiae* and AMFR (CUE1 ortholog) of *H. sapiens* have been studied as ERAD components (Spandl et al., 2011; Xie and Ng, 2010). The CUE1 sequence of *S. pombe* showed 42% similarity to MoCUE1 (MGG_12163-encoding protein), and yeast and human CUE1 exhibited 38% and 16% similarity to MoCUE1, respectively. We then retrieved four CUE1 sequences and performed

multi-sequence alignment. Ubiquitin system component Cue domain (IPR003892) was conserved in CUE1 of four species and proline (P) and leucine (L) residues, which are important for ubiquitin binding, were conserved in the Cue domain (Figure. 1B). In a previous study, CUE1 was found to participate in ERAD and plays an essential role in recruiting the UBC7 E2 conjugating enzyme (Xie and Ng, 2010). In CUE1 of four species, the UBC7 binding region (U7BR) was well-conserved on the C-terminus, and residues involved in forming a hydrogen bond or salt bridge with UBC7 were conserved (Figure. 1B). These results suggest that the Cue domain and U7BR are well-conserved in MoCUE1, as well as in yeast and human.

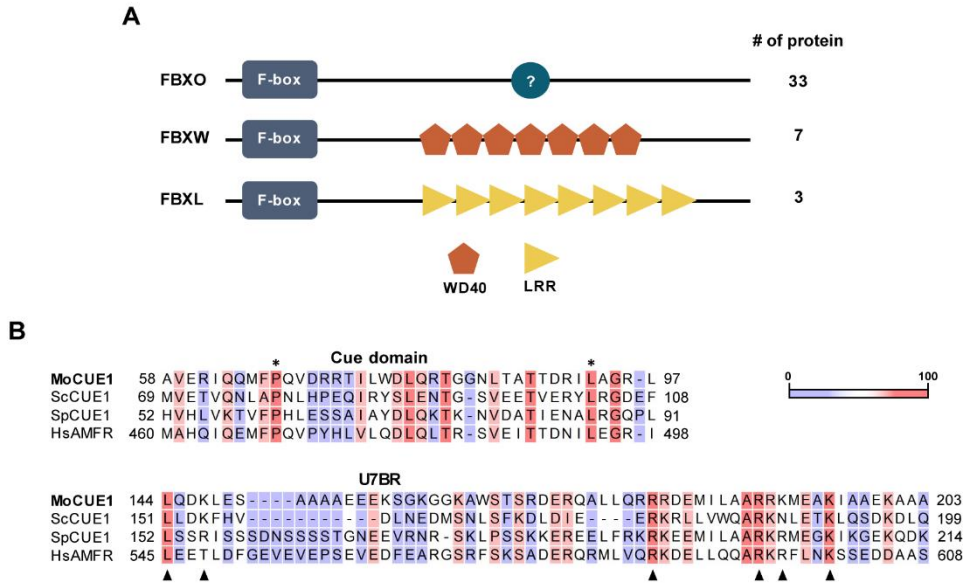

Fig. 1. Domain architecture and number of F-box proteins in *Magnaporthe oryzae* and alignment of the CUE1 protein in *M. oryzae*, *Saccharomyces cerevisiae*, *Schizosaccharomyces pombe*, and *Homo sapiens* (A) The domain architectures and numbers of proteins containing the F-box domain were determined using the InterProScan tool. FBXO, F-box only or others; FBXW, F-box with WD40 repeat; FBXL, F-box with LRR repeat. (B) Protein sequences were obtained from the CFGP database and aligned using MUSCLE tool of the MEGA v.10 software. Multiple sequence alignment was performed using the T-COFFEE server. The color bar indicates the consistency between the final aligned sequences of four species. Red regions indicate well conservation among the four species. Black asterisks indicate residues required for ubiquitin binding in the CUE domain. Black arrows indicate residues important for hydrogen bonds or salt bridges with UBC7. Mo, *M. oryzae*; Sc, *S. cerevisiae*; Sp, *S. pombe*; Hs, *H. sapiens*.

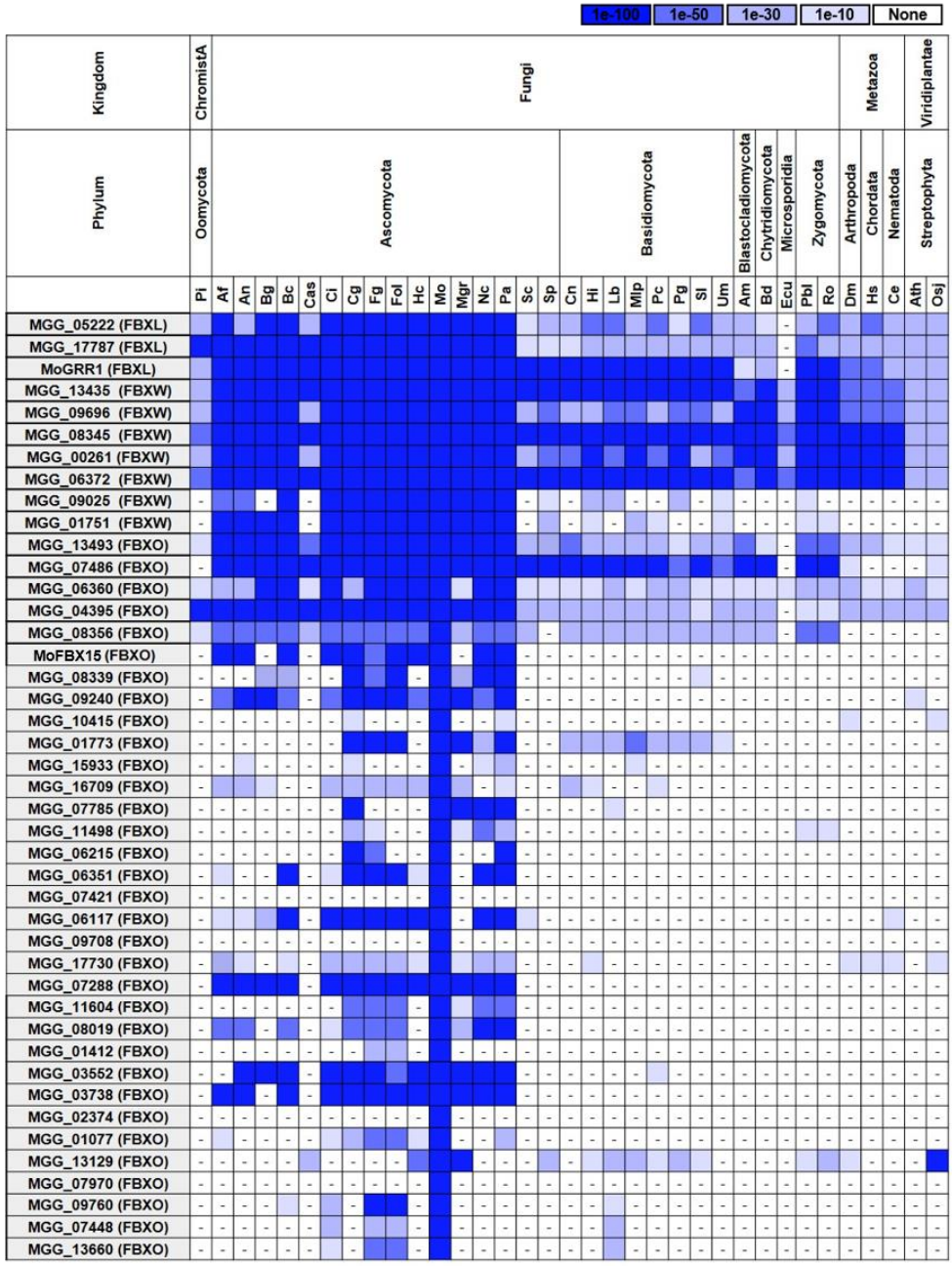
1e-100
1e-50
1e-30
1e-10
None
Kingdom
ChromistA
Fungi
Metazoa
Viridiplantae
Phylum
Oomycota
Ascomycota
Basidiomycota
Blastocladiomycota
Chytridiomycota
Microsporidia
Zygomycota
Arthropoda
Chordata
Nematoda
Streptophyta
Pi Af An Bg Bc Cas Ci Cg Fg Fol Hc Mo Mgr Nc Pa Sc Sp Cn Hi Lb Mlp Pc Pg Sl Um Am Bd Ecu Pbl Ro Dm Hs Ce Ath Osj
MGG_05222 (FBXL)
MGG_17787 (FBXL)
MoGRR1 (FBXL)
MGG_13435 (FBXW)
MGG_09696 (FBXW)
MGG_08345 (FBXW)
MGG_00261 (FBXW)
MGG_06372 (FBXW)
MGG_09025 (FBXW)
MGG_01751 (FBXW)
MGG_13493 (FBXO)
MGG_07486 (FBXO)
MGG_06360 (FBXO)
MGG_04395 (FBXO)
MGG_08356 (FBXO)
MoFBX15 (FBXO)
MGG_08339 (FBXO)
MGG_09240 (FBXO)
MGG_10415 (FBXO)
MGG_01773 (FBXO)
MGG_15933 (FBXO)
MGG_16709 (FBXO)
MGG_07785 (FBXO)
MGG_11498 (FBXO)
MGG_06215 (FBXO)
MGG_06351 (FBXO)
MGG_07421 (FBXO)
MGG_06117 (FBXO)
MGG_09708 (FBXO)
MGG_17730 (FBXO)
MGG_07288 (FBXO)
MGG_11604 (FBXO)
MGG_08019 (FBXO)
MGG_01412 (FBXO)
MGG_03552 (FBXO)
MGG_03738 (FBXO)
MGG_02374 (FBXO)
MGG_01077 (FBXO)
MGG_13129 (FBXO)
MGG_07970 (FBXO)
MGG_09760 (FBXO)
MGG_07448 (FBXO)
MGG_13660 (FBXO)

Figure 2. BLAST MATRIX analysis of 43 F-box proteins in *M. oryzae*. The sequence of 43 F-box proteins (FBXs) were retrieved from CFGP 2.0 database. BLAST MATRIX analysis was performed using Fungal Genome Gold Standard dataset and BLAST MATRIX results were visualized to blue color according to the e-value. *Phytophthora infestans* (Pi), *Aspergillus fumigatus* (Af), *Aspergillus nidulans* (An), *Blumeria graminis* f. sp. *hordei* (Bg), *Botrytis cinerea* (Bc), *Candida albicans* (Cas), *Coccidioides immitis* (Ci), *Colletotrichum graminicola* (Cg), *Fusarium graminearum* (Fg), *Fusarium oxysporum* f. sp. *lycopersici* (Fol), *Histoplasma capsulatum* (Hc), *Magnaporthe oryzae* (Mo), *Mycosphaerella graminicola* (Mgr), *Neurospora crassa* (Nc), *Podospora anserina* (Pa), *Saccharomyces cerevisiae* (Sc), *Schizosaccharomyces pombe* (Sp), *Cryptococcus neoformans* (Cn), *Heterobasidion irregulare* (Hi), *Laccaria bicolor* (Lb), *Melampsora larici-populina* (Mlp), *Phanerochaete chrysosporium* (Pc), *Puccinia graminis* f. sp. *tritici* (Pg), *Serpula lacrymans* (Sl), *Ustilago maydis* (Um), *Allomyces macrogynus* (Am), *Batrachochytrium dendrobatidis* (Bd), *Encephalitozoon cuniculi* (Ecu), *Phycomyces blakesleeanus* (Pbl), *Rhizopus oryzae* (Ro), *Drosophila melanogaster* (Dm), *Homo sapiens* (Hs), *Caenorhabditis elegans* (Ce), *Arabidopsis thaliana* (Ath), *Oryza sativa japonica* (Osj).

II. MoCUE1 is functional ortholog of CUE1 in yeast

In a previous study, CUE1, an ERAD-associated component, was found to be required for tolerance to ER stressors such as nickel chloride ($NiCl_2$) and nickel sulfate ($NiSO_4$) (Luo et al., 2016). Therefore, to determine whether the MGG_12163 coding protein plays role as CUE1, we generated a complemented strain by transforming a yeast expression vector containing MoCUE1 cDNA in a haploid *Cue1* deletion mutant of *S. cerevisiae*. Unlike the deletion mutant, which exhibited decreased growth in YPD agar medium containing 2.5 mM $NiCl_2$ and 2.5 mM $NiSO_4$, the defect of response to ER stressors was recovered in the complemented strain (Figure 3). These results indicate that MoCUE1 is a functional ortholog of ScCUE1.

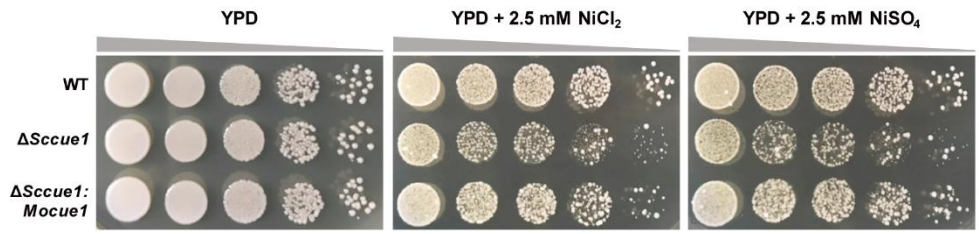

Figure 3. Δ***Sccue1*** **was functionally complemented by** ***MoCUE1.*** Wild-type (WT) and Δ*cue1 S. cerevisiae*, and functionally complemented strain were spot inoculated on YPD agar medium containing 2.5 mM each of $NiCl_2$ and $NiSO_4$.

III. Ubiquitination and SUMOylation levels decreased in Δ*Mofbx15* and Δ*Mocue1*

To confirm that the ubiquitination-associated components, MoFBX15 and MoCUE1 are required for ubiquitination in *M. oryzae*, we generated deletion mutants of each MoFBX15 and MoCUE1-encoding genes via homologous recombination. Western blot assay results showed that ubiquitination levels of Δ*Mofbx15* and Δ*Mocue1* decreased to 85% and 77% of the wild-type (WT), respectively (Figure 4A). Previous studies have identified crosstalk between the ubiquitination and SUMOylation pathway in human, fission yeast, and budding yeast (Lamoliatte et al., 2017; Parker and Ulrich, 2012). Therefore, we performed Western blotting to confirm the SUMOylation levels in the deletion mutants. The pHA-SMT3 that was generated in our previous study and transformed into the WT, Δ*Mofbx15*, and Δ*Mocue1* and total proteins were extracted after heat stress treatment (Lim et al., 2018). Under heat stress, SUMOylation levels in Δ*Mofbx15* and Δ*Mocue1* decreased to 83% and 79% of WT. However, free SUMO levels did not differ between the WT and deletion mutants at 25°C or under high temperature conditions (Figure 4B). To determine the reasons for reduced SUMOylated substrates in the deletion mutants, we confirmed transcript levels of 10 SUMOylation-associated component encoding genes using qRT-PCR (Lim et al., 2018). Remarkably, the expression of SUMO proteases, *MoULP1* (involved in SUMO maturation and deSUMOylation), *MoULP2* (involved in deSUMOylation) and *MoWSS1* (involved in deSUMOylation of substrates modified by SUMO-targeted ubiquitin ligases), increased 4- to 9-fold in Δ*Mofbx15* and Δ*Mocue1* (Figure 5). These results indicate that crosstalk between

ubiquitination-associated components and SUMOylation-related components were present in *M. oryzae*.

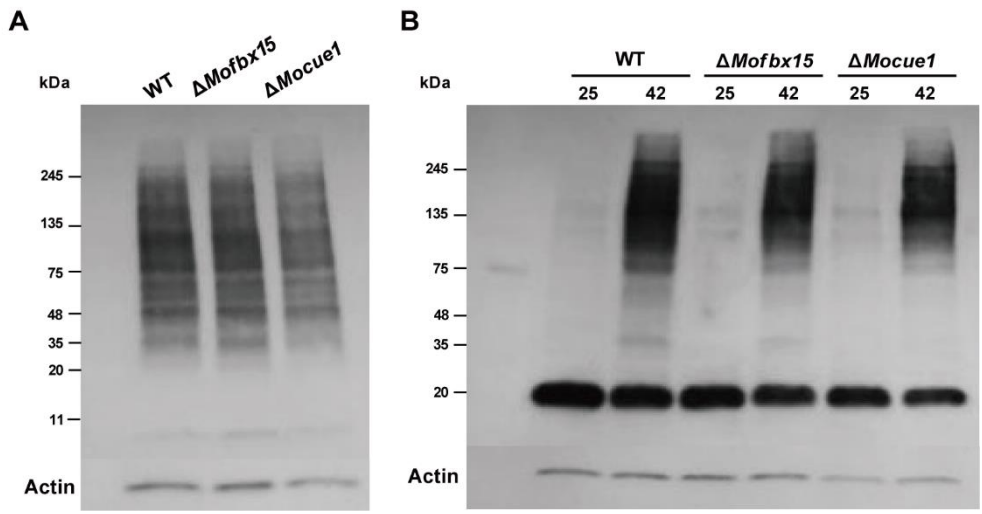

Figure 4. Levels of ubiquitination and SUMOylation decreased in Δ*Mofbx15* and Δ*Mocue1*. (A) Total proteins from the WT, Δ*Mofbx15*, and Δ*Mocue1* were extracted from mycelia cultured for 3 days in liquid CM medium. We loaded 35 μg total proteins on SDS-PAGE and Western blotting was performed using anti-ubiquitin (1:1000, Cell Signaling Technology) to detect ubiquitination levels. (B) To detect SUMOylation levels, total proteins were extracted from mycelia that were heat treated at 42°C for 45 min or not treated (25°C). Western blotting was performed using anti-HA (1:1000, BETHYL). Anti-actin (1:1000, Cell Signaling Technology) was used to control for protein loading.

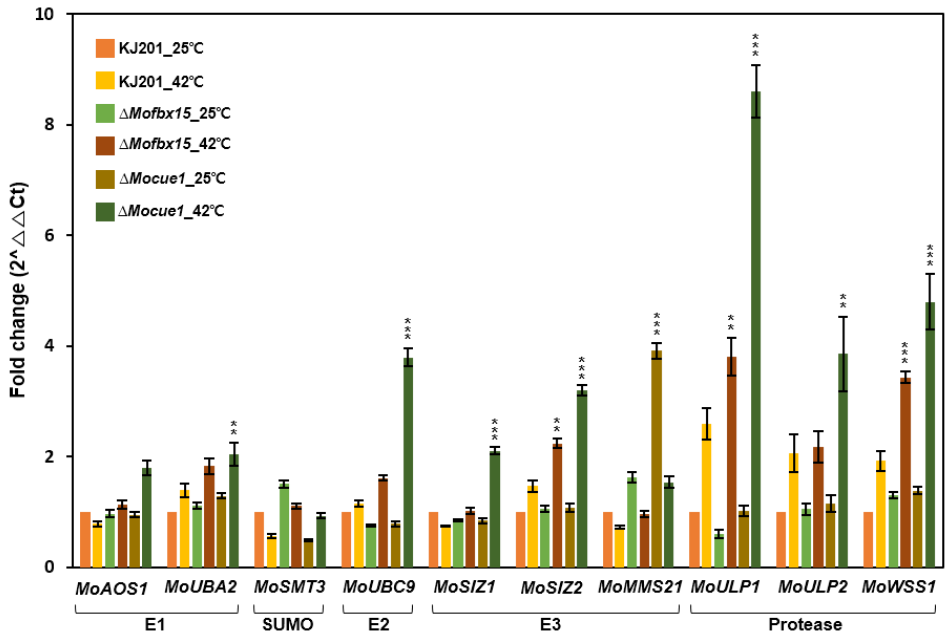

Figure 5. The expression of ten SUMOylation-associated genes in the WT, Δ*Mofbx15,* and Δ*Mocue1.* Total RNA of WT, Δ*Mofbx15*, and Δ*Mocue1* was extracted from mycelia that were heat treated (42°C) or no treated (25°C). The transcript levels of ten SUMOylation-related genes were confirmed by qRT-PCR. Statistical significance was determined using the Student's *t*-test (**, p <0.05 and ***, p <0.001).

IV. MoFBX15 and MoCUE1 are required for conidiation

Targeted gene deletion mutants were generated to examine the biological functions of *MoFBX15* and *MoCUE1* in *M. oryzae*. Targeted gene deletion mutants were confirmed using Southern blot assay and RT-PCR (Figure 6). The phenotypes of three independent Δ*Mofbx15* and two independent Δ*Mocue1* were found to be the same. Compared to the WT, mycelial growth of Δ*Mocue1* on CMA and MMA reduced by 9% and 14%, respectively. However, mycelial growth of Δ*Mofbx15* did not differ from that of the WT (Figure 7A and 7B). Δ*Mofbx15* and Δ*Mocue1* formed 2.2×10^5 /mL and 4×10^4 /mL conidia, respectively, that is significantly fewer than the WT (4.5×10^5 /mL conidia) (Figure 8A). Conidiogenesis was observed under microscope to elucidate the reduction of conidiation. Conidia produced a sympodial pattern on the conidiophore in the WT. However, in Δ*Mofbx15* and Δ*Mocue1*, fewer normal patterns were observed (Figure 8B). In addition, expression levels of conidiogenesis-related genes (*COS1*, *COM1*, *CON7*, and *HOX2*) were confirmed in the deletion mutants by performing qRT-PCR (Kim et al., 2009; Odenbach et al., 2007; Yang et al., 2010; Zhou et al., 2009). However, the expression of conidiogenesis-related genes was within 0.5- to 2-fold, with no significant difference between the WT and deletion mutants (Figure 9). Conidial germination and appressorium formation in the two deletion mutants did not differ from those in the WT (Table 3). Mycelial growth and conidiation defects were recovered in the complemented strains (Figure 8, Figure 10, and Table 3).

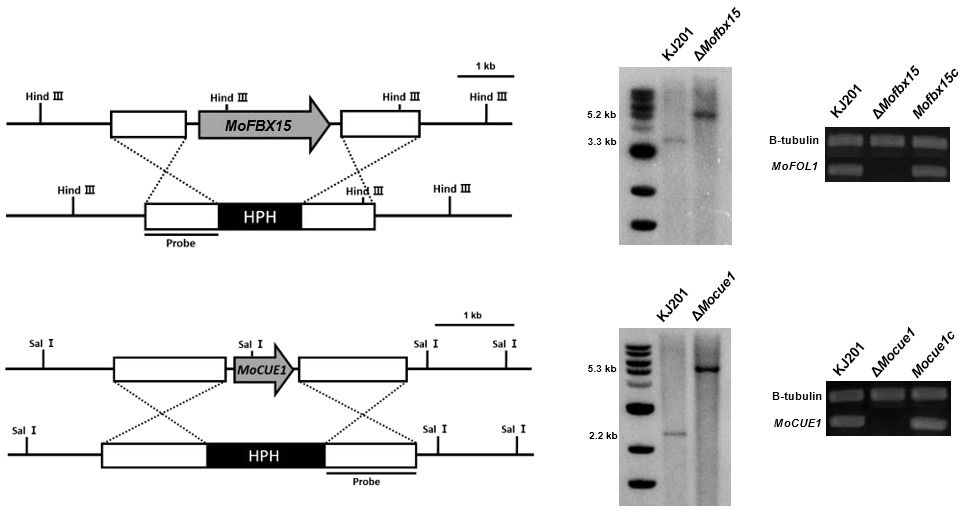

Figure 6. Southern blot analysis and RT-PCR for confirming the target deletion. Genomic DNA of WT and deletion mutants was digested with Hind III or Sal I enzyme. Upstream or downstream flanking of each genes was used for Southern blot analysis as a probe. Total RNA of the WT, deletion mutants, and complemented strains was extracted and synthesized to complementary DNA. RT-PCR was performed using the primers for confirming the deletion of target genes.

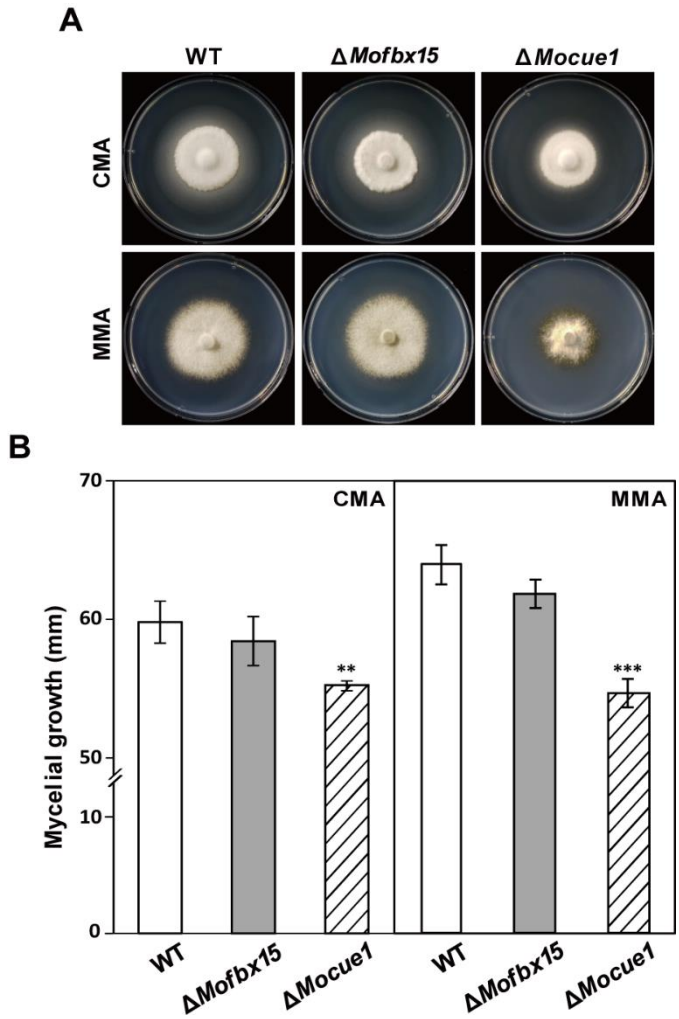

Figure 7. Δ*Mocue1* has defect in mycelial growth. WT, deletion mutants, and complemented strains were inoculated on CMA and MMA. (A) The colony morphology of the WT, Δ*Mofbx15*, and Δ*Mocue1* was observed after incubation for 9 days. (B) The mycelial growth of the WT, Δ*Mofbx15*, and Δ*Mocue1* was measured after incubation for 9 days. Statistical significance was determined using the student's *t*-test (**, $p < 0.05$ and ***, $p < 0.001$).

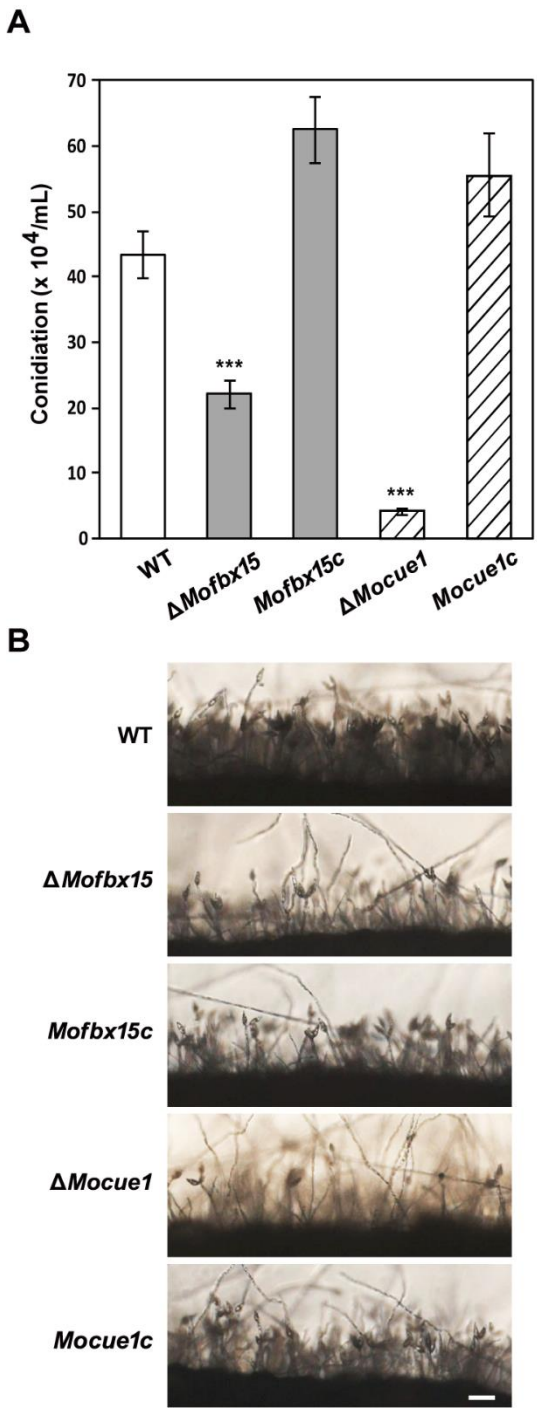
A
70
60
50
40
30
20
10
0
Conidiation (x 10^4/mL)
***
***
WT
ΔMofbx15
Mofbx15c
ΔMocue1
Mocue1c
B
WT
ΔMofbx15
Mofbx15c
ΔMocue1
Mocue1c

Figure 8. Conidiation reduced in Δ*Mofbx15* and Δ*Mocue1.* (A) Conidia of the WT, deletion mutants, and complemented strains were harvested from oatmeal agar medium after incubation for 10 days. Conidiation was measured using a hemacytometer under a microscope. Statistical significance was determined using the Student's *t*-test (***, p <0.001) (B) Conidiogenesis was observed on oatmeal agar medium after incubation for 10 days. Scale bar, 100 μm.

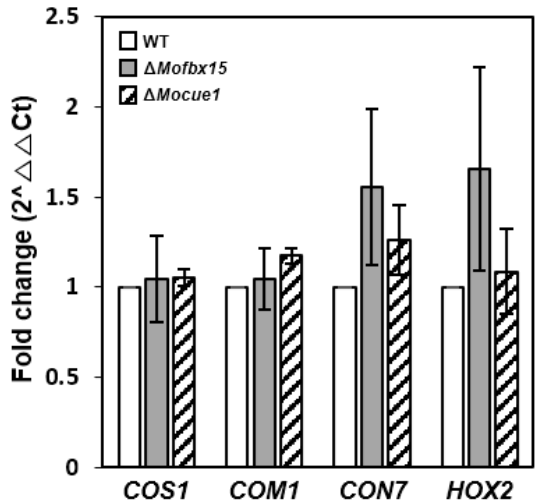

Figure 9. The expression of conidiation-related genes in the WT, Δ*Mofbx15,* and Δ*Mocue1.* The transcript levels of conidiation-related genes were confirmed by qRT-PCR during conidiation stage in the WT, Δ*Mofbx15,* and Δ*Mocue1*.

Table 3. Developmental phenotypes of the WT, deletion mutants and complemented strains.

Strain	Conidial size		Conidiation[b] (10^4/ml)	Conidial germination (%)	Appressorium formation (%)
	Length (μm)	Width (μm)			
WT	30.5±2.7	9.8±1.0	28.7±1.2	90.0±1.0	93.3±1.2
Δ*Mofbx15*	29.5±2.8	9.4±0.8	17.0±1.7***	93.7±1.2	93.0±3.6
Mofbx15c[a]	29.3±4.0	9.5±0.9	22.0±1.0	92.7±4.9	92.3±2.5
Δ*Mocue1*	27.9±4.3***	9.5±1.3	17.3±0.7***	92.0±1.0	94.0±1.0
Mocue1c	29.3±3.7	9.3±0.8	24.3±0.6	93.0±2.0	93.3±3.1

The significance was statistically determined by *t*-test with ***, $p < 0.001$.

[a]Complemented strains were named after the gene name with a "c".

[b]Conidiation was measured on V8 agar media culturing for 7days.

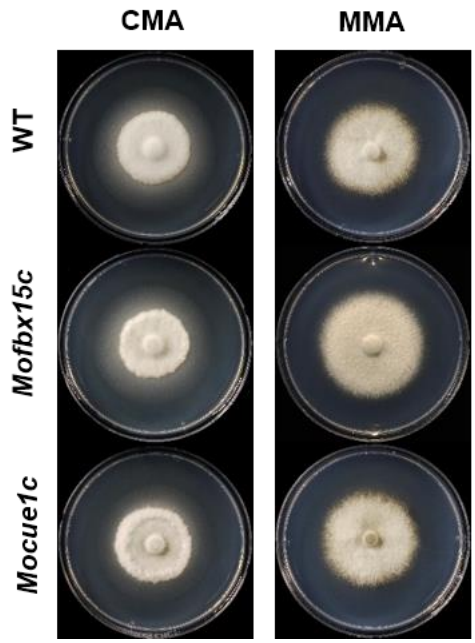

Figure 10. Mycelial growth test of the WT and complemented strains. The WT and complemented strains were inoculated on CMA and MMA. Colony morphology and mycelial growth of the WT, *Mofbx15c*, and *Mocue1c* were observed after incubation for 9 days.

V. MoFBX15 is needed for septum development in conidial hyphae

To examine the roles of *MoFBX15* and *MoCUE1* in septum development, we observed the septa of conidia and conidial hyphae stained with CFW under a fluorescent microscope. In the two deletion mutants, septum formation was normal in conidia, but aberrant in conidial hyphae (Figure 11). Compared to the WT (72 μm), cell length of Δ*Mofbx15* and Δ*Mocue1* decreased to 62 and 65 μm, respectively (Figure 11). The 1.08 septa were developed in WT, but 1.22 and 1.29 septa were formed in Δ*Mofbx15* and Δ*Mocue1*, respectively, in 100 μm of conidial hyphae. Since mycelial growth of Δ*Mofbx15* did not differ from the WT, these results suggest that *MoFBX15* is involved in septum development in conidial hyphae.

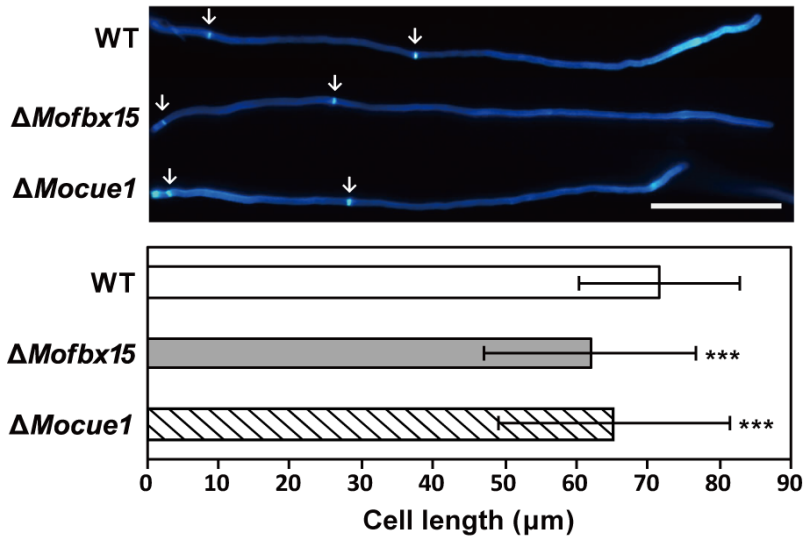

Figure 11. Cell length of Δ*Mofbx15* and Δ*Mocue1* reduced compared to the WT. The septa of conidial hyphae were stained with 10 μg/mL of CFW and the cell length of the WT and deletion mutants was measured using the ImageJ software. Scale bar, 50 μm. Statistical significance was determined using the Student's *t*-test (***, $p < 0.001$).

VI. The MoCUE1 deletion mutant has defect in ER stress response.

CUE1, a homolog of MoCUE1, is a key factor of the ERAD mechanism in yeast (Thibault and Ng, 2012). Therefore, we examined the sensitivity of *MoCUE1*-absent strain and the transcriptional expression of *MoCUE1* under ER stress conditions. To confirm sensitivity to ER stress, we measured mycelial growth of the WT, Δ*Mocue1*, and complemented strain on CMA supplemented with 2 mM DTT (an inhibitor of protein disulfide bond formation) and 0.15 μg/mL TM (an inhibitor of oligosaccharide biosynthesis), respectively. Mycelial growth of Δ*Mocue1* decreased in ER stress conditions. However, compared to inhibition rate on CMA (9%), inhibition rate on CMA with 2 mM DTT and 0.15 μg/mL TM was 9% and 16%, respectively. Therefore, Δ*Mocue1* was sensitive to ER stress induced by TM (Figure 12A and Figure 13). We confirmed transcriptional expression of *MoCUE1* with ERR1, LHS1, and KAR2 coding genes associated with the unfolded protein response (UPR) pathway and located ER (Goh et al., 2017; Yi et al., 2009). Expression of the *MoCUE1* and UPR-associated genes increased > 2-fold under both DTT- and TM-treated conditions (Figure 12B). These results indicate that Δ*Mocue1* has defect in ER stress response induced by the inhibition of oligosaccharide biosynthesis, and that like *ERR1*, *LHS1*, and *KAR2*, *MoCUE1* is related to the ER-associated response.

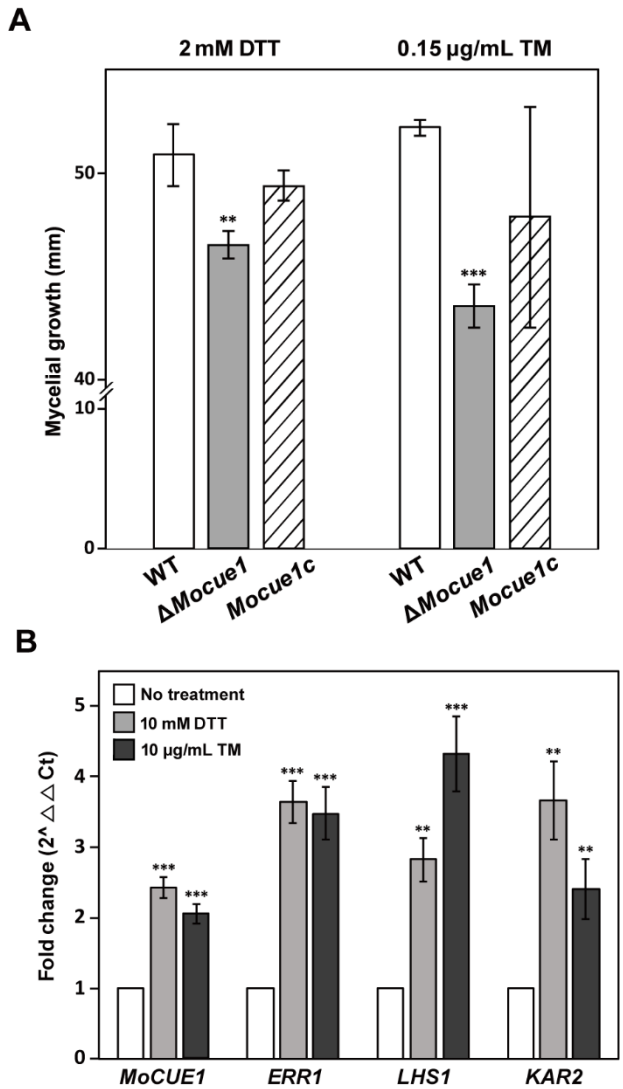

Figure 12. *MoCUE1* was needed for adaptation to ER stress conditions. (A) The mycelial growth of Δ*Mocue1* was measured on CMA containing 2 mM DTT and 0.15 μg/mL TM after incubation for 9 days. (B) The expression levels of UPR pathway-related genes including *MoCUE1* were detected in the WT that cultured in liquid CM containing 10 mM DTT and 10 μg/mL TM, respectively. Statistical significance was determined using the Student's *t*-test (**, p <0.05 and ***, p <0.001).

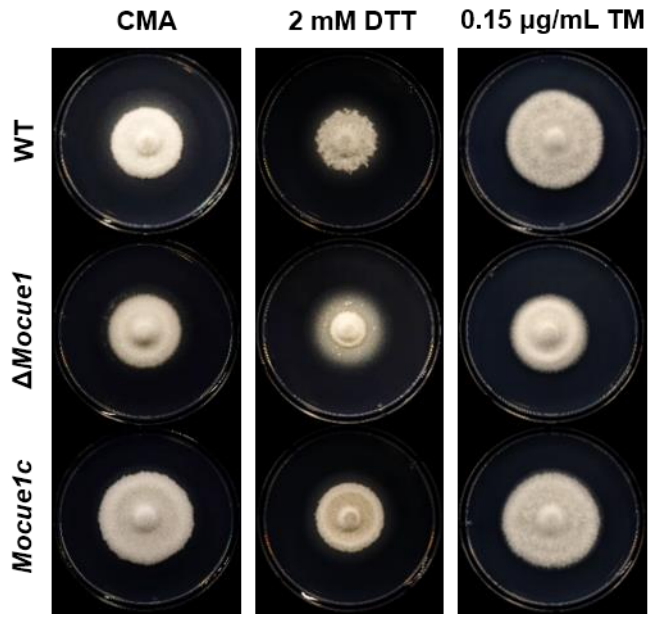

Figure 13. Colony morphology of the WT, Δ*Mocue1,* and *Mocue1c* under ER stress conditions. The WT, Δ*Mocue1,* and *Mocue1c* were inoculated on CMA and CMA containing 2 mM DTT and 0.15 μg/mL TM. The colony morphology and mycelial growth on ER stress conditions were observed after incubation for 9 days.

VII. MoCUE1 is related to cytoplasmic effector accumulation in the BIC

In this study, MoCUE1 was required for ER stress tolerance, similar to ERR1, LHS1, and KAR2, which are components involved in the UPR pathway. MoLHS1 is important for cytoplasmic effector function and localization (Yi et al., 2009). In addition, SUMOylation decreased in Δ*Mocue1*. Therefore, to determine whether *MoCUE1* is needed for the localization of effectors and whether Δ*Mosmt3* exhibits similar effector localization trends to Δ*Mocue1*, we transformed PWL2:eGFP:NLS, Avr-Pita:eGFP, and BAS4:mRFP expression plasmids into WT, Δ*Mocue1*, and Δ*Mosmt3*, respectively. PWL2 and Avr-Pita are located in the BIC on PH and IH, and BAS4 is uniformly located on the outline of PH and IH at the biotrophic stage (22–40 hpi) (Giraldo et al., 2013; Khang et al., 2010; Mosquera et al., 2009). We counted penetration sites that accumulated PWL2 in BICs at 30–32 hpi under a microscope. In WT inoculated sheath cells, PWL2 located in BICs on PH and IH of 97% of the penetration sites. However, in Δ*Mocue1,* 87% of the penetration sites were exhibited fluorescence signals in BICs and generally dispersed fluorescence signals in overall of PH and IH (Figure 14A). In Δ*Mosmt3*, 90% of the penetration sites have fluorescence signals in the BICs but, among these BICs, 80% were non-focal (Figure 14A). The PWL2 signal was observed in the 40% host nuclei in the Δ*Mocue1* inoculated sheath cells compared with the WT inoculated sheath cells (82%). In Δ*Mosmt3* inoculated sheath cells, 54% of the focal BIC-formed sites and 56% of the non-focal BIC-formed sites showed PWL2 signal in host nuclei. Like PWL2, Avr-Pita, is a cytoplasmic effector (Khang et al., 2010). Avr-Pita location

trends were not similar to those of PWL2 in Δ*Mocue1* but, trends were similar to those of PWL2 in Δ*Mosmt3*. The number of penetration sites with Avr-Pita in BICs of Δ*Mocue1* (85%) did not differ from those of the WT (88%), whereas the fluorescence intensity of Avr-Pita increased by 1.2- to 3.2-fold in Δ*Mocue1* compared with the WT. In Δ*Mosmt3*, 73% of the penetration sites showed the Avr-Pita signal in BICs, among these, 59% were non-focal BICs (Figure 14B). To examine the effects of MoCUE1 and MoSMT3 on apoplastic effector localization, we observed the localization of BAS4 in the WT, Δ*Mocue1*, and Δ*Mosmt3* inoculated sheath cells. However, similar to the WT, the BAS4 located in the extra-invasive hyphal membrane (EIHM) in Δ*Mocue1* and Δ*Mosmt3* (Figure 15). These results illustrate and suggest that *MoCUE1*, ubiquitination component related to ERAD, and SUMOylation are important for PWL2 and Avr-Pita accumulation in BICs and translocation into plants.

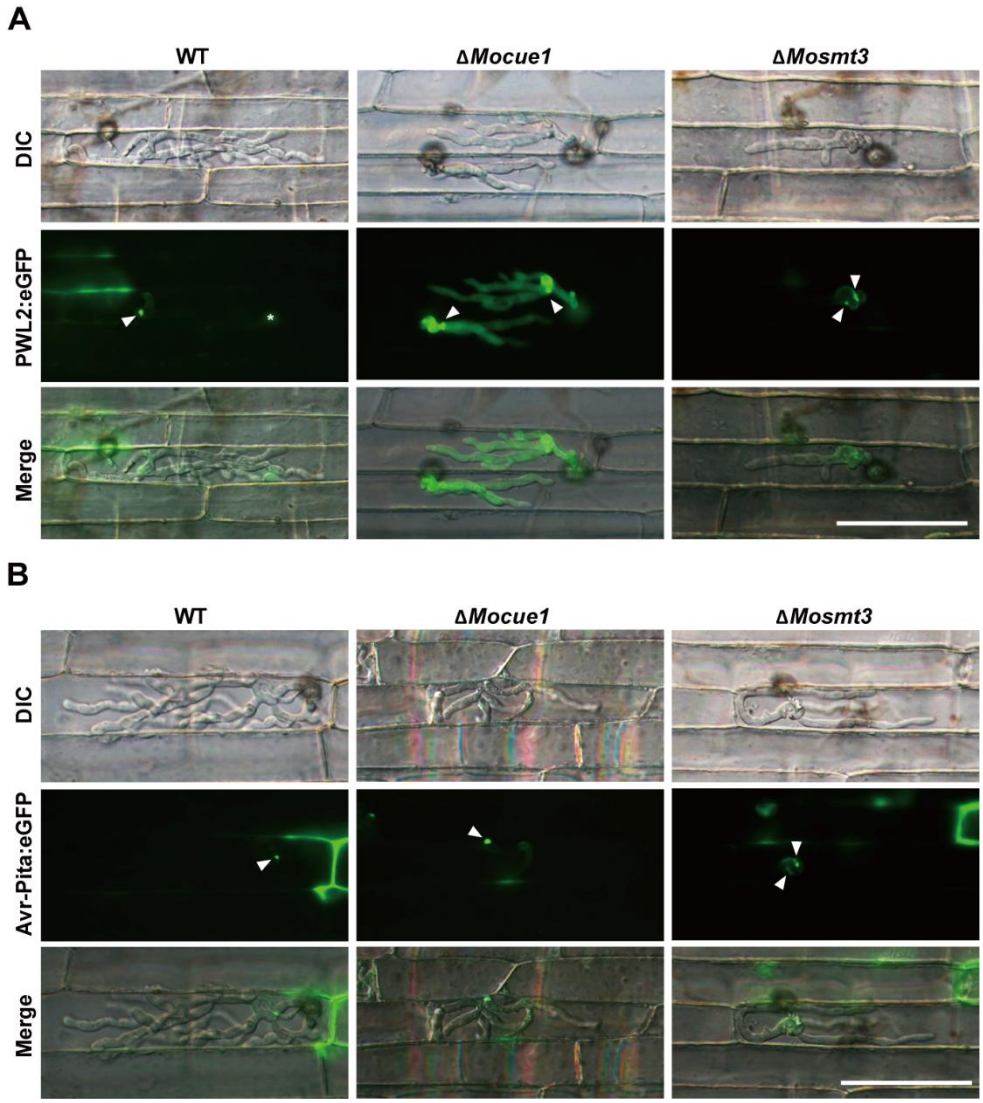
A
WT
ΔMocue1
ΔMosmt3
DIC
PWL2:eGFP
Merge
B
WT
ΔMocue1
ΔMosmt3
DIC
Avr-Pita:eGFP
Merge

Figure 14. *MoCUE1* and *MoSMT3* were related to PWL2 and Avr-Pita accumulation in BICs. Conidia suspension (2×10^4 /mL) was collected and inoculated onto sheath cells of 6-week-old susceptible rice cultivars. (A) The localization of PWL2:eGFP:NLS was observed in WT, Δ*Mocue1*, and Δ*Mosmt3* infected cells at 30–32 hpi. To observe PWL2 localization, we set the exposure times to 2, 0.5, and 1 s for WT, Δ*Mocue1*, and Δ*Mosmt3* inoculated samples, respectively. Scale bar, 50 μm. (B) The localization of eGFP expressed Avr-Pita was observed in WT, Δ*Mocue1*, and Δ*Mosmt3* inoculated sheath cells at 30–32 hpi. To observe Avr-Pita localization in the WT, Δ*Mocue1*, and Δ*Mosmt3*, we used exposure time to 1 s. Arrow heads indicate BICs and the asterisk indicates a rice nucleus. Scale bar, 50 μm.

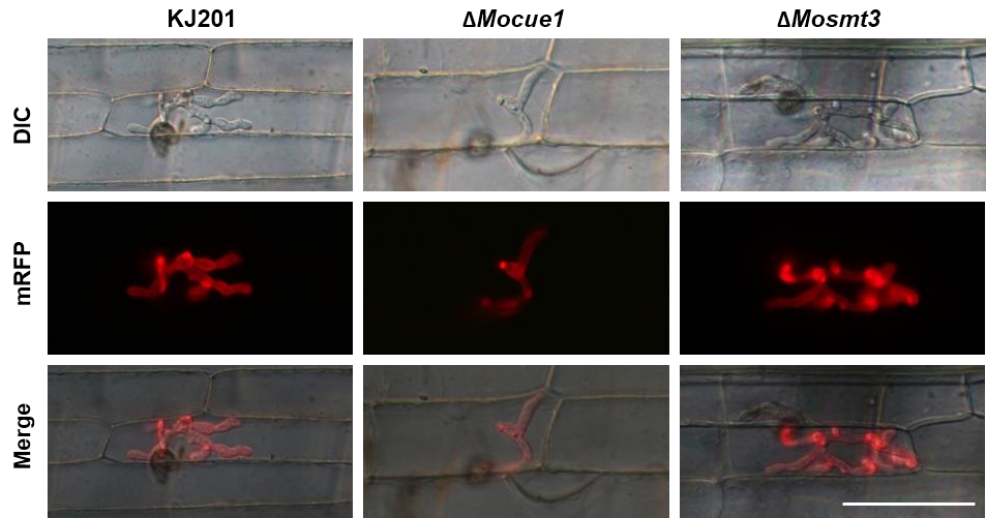

Figure 15. Localization of BAS4 during infection stage in the WT, Δ*Mocue1*, and Δ*Mosmt3* inoculated sheath cells. EF1αpro:BAS4:mRFP containing plasmid was transformed in the WT, Δ*Mocue1*, and Δ*Mosmt3*. Conidia suspensions (2 x 10^4/mL) were inoculated onto 6-week-old rice sheath cells and localization of BAS4 was observed at 30-32 hpi. Exprosure time for observing was 100 ms. Scale bar, 50 μm.

VIII. MoFBX15 and MoCUE1 are involved in pathogenicity in rice blast fungus

Recent studies have shown that various ubiquitination-associated proteins are important to pathogenicity in *M. oryzae* (Guo et al., 2015; Oh et al., 2012; Prakash et al., 2016; Shi et al., 2016; Shi et al., 2019; Wang et al., 2018). To investigate the pathogenicity of Δ*Mofbx15* and Δ*Mocue1,* conidia suspension of the WT, deletion mutants, and complemented strains was inoculated by spraying on 4-week-old rice plants. The WT formed many typical lesions, whereas deletion mutants formed smaller and fewer lesions on leaves compared to the WT (Figure 16A). To determine the reason for this phenomenon, we measured the penetration rate of deletion mutants after sheath inoculation in 6-week-old rice for 24 and 32 h. However, penetration rate did not differ between the WT and deletion mutants (data not shown). To examine invasive growth in the deletion mutants, we observed sheath cells at 48 hpi under a microscope. Colonization of IH in sheath cells was classified into three types. 1st cell colonization type for IH colonization occurred only in the penetrated cells, 2nd cell colonization type for IH spread to neighboring cells from the penetrated cells, and ≥ 3rd cell colonization type for IH extensive grow beyond the neighboring cells. In the WT, 85% of the penetrated sites exhibited 2nd and 3rd cell colonization type, whereas 51-58% of the penetrated sites exhibited 1st cell colonization type in Δ*Mofbx15* and Δ*Mocue1* (Figure 16B and 16C). When phytopathogens invade host cells, they are faced with stress conditions such as host-generated reactive oxygen species (ROS) and pH changes (Bousset et al., 2019; Segal and Wilson, 2018). ROS detoxification and pH adaptation are closely related to pathogenicity (Landraud et

al., 2013; Mir et al., 2015). To determine the response to typical stresses including oxidative and alkaline stresses, the WT, deletion mutants, and complemented strains were cultured on CMA supplemented with 5 mM H_2O_2 and CMA adjusted to pH 8.0 for each stress condition. According to the growth test results, the deletion mutants not sensitive to oxidative stress, but the deletion mutants sensitive to alkaline stress (Figure 16D and Figure 17)**.** These results suggest that significant reduction in pathogenicity was caused by delaying IH growth and sensitive to alkaline stress not caused by aberrant penetration in the deletion mutants. The reduced pathogenicity and delayed growth in IH in the deletion mutants were recovered in the complemented strains (Figure 16A, 16B, and 16C)**.**

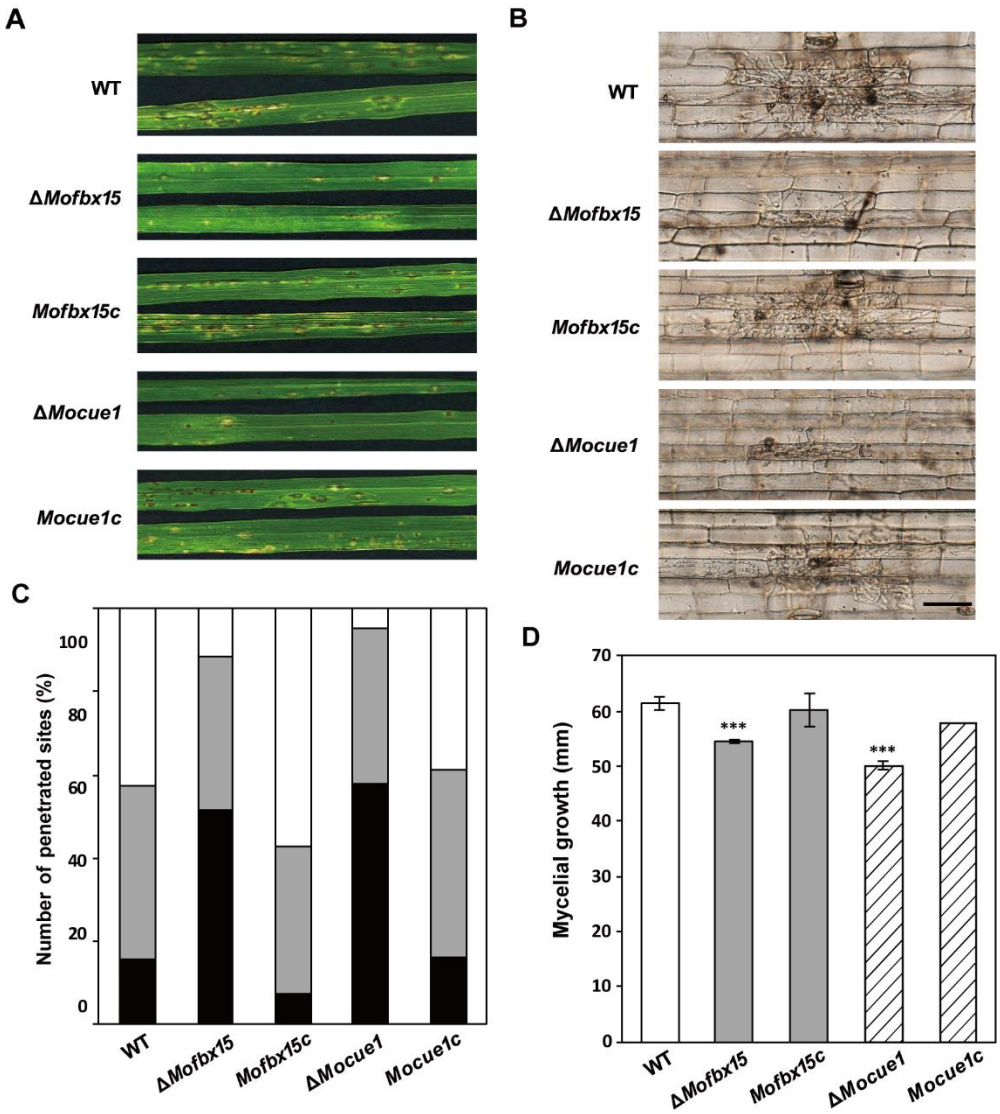
A
WT
ΔMofbx15
Mofbx15c
ΔMocue1
Mocue1c
B
WT
ΔMofbx15
Mofbx15c
ΔMocue1
Mocue1c
C
Number of penetrated sites (%)
0
20
40
60
80
100
WT
ΔMofbx15
Mofbx15c
ΔMocue1
Mocue1c
D
Mycelial growth (mm)
0
10
20
30
40
50
60
70
***
***
WT
ΔMofbx15
Mofbx15c
ΔMocue1
Mocue1c

Figure 16. *MoFBX15* and *MoCUE1* are required for pathogenicity in *M. oryzae*. (A) Conidia suspensions (5×10^4 /mL) of the WT, deletion mutants, and complemented strains were collected from V8 agar medium after incubation for 7 days and spray inoculated onto 4-week-old Nakdong rice seedlings. Inoculated leaves were harvested after incubation for 6 days at 28°C. (B) Conidia suspensions (2×10^4 /mL) of the WT, deletion mutants, and complemented strains were inoculated onto sheath cells of 6-week-old Nakdong rice seedling. Invasive hyphal growth was observed at 48 hpi under a microscope. Scale bar; 50 μm. (C) Type of invasive hyphae growth of the WT, deletion mutants, and complemented strains was classified as 1st cell (black bars), 2nd cell (gray bars), or ≥ 3rd cell colonization (white bars) according to the growth from the penetrated sites. (D) The mycelial growth of the WT, deletion mutants, and complemented strains was measured on alkaline stress media adjusted to pH 8.0 after incubation for 9 days. Statistical significance was determined using the Student's *t*-test (***, $p < 0.001$).

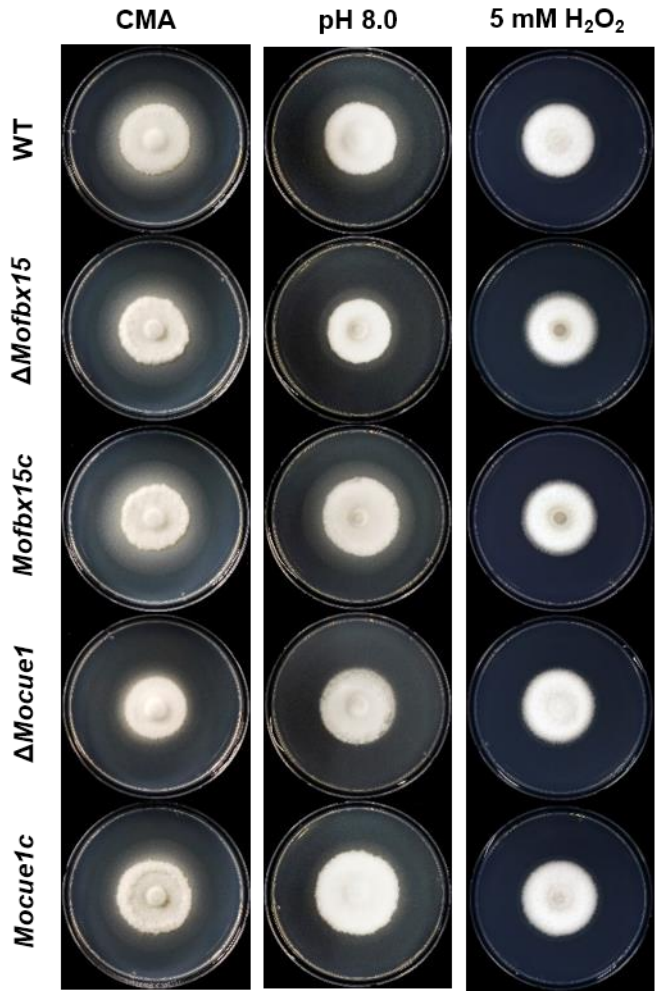

Figure 17. Mycelial growth of the WT, deletion mutants, and complementation strains under oxidative and alkaline stress conditions. The WT, deletion mutants, and complementation strains were inoculated on CMA, pH 8.0 adjusted CMA, and and CMA containing 5 mM H_2O_2. Colony morphology and mycelial growth on oxidative and alkaline stress conditions were observed after incubation for 9 days.

DISCUSSION

PTM by UBLs is essential for multiple biological mechanisms in eukaryotes (Liu and Xue, 2011; Oh et al., 2012). In recent decades, ubiquitination and SUMOylation have been actively studied as major PTMs by UBLs in relation to fungal development and pathogenicity in rice blast fungi (Guo et al., 2015; Lim et al., 2018; Liu et al., 2018; Oh et al., 2012; Prakash et al., 2016; Shi et al., 2016; Wang et al., 2018). In particular, the functions of MoSKP1, a component of the SCF complex, and FBXL (MoGRR1), FBXW (MoCDC4 and MoFWD1), and FBXO (MoFBX15) have been studied, but F-box only proteins in crosstalk between two PTMs, ubiquitination and SUMOylation is still uncharacterized in plant pathogenic fungi including *M. oryzae* (Guo et al., 2015; Prakash et al., 2016; Shi et al., 2019). In addition, the ERAD complex, which plays an important role in protein quality control and degradation in the ER, remains poorly understood in fungal plant pathogens (Thibault and Ng, 2012). Therefore, we comprehensively characterized the functions of F-box only protein and ERAD-associated components of *M. oryzae* in this study.

I. Ubiquitination and SUMOylation are correlated in *M. oryzae*

In this study, SUMO-modified proteins levels decreased and the expression of SUMO proteases increased in ubiquitination-associated component deletion mutants including Δ*Mofbx15* and Δ*Mocue1* (Figure 4B and Figure 5). In addition, *MoCUE1*

and *MoSMT3* were involved in the localization of cytoplasmic effectors including PWL2 and Avr-Pita in the BICs and their translocation in the host (Figure 14A and 14B). However, *MoCUE1* and *MoSMT3* may not directly interact because the localization trends of PWL2 and Avr-Pita were not similar between Δ*Mocue1* and Δ*Mosmt3* (Figure 14A and 14B). Most of our knowledge of the interactions between ubiquitination and SUMOylation pathway is derived from studies of model species including human and yeast (Lamoliatte et al., 2017; Parker and Ulrich, 2012). Five evidences have demonstrated crosstalk between these pathways, 1) Ubiquitin and SUMO are added to the same K residue of the substrate (Wilson and Heaton, 2008). Ubiquitination of K164 in proliferating cell nuclear antigen (PCNA), a factor of DNA replication and cell cycle regulation, is involved in reducing DNA repair errors, and SUMOylation is involved in recruiting Srs2 helicase during S-phase (Gali et al., 2012; Zhang et al., 2011). In H2B, ubiquitination and SUMOylation occur on K121. Ubiquitination on the H2B is needed to regulate the transcriptional process, but the function of SUMOylation is unknown (Lamoliatte et al., 2017). Crosstalk between ubiquitin and SUMO on the PCNA is not competitive whereas two modifications on the H2B are competitive (Gali et al., 2012; Lamoliatte et al., 2017; Zhang et al., 2011). 2) Ubiquitin and SUMO are attached to different K residues of one substrate for co-regulation (Wilson and Heaton, 2008). In yeast, ubiquitin and SUMO modifications occur in K123 and K6/7 of the H2B histone protein, respectively (Trujillo et al., 2011). It remains unknown whether the H2B is simultaneously modified by ubiquitin and SUMO, but SUMOylation is negatively regulated by ubiquitination in the H2B (Nathan et al., 2006). 3) Ubiquitination-associated

components are directly modified by SUMO (Wilson and Heaton, 2008). Mdm2, an ubiquitin E3 ligase, is modified by the participation of the SUMO E3 ligases, RanBP2 and PIAS, and SUMOylation in Mdm2 inhibits self-ubiquitination and degradation (Miyauchi et al., 2002). 4) Some E3 ligases are simultaneously involved in SUMOylation and ubiquitination (Wilson and Heaton, 2008). TOP1 binding arginine/serine rich protein (TOPORS), an E3 ligase, has dual activity of SUMO and ubiquitin ligase in mammals and yeast (Pungaliya et al., 2007). 5) SUMO interaction motifs of SUMO-targeted ubiquitin ligases (STUBLs) recognize SUMOylated substrates, and then ubiquitin is added to SUMOylated substrates (Sriramachandran and Dohmen, 2014; Wilson and Heaton, 2008). Ris1-Nis1, a STUBL complex, is important for the homeostasis of SUMOylation in eukaryotes (Alonso et al., 2012), and RNF4, a STUBL, is involved in the DNA-damage repair system by recognizing SUMOylated MDC1 and BRCA1 (Galanty et al., 2012; Kumar et al., 2017; Luo et al., 2012). We previously reported that levels of ubiquitinated proteins in SUMOylation-associated deletion mutants did not differ from those of the WT (Lim et al., 2018). These results and those of previous studies provide evidence that ubiquitination crosstalks with SUMOylation as an upstream pathway in *M. oryzae*.

II. The F-box domain and tolerance for alkaline stress are important to pathogenicity in *M. oryzae.*

In a previous study of *MoGRR1*, the F-box domain played an important role in conidiation and pathogenicity than LRR, which is needed to bind with substrates (Guo et al., 2015). Our results also showed that Δ*Mofbx15*, a FBXO protein, is

required for conidiation and pathogenicity in *M. oryzae* (Figure 8 and Figure 16). To determine the reason for decreased pathogenicity, we measured rates of conidial germination, appressorium formation, penetration, as well as oxidative and alkaline stress responses in Δ*Mofbx15*. Alkaline stress sensitivity increased in Δ*Mofbx15* compared to the WT (Figure 16D). Adaptations to the environment including host plant pH changes are essential for reproduction and survival in plant pathogenic fungi (Fernandes et al., 2017; Vylkova, 2017). Some fungal plant pathogens including *M. oryzae* prefer acidic pH during the life cycle, but this fungus needs to acclimate to mildly acidic pH environment to recognize the host plant surface and form infection structure (Landraud et al., 2013; Shnaiderman et al., 2013). During colonization after successful penetration, *M. oryzae* takes nutrients from the host and releases NH_4^+ produced by protein catabolism, converting the plant environment to alkaline pH (Bi et al., 2016). Therefore, adaptation to alkaline pH is important for *M. oryzae* survival and pathogenicity. A previous study showed that MoPACC, a transcription factor that regulates genes involved in the pH-controlling pathway, is required for conidiation and pathogenicity under alkaline conditions (Landraud et al., 2013). Therefore, we speculate that pathogenicity reduction may be due to absence of F-box domain and decrease in alkaline stress tolerance in Δ*Mofbx15*.

III. ER function homeostasis is interconnected with effector localization and pathogenicity in *M. oryzae*

In this study, the *MoCUE1* complemented strain was recovered sensitivity to ER stress in *S. cerevisiae* (Figure 3). These results indicate that *MoCUE1* plays a similar

role as *ScCUE1*. Δ*Mocue1* exhibited defects in mycelial growth, conidiation, resistance to ER and alkaline stress, cytoplasmic effector accumulation, and pathogenicity (Figure 7, Figure 8, Figure 12A, Figure 14, and Figure 16). Furthermore, *MoCUE1* expression increased by ER stressors such as DTT and TM (Figure 12B). The ER is an essential organelle in eukaryotes with several biological roles including protein synthesis, folding, and transport, lipid biogenesis, and carbohydrate and calcium metabolism (Krishnan and Askew, 2014; Schwarz and Blower, 2016). The ER is also involved in the elimination of incompletely folded proteins through the ERAD pathway and stimulation of UPR (Krishnan and Askew, 2014). The correlation of ER function-related proteins and pathogenicity has been well-characterized in human and plant fungal pathogens including *M. oryzae* (Cheon et al., 2011; Feng et al., 2011; Goh et al., 2017; Miyazaki and Kohno, 2014; Miyazaki et al., 2010a; Miyazaki et al., 2010b; Yi et al., 2009). Ire1/IreA, a regulating protein of the UPR signaling pathway, is associated with tolerance for antifungal drugs and ER stress and virulence in *A. fumigatus*, *Cryptococcus neoformans*, *C. grabrata* (Cheon et al., 2011; Feng et al., 2011; Miyazaki and Kohno, 2014). Crz1 and Slt2 are involved in Ca^{2+} flow and the ER stress surveillance pathway, respectively, and are required for fungal virulence in *C. grabrata* (Miyazaki et al., 2010a; Miyazaki et al., 2010b). In. *M. oryzae*, LHS1 and ERR1 have been studied as representative ER function-related proteins. LHS1, a member of the heat shock proteins 70 (Hsp70) family, and ERR1, an ER retention receptor, are important for protein folding and translocation, as well as ER integrity (Goh et al., 2017; Yi et al., 2009). These proteins play pivotal roles in fungal development and pathogenicity (Goh et al., 2017;

Yi et al., 2009). LHS1 is particularly important for cytoplasmic effector secretion in *M. oryzae* (Yi et al., 2009). Other recent studies of secretion pathway components have shown that in strains lacking MoEXO70 and MoSEC5, which are exocyst components, the PWL2 signal is accumulated not only in the BIC, but also within IH (Giraldo et al., 2013). In the absence of MoSSO1, MoSYN8, and MoSEC4, which are t-soluble N-ethylmaleimide-sensitive factor attachment protein receptor (SNARE), and Qc-SNARE proteins and an exocyst component, respectively, BICs are abnormally formed on IH and the secretion of cytoplasmic effectors including Avr-Pia and Avr-Piz-t is defective; however, the secretion of the apoplastic effector, BAS4, was not affected (Giraldo et al., 2013; Qi et al., 2016; Zheng et al., 2016). MoRBF1, a glycine-rich secretion protein, is involved in BIC formation, PH length, and PWL2 translocation into the rice cytoplasm (Nishimura et al., 2016). As reported in previous studies, several proteins related to effector localization and BIC formation are essential for pathogenicity in *M. oryzae*. In Δ*Mocue1*, PWL2 localized throughout the IH as well as the BIC, and the rates of BIC accumulation and host nucleus accumulation in inoculated cells decreased compared to the WT. The fluorescence intensity of Avr-Pita in BICs increased in Δ*Mocue1* (Figure 14). However, *MoCUE1* was dispensable for BIC formation and was not involved in BAS4 localization during infection (Figure 15). Therefore, we suggest that pathogenicity decline in Δ*Mocue1* is correlated with phenotypes of cytoplasmic effector mislocalization and ER homeostasis including ERAD functionality.

In this study, we elucidated the roles of ubiquitination-associated components, including the F-box domain only protein (MoFBX15) and CUE protein (MoCUE1),

in fungal development, stress tolerance, SUMOylation, and pathogenicity in *M. oryzae*. This study provides a novel perspective on the correlation of ubiquitination, SUMOylation, and pathogenesis in rice blast fungus and other plant pathogenic fungi.

LITERATURE CITED

Alonso, A., D'Silva, S., Rahman, M., Meluh, P. B., Keeling, J., Meednu, N., Hoops, H.J., and Miller, R.K. 2012. The yeast homologue of the microtubule-associated protein Lis1 interacts with the sumoylation machinery and a SUMO-targeted ubiquitin ligase. Mol. Biol. Cell. 23:4552–4566.

Atir-Lande, A., Gildor, T., and Kornitzer, D. 2005. Role for the SCFCDC4 ubiquitin ligase in *Candida albicans* morphogenesis. Mol. Biol. Cell. 16:2772-2785.

Bi, F., Barad, S., Ment, D., Luria, N., Dubey, A., Casado, V., Glam, N., Minguez, J.D., Espeso, E.A., Fluhr, R., and Prusky, D. 2016. Carbon regulation of environmental pH by secreted small molecules that modulate pathogenicity in phytopathogenic fungi. Mol. Plant Pathol. 17:1178-1195.

Bousset, L., Ermel, M., Soglonou, B., and Husson, O. 2019. A method to measure redox potential (Eh) and pH in agar media and plants shows that fungal growth is affected by and affects pH and Eh. Fungal Biol. 123:117-124.

Cheon, S.A., Jung, K.-W., Chen, Y.-L., Heitman, J., Bahn, Y.-S., and Kang, H.A. 2011. Unique evolution of the UPR pathway with a novel bZIP transcription factor, Hxl1, for controlling pathogenicity of *Cryptococcus neoformans*. PLOS Pathog. 7:e1002177.

Choi, J., Cheong, K., Jung, K., Jeon, J., Lee, G.-W., Kang, S., Kim, S., Lee, Y.-W., and Lee, Y.-H. 2012. CFGP 2.0: a versatile web-based platform for supporting comparative and evolutionary genomics of fungi and *Oomycetes*. Nucleic Acids Res. 41:714-719.

Dean, R. A., Talbot, N. J., Ebbole, D. J., Farman, M. L., Mitchell, T. K., Orbach, M.

J., Thon, M., Kulkarni, R., Xu, J.-R., Pan, H., Read, N. D., Lee, Y.-H., Carbone, I., Brown, D., Oh, Y., Donofrio, N., Jeong, J. S., Soanes, D. M., Djonovic, S., Kolomiets, E., Rehmeyer, C., Li, W., Harding, M., Kim, S., Lebrun, M.-H., Bohnert, H., Coughlan, S., Butler, J., Calvo, S., Ma, L.-J., Nicole, R., Purcell, S., Nusbaum, C., Galagan, J. E. and Birren, B. W. 2005. The genome sequence of the rice blast fungus *Magnaporthe grisea*. Nature. 434:980.

Dielen, A.-S., Badaoui, S., Candresse, T., and German-Retana, S. 2010. The ubiquitin/26S proteasome system in plant-pathogen interactions: a never-ending hide-and-seek game. Mol. Plant Pathol. 11:293-308.

Dürr, M., Escobar-Henriques, M., Merz, S., Geimer, S., Langer, T., and Westermann, B. 2006. Nonredundant roles of mitochondria-associated F-box proteins Mfb1 and Mdm30 in maintenance of mitochondrial morphology in yeast. Mol. Biol. Cell. 17:3745-3755.

Feng, X., Krishnan, K., Richie, D.L., Aimanianda, V., Hartl, L., Grahl, N., Powers-Fletcher, M.V., Zhang, M., Fuller, K.K., Nierman, W.C., Lu, L.J., Latgé, J.-P., Woollett, L., Newman, S.L., Cramer Jr, R.A., Rhodes, J.C., and Askew, D.S. 2011. HacA-independent functions of the ER stress sensor IreA synergize with the canonical UPR to influence virulence traits in *Aspergillus fumigatus*. PLOS Pathog. 7:e1002330.

Fernandes, T. R., Segorbe, D., Prusky, D., and Di Pietro, A. 2017. How alkalinization drives fungal pathogenicity. PLOS Pathog. 13:e1006621.

Galanty, Y., Belotserkovskaya, R., Coates, J., and Jackson, S. P. 2012. RNF4, a SUMO-targeted ubiquitin E3 ligase, promotes DNA double-strand break

repair. Genes Dev. 26:1179-1195.

Gali, H., Juhasz, S., Morocz, M., Hajdu, I., Fatyol, K., Szukacsov, V., Burkovics, P., and Haracska, L. 2012. Role of SUMO modification of human PCNA at stalled replication fork. Nucleic Acids Res. 40:6049-6059.

Gill, G. 2004. SUMO and ubiquitin in the nucleus: different functions, similar mechanisms? Genes Dev. 18:2046-2059.

Giraldo, M.C., Dagdas, Y.F., Gupta, Y. K., Mentlak, T. A., Yi, M., Martinez-Rocha, A. L., Saitoh, H., Terauchi, R., Talbot, N.J., and Valent, B. 2013. Two distinct secretion systems facilitate tissue invasion by the rice blast fungus *Magnaporthe oryzae*. Nat. Commun. 4:1996.

Goh, J., Jeon, J., and Lee, Y.-H. 2017. ER retention receptor, MoERR1 is required for fungal development and pathogenicity in the rice blast fungus, *Magnaporthe oryzae*. Sci. Rep. 7:1259.

Goh, J., Kim, K.S., Park, J., Jeon, J., Park, S.-Y., and Lee, Y.-H. 2011. The cell cycle gene MoCDC15 regulates hyphal growth, asexual development and plant infection in the rice blast pathogen *Magnaporthe oryzae*. Fungal Genet. Biol. 48:784-792.

Guo, M., Gao, F., Zhu, X., Nie, X., Pan, Y., and Gao, Z. 2015. MoGrr1, a novel F-box protein, is involved in conidiogenesis and cell wall integrity and is critical for the full virulence of *Magnaporthe oryzae*. *Appl.* Microbiol. Biotechnol. 99:8075-8088.

Jonkers, W., and Rep, M. 2009. Lessons from fungal F-box proteins. Eukaryot. Cell. 8:677-695.

Kaneko, M., Iwase, I., Yamasaki, Y., Takai, T., Wu, Y., Kanemoto, S., Matsuhisa,

K., Asada, R., Okuma, Y., Watanabe, T., Imaizumi, K., and Nomura, Y. 2016. Genome-wide identification and gene expression profiling of ubiquitin ligases for endoplasmic reticulum protein degradation. Sci. Rep. 6:30955.

Khang, C.H., Berruyer, R., Giraldo, M.C., Kankanala, P., Park, S.-Y., Czymmek, K., Kang, S., Valent, B. 2010. Translocation of *Magnaporthe oryzae* effectors into rice cells and their subsequent cell-to-cell movement. Plant Cell. 22:1388-1403.

Kim, K.S., and Lee, Y.-H. 2012. Gene expression profiling during conidiation in the rice blast pathogen *Magnaporthe oryzae*. PLoS One. 7:e43202.

Kim, S., Ahn, I.-P., Rho, H.-S., and Lee, Y.-H. 2005. MHP1, a *Magnaporthe grisea* hydrophobin gene, is required for fungal development and plant colonization. Mol. Microbiol. 57:1224-1237.

Kim, S., Park, S.-Y., Kim, K.S., Rho, H.-S., Chi, M.-H., Choi, J., Park, J., Kong, S., Park, J., Goh, J., and Lee, Y.-H. 2009. Homeobox transcription factors are required for conidiation and appressorium development in the rice blast fungus *Magnaporthe oryzae*. PLoS Genet. 5:e1000757.

Kong, S., Park, S.-Y., and Lee, Y.-H. 2015. Systematic characterization of the bZIP transcription factor gene family in the rice blast fungus, *Magnaporthe oryzae*. Environ. Microbiol. 17:1425-1443.

Kornitzer, D. 2006. The ubiquitin system and morphogenesis of fungal pathogens. Isr. Med. Assoc. J. 8:243-245.

Krishnan, K., and Askew, D.S. 2014. Endoplasmic reticulum stress and fungal pathogenesis. Fungal Biol. Rev. 28:29-35.

Kumar, R., González-Prieto, R., Xiao, Z., Verlaan-de Vries, M., and Vertegaal, A. C. 2017. The STUbL RNF4 regulates protein group SUMOylation by targeting the SUMO conjugation machinery. Nat. Commun. 8:1809.

Lamoliatte, F., McManus, F.P., Maarifi, G., Chelbi-Alix, M.K., and Thibault, P. 2017. Uncovering the SUMOylation and ubiquitylation crosstalk in human cells using sequential peptide immunopurification. Nat. Commun. 8:14109.

Landraud, P., Chuzeville, S., Billon-Grande, G., Poussereau, N., and Bruel, C. 2013. Adaptation to pH and role of PacC in the rice blast fungus *Magnaporthe oryzae*. PLoS One. 8:e69236.

Lee, J., Lee, T., Lee, Y.-W., Yun, S.-H., and Turgeon, B.G. 2003. Shifting fungal reproductive mode by manipulation of mating type genes: obligatory heterothallism of *Gibberella zeae*. Mol. Microbiol. 50:145-152.

Lim, Y.-J., Kim, K.-T., and Lee, Y.-H. 2018. SUMOylation is required for fungal development and pathogenicity in the rice blast fungus *Magnaporthe oryzae*. Mol. Plant Pathol. 19:2134-2148.

Liu, C., Li, Z., Xing, J., Yang, J., Wang, Z., Zhang, H., Chen, D., Peng, Y.-L., and Chen, X.-L. 2018. Global analysis of sumoylation function reveals novel insights into development and appressorium-mediated infection of the rice blast fungus. New Phytol. 219:1031-1047.

Liu, T.-B., and Xue, C. 2011. The ubiquitin-proteasome system and F-box proteins in pathogenic fungi. Mycobiology. 39:243-248.

Luo, C., Cao, C., and Jiang, L. 2016. The endosomal sorting complex required for transport (ESCRT) is required for the sensitivity of yeast cells to nickel ions in *Saccharomyces cerevisiae*. FEMS Yeast Res. 16.

Luo, K., Zhang, H., Wang, L., Yuan, J., and Lou, Z. 2012. Sumoylation of MDC1 is important for proper DNA damage response. EMBO J. 31:3008-3019.

Malaker, P.K., Barma, N.C.D., Tiwary, T.P., Collis, W.J., Duveiller, E., Singh, P.K., Joshi, A.K., Singh, R.P., Braun, H.-J., Peterson, G.L., Pedley, K.F., Farman, M.L., and Valent, B. 2016. First report of wheat blast caused by *Magnaporthe oryzae* pathotype *triticum* in Bangladesh. Plant Dis. 100:2330.

Mathur, R., Yen, J.L., and Kaiser, P. 2015. Skp1 independent function of Cdc53/Cul1 in F-box protein homeostasis. PLoS Genet. 11:e1005727.

Mir, A.A., Park, S.-Y., Sadat, M.A., Kim, S., Choi, J., Jeon, J., and Lee, Y.-H. 2015. Systematic characterization of the peroxidase gene family provides new insights into fungal pathogenicity in *Magnaporthe oryzae*. Sci. Rep. 5:11831.

Miyauchi, Y., Yogosawa, S., Honda, R., Nishida, T., and Yasuda, H. 2002. Sumoylation of Mdm2 by protein inhibitor of activated STAT (PIAS) and RanBP2 enzymes. J. Biol. Chem. 7:50131-50136.

Miyazaki, T., Inamine, T., Yamauchi, S., Nagayoshi, Y., Saijo, T., Izumikawa, K., Seki, M., Kakeya, H., Yamamoto, Y., Yanagihara, K., Miyazaki, Y., and Kohno, S. 2010. Role of the Slt2 mitogen-activated protein kinase pathway in cell wall integrity and virulence in *Candida glabrata*. FEMS Yeast Res. 10:343-352.

Miyazaki, T., and Kohno, S. 2014. ER stress response mechanisms in the pathogenic yeast *Candida glabrata* and their roles in virulence. Virulence. 5:365-370.

Miyazaki, T., Yamauchi, S., Inamine, T., Nagayoshi, Y., Saijo, T., Izumikawa, K., Seki, M., Kakeya, H., Yamamoto, Y., Yanagihara, K., Miyazaki, Y., and Kohno, S. 2010. Roles of calcineurin and Crz1 in antifungal susceptibility

and virulence of *Candida glabrata*. Antimicrob. Agents Chemother. 54:1639-1643.

Mosquera, G., Giraldo, M.C., Khang, C.H., Coughlan, S., and Valent, B. 2009. Interaction transcriptome analysis identifies *Magnaporthe oryzae* BAS1-4 as biotrophy-associated secreted proteins in rice blast disease. Plant Cell. 21:1273-1290.

Müller, S., Hoege, C., Pyrowolakis, G., and Jentsch, S. 2001. Ubiquitin and proteasomes: Sumo, ubiquitin's mysterious cousin. Nat. Rev. Mol. Cell Biol. 2:202.

Nathan, D., Ingvarsdottir, K., Sterner, D.E., Bylebyl, G.R., Dokmanovic, M., Dorsey, J.A., Whelan, K.A., Krsmanovic, M., Lane, W.S., Meluh, P.B., Johnson, E.S., and Berger, S.L. 2006. Histone sumoylation is a negative regulator in *Saccharomyces cerevisiae* and shows dynamic interplay with positive-acting histone modifications. Genes Dev. 20:966-976.

Nelson, D.E., Randle, S.J., and Laman, H. 2013. Beyond ubiquitination: the atypical functions of Fbxo7 and other F-box proteins. Open Biol. 3:130131.

Nishimura, T., Mochizuki, S., Ishii-Minami, N., Fujisawa, Y., Kawahara, Y., Yoshida, Y., Okada, K., Ando, S., Matsumura, H., Terauchi, R., Minami, E., and Nishizawa, Y. 2016. *Magnaporthe oryzae* glycine-rich secretion protein, Rbf1 critically participates in pathogenicity through the focal formation of the biotrophic interfacial complex. PLOS Pathog. 12,:e1005921.

Odenbach, D., Breth, B., Thines, E., Weber, R.W.S., Anke, H., and Foster, A.J. 2007. The transcription factor Con7p is a central regulator of infection-related morphogenesis in the rice blast fungus *Magnaporthe grisea*. Mol. Microbiol.

64:293-307.

Oh, Y., Franck, W.L., Han, S.-O., Shows, A., Gokce, E., Muddiman, D.C., and Dean, R.A. 2012. Polyubiquitin is required for growth, development and pathogenicity in the rice blast fungus *Magnaporthe oryzae*. PLoS One. 7:e42868.

Parker, J.L., and Ulrich, H.D. 2012. A SUMO-interacting motif activates budding yeast ubiquitin ligase Rad18 towards SUMO-modified PCNA. Nucleic Acids Res. 40:11380-11388.

Pham, K.T.M., Inoue, Y., Van Vu, B., Nguyen, H.H., Nakayashiki, T., Ikeda, K.-I., and Nakayashiki, H. 2015. MoSET1 (Histone H3K4 Methyltransferase in *Magnaporthe oryzae*) regulates global gene expression during infection-related morphogenesis. PLoS Genet. 11:e1005385.

Prakash, C., Manjrekar, J., and Chattoo, B.B. 2016. Skp1, a component of E3 ubiquitin ligase, is necessary for growth, sporulation, development and pathogenicity in rice blast fungus (*Magnaporthe oryzae*). Mol. Plant Pathol. 17:903-919.

Pungaliya, P., Kulkarni, D., Park, H.-J., Marshall, H., Zheng, H., Lackland, H., Saleem, A., and Rubin, E.H. 2007. TOPORS functions as a SUMO-1 E3 ligase for chromatin-modifying proteins. J. Proteome Res. 6:3918-3923.

Qi, Z., Liu, M., Dong, Y., Zhu, Q., Li, L., Li, B., Yang, J., Li, Y., Ru, Y., Zhang, H., Zheng, X., Wang, P., and Zhang, Z. 2016. The syntaxin protein (MoSyn8) mediates intracellular trafficking to regulate conidiogenesis and pathogenicity of rice blast fungus. New Phytol. 209:1655-1667.

Ruggiano, A., Foresti, O., and Carvalho, P. 2014. ER-associated degradation:

Protein quality control and beyond. J. Cell Biol. 204:869-879.

Schwarz, D.S., and Blower, M.D. 2016. The endoplasmic reticulum: structure, function and response to cellular signaling. Cell. Mol. Life Sci. 73:79-94.

Segal, L.M., and Wilson, R.A. 2018. Reactive oxygen species metabolism and plant-fungal interactions. Fungal Genet. Biol. 110:1-9.

Shi, H.-B., Chen, G.-Q., Chen, Y.-P., Dong, B., Lu, J.-P., Liu, X.-H., and Lin, F.-C. 2016. MoRad6-mediated ubiquitination pathways are essential for development and pathogenicity in *Magnaporthe oryzae*. Environ. Microbiol. 18:4170-4187.

Shi, H.-B., Chen, N., Zhu, X.-M., Liang, S., Li, L., Wang, J.-Y., Lu, J.-P., Lin, F.-C., and Liu, X.-H. 2019. F-box proteins MoFwd1, MoCdc4 and MoFbx15 regulate development and pathogenicity in the rice blast fungus *Magnaporthe oryzae*. Environ. Microbiol. 21: 3027-3045.

Shnaiderman, C., Miyara, I., Kobiler, I., Sherman, A., and Prusky, D. 2013. Differential activation of ammonium transporters during the accumulation of ammonia by *Colletotrichum gloeosporioides* and its effect on appressoria formation and pathogenicity. MPMI, 26:345-355.

Smith, M.H., Ploegh, H.L., and Weissman, J.S. 2011. Road to ruin: Targeting proteins for degradation in the endoplasmic reticulum. Science, 334:1086-1090.

Spandl, J., Lohmann, D., Kuerschner, L., Moessinger, C., and Thiele, C. 2011. Ancient ubiquitous protein 1 (AUP1) localizes to lipid droplets and binds the E2 ubiquitin conjugase G2 (Ube2g2) via its G2 binding region. J. Biol. Chem. 286:5599-5606.

Sriramachandran, A.M., and Dohmen, R.J. 2014. SUMO-targeted ubiquitin ligases. Biochim. Biophys. Acta. 1843:75-85.

Thibault, G., and Ng, D.T.W. 2012. The endoplasmic reticulum-associated degradation pathways of budding yeast. Cold Spring Harb Perspect. Biol. 4:a013193.

Thomas, D., Kuras, L., Barbey, R., Cherest, H., Blaiseau, P.-L., and Surdin-Kerjan, Y. 1995. Met30p, a yeast transcriptional inhibitor that responds to S-adenosylmethionine, is an essential protein with WD40 repeats. Mol. Cell. Biol. 15:6526-6534.

Trujillo, K.M., Tyler, R.K., Ye, C., Berger, S.L., and Osley, M.A. 2011. A genetic and molecular toolbox for analyzing histone ubiquitylation and sumoylation in yeast. Methods. 54:296-303.

Valent, B. 1990. Rice blast as a model system for plant pathology. Phytopathology. 80:33-36.

von Delbrück, M., Kniss, A., Rogov, V.V., Pluska, L., Bagola, K., Löhr, F., Güntert, P., Sommer, T., and Dötsch, V. 2016. The CUE domain of Cue1 aligns growing ubiquitin chains with Ubc7 for rapid elongation. Mol. Cell. 62:918-928.

Vylkova, S. 2017. Environmental pH modulation by pathogenic fungi as a strategy to conquer the host. PLOS Pathog. 13:e1006149.

Wang, Z., Zhang, H., Liu, C., Xing, J., and Chen, X.-L. 2018. A deubiquitinating enzyme Ubp14 is required for development, stress response, nutrient utilization, and pathogenesis of *Magnaporthe oryzae*. Front. Microbiol. 9:769.

Wilson, V.G., and Heaton, P.R. 2008. Ubiquitin proteolytic system: focus on SUMO. Expert Rev. Proteomic. 5:121-135.

Xie, W., and Ng, D.T.W. 2010. ERAD substrate recognition in budding yeast. *Semin.* Cell Dev. Biol. 21:533-539.

Xu, G., Ma, H., Nei, M., and Kong, H. 2009. Evolution of F-box genes in plants: Different modes of sequence divergence and their relationships with functional diversification. Proc. Natl. Acad. Sci. U.S.A. 106:835-840.

Yang, J., Zhao, X., Sun, J., Kang, Z., Ding, S., Xu, J.-R., and Peng, Y.-L. 2010. A novel protein Com1 is required for normal conidium morphology and full virulence in *Magnaporthe oryzae*. MPMI. 23:112-123

Yi, M., Chi, M.-H., Khang, C.H., Park, S.-Y., Kang, S., Valent, B., and Lee, Y.-H. 2009. The ER chaperone LHS1 is involved in asexual development and rice infection by the blast fungus *Magnaporthe oryzae*. Plant Cell. 21:681-695.

Yochem, J., and Byers, B. 1987. Structural comparison of the yeast cell division cycle gene CDC4 and a related pseudogene. J. Mol. Biol. 195:233-245.

Yu, H., Wu, J., Xu, N., and Peng, M. 2007. Roles of F-box Proteins in Plant Hormone Responses. Acta Biochim. Biophys. Sin. 39:915-922.

Zhang, W., Qin, Z., Zhang, X., and Xiao, W. 2011. Roles of sequential ubiquitination of PCNA in DNA-damage tolerance. FEBS Lett. 585:2786-2794.

Zheng, H., Chen, S., Chen, X., Liu, S., Dang, X., Yang, C., Giraldo, M.C., Oliveira-Garcia, E., Zhou, J., Wang, Z., and Valent, B. 2016. The Small GTPase MoSec4 is involved in vegetative development and pathogenicity by regulating the extracellular protein secretion in *Magnaporthe oryzae*. Front. Plant Sci. 7:1458.

Zhou, Z., Li, G., Lin, C., and He, C. 2009. Conidiophore stalk-less1 encodes a putative zinc-finger protein involved in the early stage of conidiation and mycelial infection in *Magnaporthe oryzae*. MPMI. 22:402-410.

벼 도열병균의 발달과 병원성에 대한 수모화의 기능 구명

임 유 진

초 록

번역 과정은 DNA에서 RNA를 거쳐 단백질을 만들어내는 ‘central dogma’의 마지막 단계이다. 그러나 생물은 번역 과정에서 한 단계 더 나아가 번역 후 수정 과정을 거쳐 생물학적 기능의 다양성을 이룬다. 단백질 번역 후 수정 과정은 특정 작용기 또는 작은 단백질을 기질 단백질에 결합하는 것으로, 대표적으로 인산화, 메틸화, 아세틸화, 글리코실화, 유비퀴틴화(ubiquitination), 수모화(SUMOylation)가 있다. 대부분의 단백질 번역 후 수정 과정은 전 세계적으로 식량안보에 큰 피해를 끼치는 식물 병원성 곰팡이의 생장과 병원성에 중요하다고 연구되어 왔으나, 수모화는 연구가 이루어진 바 없다. 수모화는 수모 단백질(SUMO), E1 활성화효소, E2 접합효소, E3 결합효소, 단백질 분해효소와 같이 5개의 핵심 단백질들의 참여로 세포주기, DNA 수정, 전사조절과 같은 중요한 생물학적 과정들에 관여한다. 벼 도열병균은 벼와 밀에 침입하여 전 생육기에 걸쳐 발병시켜 사회경제적 피해를 주며, 기주 병원체 상호작용의 모델 생물체로 연구되어왔다. 따라서 본 연구에서는 벼 도열병균의 병원성에 대한 단백질 번역 후 수정 과정의 역할을 알아보기 위해 식물 병원

성 곰팡이 최초로 수모화에 참여하는 단백질들을 동정하였다. 동정된 참여 단백질 중 수모 단백질(MoSMT3), 2개의 E1 활성화효소(MoAOS1, MoUBA2), E2 접합효소(MoUBC9)을 부호화하는 유전자의 삭제를 통해 균사생장, 분생포자와 침입 기관의 형성과 병원성에 중요한 역할을 하는 것을 밝혔다. 또한, 이 참여 단백질들이 벼 도열병균의 수모화에 필수적이며 영양결핍, DNA 수정 과정 방해와 산화 스트레스에 대한 저항성에 관여하고 있었다. 기주식물을 침입할 때 노출되는 환경 스트레스 중 하나인 산화 스트레스에 의해 4개의 단백질 모두 핵에 위치하는 것으로 보아 핵단백질의 수모화는 식물 병원성 곰팡이의 스트레스 저항성에 관여할 것이라는 가능성과 함께 병원성에 대한 수모화의 역할에 대한 새로운 시각을 제시하였다. 또 다른 단백질 번역 후 수정 과정인 유비퀴틴화는 수모화와 같은 도메인을 공유지만 수모화 참여 단백질과는 다른 종류의 E1 활성화효소, E2 접합효소, E3 결합효소의 순차적 참여에 의해 기질 단백질에 유비퀴틴을 결합시킨다. 유비퀴틴화는 수모화와 달리 단백질의 분해과정에 참여하여 단백질의 품질을 관리하는 중요한 역할을 하며, 그 기질을 선택하는 데 있어 유비퀴틴화의 E3 결합효소는 매우 필수적이다. 벼 도열병균에서 유비퀴틴화에 참여하는 단백질과 병원성에 대한 연구는 다소 이루어져 있지만, Skp1/Cullin/F-box (SCF) 복합체를 이루는 F-box 도메인만을 가지고 있는 단백질(F-box only protein)과 소포체 관련 분해(endoplasmic reticulum-associated degradation (ERAD)) 복합체에 참여하는 E3 결합효소에 대한 이해는 매우 부족하

다. 본 연구에서는 각 복합체에 참여하는 MoFBX15(F-box only protein)과 MoCUE1 (ubiquitin system component cue)의 기능분석을 수행하였다. MoFBX15와 MoCUE1은 벼 도열병균의 발달과 병원성에 관여하는데, 특히 MoCUE1은 소포체 스트레스 저항성과 식물 병원균의 병원성 인자인 이펙터(effector)의 분비와 이동에 중요하다. 게다가 각각의 E3 결합효소 부호화 유전자를 삭제한 돌연변이체에서 유비퀴틴화뿐만 아니라 수모화가 감소하였고, 수모 단백질을 기질에서 분리시켜주는 단백질 분해효소의 발현이 감소하였다. 이를 통해 벼 도열병균의 병원성에 대한 유비퀴틴화의 역할뿐만 아니라 수모화와 유비퀴틴화의 상호작용(cross-talk)에 대한 가능성을 제시하였다. 따라서 본 연구는 식물 병원성 곰팡이의 병원성에 대한 단백질 번역 후 수정과정의 역할의 이해를 도우며, 독립적안 단백질 번역 후 수정 과정이면서 상호작용하는 수모화와 유비퀴틴화의 관계를 조명함으로써 도열병균을 포함한 식물 병원성 곰팡이에서 단백질 번역 후 수정 과정에 대한 새로운 연구방향을 제시한다.

주요어 : 벼 도열병균, 병원성, 단백질 번역 후 수정과정, 벼 도열병, 수모화, 유비퀴틴화

학번 : 2015-21792